

New populations of neurons reveal novel mechanisms of cell death and astrocyte-dependent neurite pruning

by

Katherine Sarah Lehmann

A dissertation submitted in partial fulfillment
of the requirements for the degree of
Doctor of Philosophy
Neuroscience Graduate Program
at Oregon Health and Science University
September 2023

Doctoral Committee:

Dr. Gary Westbrook (chair)
Dr. Kelly Monk
Dr. Anusha Mishra
Dr. Marc Freeman
Dr. Bret Pearson

Katherine S. Lehmann ORCID iD:

0000-0002-0323-879X

Certificate of approval

Acknowledgements

This work is the culmination of many people supporting me, cheering me on, and taking risks on and for me. It takes a village and I have been incredibly lucky to have many, wonderful villages.

To my parents: thank you for the decades of support and for sharing your awe of the natural world with me. I've come a long way (I think) from burying Goldfish crackers in the backyard as a science project. I don't where I'd be without the library trips, museum excursions, weeks of camping, fossil fests, cleanways clean ups, scout meetings, bike rides, days on the water fishing, hikes, sports games, and books (so many books). A world without all of those things is duller. Thank you for giving Danny and I a bright, wonder inspiring world. And thank you for showing us how important it is to share and create that world for others.

My brother and extended family have also provided me an immense amount of support and encouragement. From warm home cooked meals, to encouraging emails and texts, to long hikes and cold river crossings, thank you for all of it.

Graduate school is what it is but being able to spend much of my twenties with kind, thoughtful, funny people has been the best part of the experience. I think my memories of this time will be filled with outdoor adventures, playing and watching soccer, game nights, park hang outs, climbing, pinball and Friendsgivings; how lucky I've been to have shared this time with such good friends. I'm sorry that I've gotten almost all of you lost in the woods at one point or another.

To all the members of the Freeman lab, thank you. I could write pages about all the ways that every single person in the lab has helped me. Leo said it well at his defense; I've been so lucky to be surrounded by people who happen to smart and chose every day to be kind.

Thank you to Marc Freeman for the mentorship, thought provoking conversations, scientific advice, wild ideas and impossible experiments. And thank you for letting me ask, and trying to answer, all of my non-scientific questions about leadership and institutions and structural change.

I'm not supposed to say thank you to Yunsik Kang, but I think in this instance it might be ok. Thank you for encouraging me and this unwieldy project. For being excited about all the data I've brought you. For pushing me to think about lots of ideas, to try outlandish ones and then gently redirecting me back on to the path when I follow one of those ideas into the wilderness. Your future graduate students are lucky to have such a kind, enthusiastic, brilliant person as their PI. And for everyone's sake, never tell your future trainees something will be simple; you'll curse whatever it is that they're trying to do forever.

With regards to this project there are a few people who literally made it possible. My committee has provided constructive feedback, helped me narrow the scope of this project and has asked questions that have led to uncovering cool new biology. Amy Sheehan started the project, verified lines and took hundreds of images to get it off the ground. Amy also solved many of the cloning projects that came with this project and made the lines that let me push the project forward. Amanda Jefferson, Ya-Chen Cheng and Yunsik Kang took over and ran with the project before handing me a paired down, much more manageable set of lines to work with. Amanda Jefferson taught me technical skills and has continued to help with dissections and imaging. Rachel De La Torre has

shared tools, reagents and helpful conversations, I've been very fortunate that we've gotten to share much of our grad school in lab. Tobi Stork keeps things from crumbling to the ground and taught me microscopy, provided thoughtful feedback and criticism of ideas and shared many lines with me. Jiakun Chen showed me how to use the Imaris software that allowed me to do the single cell quantification and has been a wonderful colleague. Leire and I performed the astrocyte screen together and I'm very grateful to her for putting up with the months of brutal dissections, imaging and analysis days. Madie Hupp and Adele Avetisyan were both integral to the Abd-B part of this project. And finally, to Dan. No matter what is happening in lab, I come home every day to a smile and a long-complicated story about some obscure football stat, or podcast, or weird poisonous plant, that almost certainly will get derailed before you tell me the punch line. Listening to your stories, telling you mine, and getting to share the past four years with you has been a blast. I'm so excited to share many more.

Table of Contents

Acknowledgements.....	iii
List of Tables	ix
List of Figures	x
List of Appendices	xii
Abstract.....	xiii
Chapter 1 Introduction	15
1.1 Developmental neuronal remodeling.....	16
1.2 Neuronal mechanisms that drive developmental remodeling.....	20
1.3 Glia cells can regulate apoptotic death in neurons.....	22
1.4 Neuron-glia communication in neurite pruning.....	24
1.5 <i>Drosophila</i> as a model to understand neuronal remodeling	26
1.6 Cell death during <i>Drosophila</i> metamorphosis	30
1.7 Local neurite pruning during <i>Drosophila</i> metamorphosis.....	33
1.8 Glia in <i>Drosophila</i> neuronal remodeling	38
1.9 Thesis Overview	40
Chapter 2 Beat-Vaneurons reveal mechanisms driving segment-dependent cell death and astrocyte-dependent neurite pruning.....	41
2.1 Introduction.....	42
2.2 Results.....	46

2.2.1 Beat-Va neurons undergo cell death or local pruning during metamorphosis	46
2.2.2 Local pruning in Beat-Va _M neurons is not driven by Ecdysone receptor (EcR).....	48
2.2.3 Astrocytes non-cell-autonomously regulate Beat-Va _M neuron pruning	51
2.2.4 The TGFβ molecule Myoglianin activates EcR expression in astrocytes to drive Beat-Va _M neuron local pruning	52
2.2.5 Translation profiling of astrocytes identified candidate astrocyte-derived activators of Beat-Va _M neuron local pruning.....	54
2.2.6 Beat-Va _L neurons are eliminated through segment-specific, steroid-dependent apoptotic cell death.....	57
2.2.7 Abdominal-B regulates segment-specific cell death in Beat-Va _L neurons..	57
2.3 Figures.....	60
2.4 Discussion.....	90
2.5 Methods and notes	95
2.5.1 Key Resource Table.....	96
2.5.2 Drosophila Genetics.....	101
2.5.3 Immunohistochemistry	102
2.5.4 Translating Ribosome Affinity Purification Sequencing.....	102
2.5.5 Image Analysis and Processing	105
2.5.6 Analysis and statistics	105
2.5.7 Generating BeatVa-LexA Stock	106
2.5.8 Generating LexAop-EcR ^{DN} Stock.....	106
2.5.9 BeatVa-Gal4 turns on embryonically	107
Chapter 3 Discussion	109
3.1 Identifying new populations of neurons that remodel during metamorphosis ...	110

3.2 The role of ecdysone signaling in <i>Drosophila</i> neurite pruning	111
3.3 Caspase signaling in neuronal remodeling	115
3.4 Hox genes in <i>Drosophila</i> neurodevelopment	116
3.5 Hox genes in mammalian neurodevelopment and cell death.....	121
3.6 Synaptic vs neurite remodeling.....	122
3.7 Identifying astrocytic molecules that drive remodeling.....	124
3.8 Identifying new molecules used in astrocyte driven debris clearance	126
Appendices.....	129
Bibliography	183

List of Tables

<i>Table 1 Neurons that die during metamorphosis</i>	33
<i>Table 2 Neurons that undergo neurite pruning during metamorphosis</i>	37

List of Figures

<i>Figure 1 Neuronal remodeling in Drosophila</i>	27
<i>Figure 2 Ecdysone signaling in Drosophila metamorphosis</i>	29
<i>Figure 3 Ecdysone-driven, caspase-mediated apoptosis</i>	30
<i>Figure 4 Beat-Va neurons undergo neurite pruning and cell death during metamorphosis</i>	61
<i>Figure 5 Beat-Va neurons undergo neurite pruning and cell death during metamorphosis</i>	63
<i>Figure 6 Beat-Va_M neurons remodel when EcR signaling or expression is inhibited</i>	65
<i>Figure 7 Manipulation of EcR-B1 expression in Beat-Va neurons</i>	67
<i>Figure 8 Genetic depletion of EcR by targeting upstream regulators does not block Beat-Va_M neuron remodeling</i>	69
<i>Figure 9 Cell specific expression of EcR^{DN} blocks astrocyte transformation</i>	71
<i>Figure 10 Astrocyte-derived signals converge with intrinsic Beat-Va_M neuron EcR signaling to execute local pruning</i>	73
<i>Figure 11 Supplemental: Verification of newly constructed BeatVa-LexA line</i>	75
<i>Figure 12 Pan-glial Myoglianin expression drives phagocytic astrocyte transformation</i>	77
<i>Figure 13 Translational profile of transforming astrocytes reveal regulators of debris clearance and neurite fragmentation</i>	79
<i>Figure 14 Visualization of Beat-Va_M neurons from all hits in the astrocyte screen</i>	81
<i>Figure 15 Astrocyte transformation tightly correlates with neurite remodeling phenotype categories</i>	82
<i>Figure 16 Beat-Va_L neurons undergo hormone-dependent, caspase-activated apoptosis</i>	84

<i>Figure 17 Hox gene Abd-B dictates caspase-dependent Beat-Va_L neuron cell death</i>	86
<i>Figure 18 Abd-B expression in Beat-Va neurons</i>	88
<i>Figure 19 BeatVa-Gal4 turns on in Drosophila embryos</i>	108
<i>Figure 20 New populations of neurons that remodel during metamorphosis</i>	111
<i>Figure 21 Abd-B dependent, EcR mediated, caspase driven apoptotic cell death</i>	120
<i>Figure 22 CadN neurons undergo neurite pruning during metamorphosis.</i>	131
<i>Figure 23 Neither caspase nor ecdysone signaling drives CadN neuron pruning</i>	132
<i>Figure 24 CadN neurons express EcR-B1</i>	133
<i>Figure 25 Pvf3 neuron refinement during metamorphosis</i>	136
<i>Figure 26 Pvf3_B cell visualized through MCFO approach</i>	137
<i>Figure 27 Pvf3 branching ladder cell at WL3</i>	138
<i>Figure 28 Pvf3 stick cell at WL3</i>	139
<i>Figure 29 Pvf3_B and Pvf3 stick neurons use different mechanisms to carry out neurite refinement</i>	141
<i>Figure 30 Pvf3 cells express the ecdysone receptor</i>	142
<i>Figure 31 Pvf3 labeled with mCD4::GFP</i>	144
<i>Figure 32 Fine projection refinement persists in vCrz neurons when cell death is blocked</i>	146
<i>Figure 33 A7 Beat-Va_M cell morphology</i>	149
<i>Figure 34 Knockdown of Draper stops some Beat-Va_M neurite fragmentation</i>	151
<i>Figure 35 Draper is necessary for proper astrocyte transformation</i>	153
<i>Figure 36 Abd-B does not define the Beat-Va_L cell death pattern</i>	157

List of Appendices

Appendix A: CadN neurons.....	130
Appendix B: Pvf3 neurons.....	135
B.1 A technical note on Pvf3 neurons	142
Appendix C: Corazonin neurons remodel when caspase and ecdysone signaling is blocked.....	145
Appendix D: More information on Beat-Va neurons	148
D.1 A technical note on Beat-Va _M A7 neurons	148
Appendix E: Astrocytic Draper is necessary for proper astrocyte transformation	150
Appendix F: Abd-A patterning does not reflect Beat _L cell death patterns	155
Appendix G: FlyLight lines evaluated at WL3 for GAL4 strength and expression pattern	159
Appendix H: FlyLight lines evaluated at WL3, 6APF and 18APF for remodeling	165
Appendix I: Astrocyte screen results	169

Abstract

During animal development, nervous systems over-wire and then refine to ultimately shape precise neuronal circuitry. This developmental neuronal remodeling, observed across evolution in animals with complex nervous systems, involves the selective pruning of synapses, neurites or whole neurons, to refine circuit connectivity, however the molecular mechanisms that drive this process have proven to be complex and diverse. To untangle this complexity, we performed a large-scale screen in *Drosophila*—which offer an unmatched molecular-genetic toolkit and, a highly stereotyped nervous system that remodels in temporally reproducible matter during metamorphosis— to discover new mechanisms of developmental neuronal remodeling. Here I describe two newly-identified populations of *Drosophila* neurons, tracked temporally at single-cell resolution, that remodel in a novel manner. The neurons—which we refer to as the Beat-Va lateral (Beat-Va_L) and Beat-Va medial (Beat-Va_M) populations—undergo cell local pruning and cell death, respectively. Beat-Va_L cells use hormonal signaling, caspase activation and Hox genes to execute cell death. This is the first time that both hormonal signaling and Hox genes have been shown to be necessary for neuronal cell death in the same population of neurons. In the Beat-Va_M population, astrocytes are necessary for the fragmentation step of remodeling. This is the first-time astrocytes specifically have been implicated in a non-redundant fashion in neuronal fragmentation in the fly. These findings demonstrate 1) a

new mechanism for cell death that relies on intersectional Hox gene and hormone receptor expression 2) a novel mechanism for neurite pruning involving astrocytes and 3) that astrocytes play unique and crucial roles at specific stages during the remodeling process. Furthermore, I present preliminary data on three other populations of neurons that remodel during metamorphosis, and which could be informative in future studies.

Chapter 1 Introduction

1.1 Developmental neuronal remodeling

During development, complex nervous systems massively over-wire and overpopulate with neurons but are then refined through selective elimination of superfluous neurons, axon or dendritic branches and/or synaptic connections. This process, termed “developmental neuronal remodeling” allows for fine-tuning of neural connectivity, ultimately leading to an optimized, functional circuit in mature animals. How neuronal remodeling occurs in a developing nervous system has only been studied in a handful of cell types in mammals or *Drosophila*. These studies have highlighted the complexity of neuronal remodeling—each group of cells appears to use different molecular machinery to drive remodeling events (Lee, Marticke et al. 2000, Stevens, Allen et al. 2007, Kirilly, Gu et al. 2009, Zhang, Wang et al. 2014, Bornstein, Zahavi et al. 2015, Sipe, Lowery et al. 2016, Choo, Miyazaki et al. 2017, Gunner, Cheadle et al. 2019, Bu, Lau et al. 2023, Maysseless, Shapira et al. 2023).

Four primary types of changes occur at a cellular level during neuronal remodeling—cell death, local axon/dendrite pruning, synaptic pruning, and neurite retraction. Neuronal cell death occurs in many developing nervous systems and leads to a loss of all associated synaptic connections. For example, 50% of chick ciliary ganglion cells die after they have integrated into circuits (Oppenheim 1985, Furber, Oppenheim et al. 1987). The extent of cell death varies across organisms and brain region. Still, cell death during CNS development appears across the evolutionary spectrum, including in organisms that can actively regenerate their nervous systems, such as flatworms (Hughes

1961, Simpson 1977, Stuart, Blair et al. 1987, Truman, Thorn et al. 1992, Marois and Carew 1997, Thomaidou, Mione et al. 1997, Hwang, Kobayashi et al. 2004, Thompson 2011, Toyoshima, Sekiguchi et al. 2012, Yamaguchi and Miura 2015). Why nervous systems produce neurons that are destined to die remains unclear, but cell death represents a crucial feature of healthy nervous system development, as mutations in cell death pathways can lead to childhood cancer and severe brain malformations (Mendrysa, Ghassemifar et al. 2011). Also of note, individuals with neurodevelopmental disorders are at a higher risk of cancer. These observations may suggest a link between cell death regulation and normal neurodevelopment (Nussinov, Tsai et al. 2022, Stephenson, Costain et al. 2022). Finally, normal cell death mechanisms in development may be maladaptive in disease. Neuronal cell death is a hallmark of neurodegenerative diseases like Alzheimer's Disease (AD) (Serrano-Pozo, Frosch et al. 2011). Whether neuronal death in disease results from inappropriate activation of the developmental cell death pathways remains unclear, but a deeper understanding of cell death mechanisms that drive developmental neuronal cell death could answer this question.

While cell death causes the loss of all synaptic connections, other types of remodeling events, such as local pruning of neurites, synaptic pruning, and axonal/synaptic retraction, eliminate only a subset of synapses on an individual neuron. Such remodeling events enable neurons to correct errors in axon pathfinding or selectively eliminate superfluous synaptic connections. Local neurite pruning, synaptic pruning, and retraction events each have unique cell biology. Local neurite pruning occurs when a neurite physically breaks, often near a branch point, and then fragments

and degenerates, leading to the loss of all synapses on the arbor (Luo and O'Leary 2005). Synaptic pruning entails the removal of specific synapses through phagocytosis while leaving the parent branch intact. Finally, axonal or synaptic retraction occurs when the structure retracts and is reabsorbed into the parent arbor (Luo and O'Leary 2005). Retraction has been beautifully imaged in the barrel cortex and tongue. Interestingly, axons shorter than $\sim 200 \mu\text{m}$ retract, but pruning of longer projections causes arbor fragmentation and subsequent clearance by surrounding glia (Portera-Cailliau, Weimer et al. 2005, Nakazawa, Mizuno et al. 2018, Whiddon, Marshall et al. 2023). Local neurite pruning has been well studied in *Drosophila* mushroom body (MB) γ neurons. In these cells, dorsal and medial axon projections of the larval (MB) γ neurons physically separate from the parent arbor at the same branch point, fragment, and are ultimately engulfed by surrounding glia (Watts, Hoopfer et al. 2003, Whiddon, Marshall et al. 2023). Intrinsic cues, neuronal activity, and cues from surrounding cells like glia can drive retraction, local neurite pruning, and synapse elimination, but how populations of neurons respond to activity and cues, and how those stimuli then selectively trigger any of the remodeling mechanisms, has been difficult to untangle (Stevens, Allen et al. 2007, Schafer, Lehrman et al. 2012, Turrigiano 2012).

The broad evolutionary conservation of neuronal remodeling argues for its importance in circuit refinement. In addition, dysregulation of neuronal remodeling likely underlies human neurodevelopmental disorders such as autism spectrum disorders and schizophrenia (Tang, Gudsnuik et al. 2014). Schizophrenia has been attributed to developmental neurite over-pruning since the 1980s (Feinberg 1982), an idea supported

by recent genetic studies that have linked schizophrenia to proteins involved in pruning (Sekar, Bialas et al. 2016). Increased synaptic pruning has also been correlated with cognitive decline in AD (Terry, Masliah et al. 1991).

Is adult activity-dependent plasticity at synapses the same as that which occurs during development? Adult activity-dependent plasticity entails significant changes in dendritic spines, which appears morphologically similar to synaptic pruning or retraction. However, I will use the term developmental neuronal remodeling to refer to physical changes in neurons that result in changed neural connectivity during development. Generally, these are large scale changes that reshape the circuit wiring diagram (Shatz 1990, Stevens, Allen et al. 2007, Dorothy, Emily et al. 2012). In contrast, activity-dependent plasticity, which can happen during development and in adults, drives more subtle changes in circuits by modifying existing synapses to dynamically change a circuit output (Ganguly and Poo 2013). For instance, adult memory formation entails long-lasting changes in the physical structure of spines and their synapses, encoding some aspects of memory (Leuner and Shors 2004). Likewise, homeostatic plasticity leads to changes in neurons or circuits that stabilize activity around a given set-point (Turrigiano 2012). Despite the differences between these processes and developmental neuronal remodeling, studies of developmental neuronal remodeling may identify cellular mechanisms used in activity-dependent and homeostatic plasticity.

1.2 Neuronal mechanisms that drive developmental remodeling

Changes in neural circuits during developmental neuronal remodeling entail a conversation between neurons and glia. During development, neurons display extracellular signals, possibly to indicate that they are competent for pruning. Glia respond to these cues, and then likely help neurons execute their appropriate remodeling events. Here I discuss examples of neuron intrinsic mechanisms used to drive cell death and local pruning, and in the next section I will discuss how glia participate in the process.

In vitro cultured dorsal root ganglion sensory neurons die upon nerve growth factor (NGF) withdrawal leading to degeneration of axons and apoptosis of cell bodies (Levi 1942, Levi-Montalcini 1987). These *in vitro* experiments likely recapitulate DRG neuron development *in vivo*; DRG axons compete for space on NGF-expressing tissues in the periphery. Those that fail to wire and do not receive the pro-survival signal NGF undergo apoptosis (Kalcheim, Barde et al. 1987, Levi-Montalcini 1987, Lin, Ro et al. 2011). This mechanism enables the appropriate matching of DRG number to the amount of target tissue, which can vary along the anteroposterior axis. In the presence of NGF, TrkA receptors on DRG neurons signal via Akt to promote cell survival (Molliver and Snider 1997, Kiris, Wang et al. 2014). NGF withdrawal stops this pro-survival signaling and a retrograde signaling cascade initiates neuron death (Xu, Das et al. 2011). Part of this mechanism entails the c-Jun-dependent activation of Puma, which inhibits the expression of the anti-apoptotic factors Bcl-w and Bcl-xl, to enable cell death (Simon, Pitts et al. 2016)

In other populations, neurons use intrinsic mechanisms to drive selecting refinement of over-wired circuits via axon or dendrite pruning. In the cerebellum, inferior olive neuron climbing fibers over-innervate multiple Purkinje cells during development. Throughout development, the connection between a climbing fiber and a single Purkinje cell strengthens while all other Purkinje cell/climbing fiber connections are eliminated (Sugihara 2006). Disrupting this circuit's development leads to motor coordination loss in mice (Wilson, Schalek et al. 2019). The initial over-innervation of climbing fibers allows for full coverage of the Purkinje cells, and signaling from Purkinje cells to climbing fibers drives the pruning of unneeded connections (Wilson, Schalek et al. 2019). Purkinje cells release brain derived neurotrophic factor (BDNF) onto the unnecessary climbing fibers which binds to TrkB—a neurotrophin receptor displayed by climbing fibers—and drives the destruction of the climbing fibers, acting as a punishment signal that eliminates selective climbing fibers but does not induce whole cell death (Choo, Miyazaki et al. 2017, Wilson, Schalek et al. 2019).

The dorsal Lateral Geniculate Nucleus (dLGN) acts as a relay point in processing visual information and undergoes significant activity-dependent refinement of synaptic connectivity during development. Briefly, retinal ganglion cells (RGCs) project to the dLGN onto a post synaptic target which sends information to the visual cortex. Initially inputs from RGCs intermingle, but during development they separate into clearly defined layers (Shatz 1990, Corriveau, Huh et al. 1998, Penn, Riquelme et al. 1998). Axons that are targeted to the incorrect layer express MHC Class I molecules and C1q, and these proteins tag the axons, and perhaps individual synapses for removal (Corriveau, Huh et

al. 1998, Huh, Boulanger et al. 2000, Stevens, Allen et al. 2007, Dorothy, Emily et al. 2012, Lee, Brott et al. 2014). Knock out of either of these molecules leads to incorrect segregation of layers in the dLGN and extra, functional synapses (Stevens, Allen et al. 2007, Lee, Brott et al. 2014).

1.3 Glia cells can regulate apoptotic death in neurons

Neuron autonomous mechanisms may drive some death, but glia cells can also dictate or assist neurons in carrying out cell death. For example, in the cerebellum, in addition to climbing fiber refinement, a subset of Purkinje cells die early in development (Ghoumari, Wehrlé et al. 2000). Microglia localize to the dying Purkinje cells prior to their death, which raises the question of whether microglia simply clear dead cells or if they actively help Purkinje cells to carry out apoptosis (Marín-Teva, Dusart et al. 2004). Many Purkinje cells in the developing cerebellum become positive for low levels of activated Caspase-3, which drives a cell towards apoptosis. Microglia are recruited to these cells and release superoxides onto them. When the neurons detect the superoxides they die and are ultimately engulfed by microglia. These observations imply that some Purkinje cells initiate a death program, but that cells must receive the microglial-derived signal to undergo apoptosis. Indeed, inhibition of microglial superoxide signaling resulted in about the same number of Purkinje cells upregulating low levels Caspase-3, however, in the absence of microglial superoxide signaling, Purkinje cells then down regulate caspase activity and ultimately survive (Lang and Bishop 1993, Marín-Teva, Dusart et al. 2004). This suggests a role for microglia in “assisted suicide” of some Purkinje neurons.

Other systems have offered insight into the diversity of mechanisms that microglia can use to drive cell death. In the developing retina, microglia migrate into the tissue and release nerve growth factor (NGF) that, when detected by the p75 neurotrophin receptor on retinal neurons, induces a wave of cell death (Frade and Barde 1998). This suggests that in addition to directly driving cell death through caspase signaling, microglia can selectively initiate death through releasing trophic factors. Conversely, in other areas of the brain, microglia are needed to promote neuronal survival directly via the secretion of trophic factors like IGF1 (Ueno, Fujita et al. 2013). Why would certain neurons in specific regions need microglia to carry out cell death while other neurons in other regions need microglia to promote survival? Likely, the neurons are intrinsically programmed to respond to specific microglial-derived signals and ignore others, perhaps due to neuronal sub-population specificity, specific maturation time points, or brain region location.

Unlike microglia, it is unclear if astrocytes can induce or influence developmental neuronal cell death. Astrocytes induce cell death in disease and injury states through the release of long-chain fatty acids (Guttenplan, Weigel et al. 2021), and recent work has implicated astrocytes in neuronal cell death in stroke models through astrocytic control of neuronal lactate supply (Kang, Choi et al. 2023). Thus far, no evidence has emerged to suggest the astrocytic mechanisms used in injury and disease are re-engaged in development.

1.4 Neuron-glia communication in neurite pruning

Glia can shape various developing circuits through selective elimination of portions of neurons. Like cell death in the cerebellum, complex molecular conversations between neurons and glia appear to allow neurons to signal to glia to drive pruning of axons or dendrites. In the dLGN, glia are critical for the recognition of RGC axons that are going to be pruned. As discussed, neurons display MHC Class I molecules and C1q. Glia can recognize C1q or MHC class-1 proteins and prune axons (Stevens, Allen et al. 2007, Tremblay, Lowery et al. 2010, Schafer, Lehrman et al. 2012, Sipe, Lowery et al. 2016). Microglia in the dLGN express CD94/NKG2C, a receptor for Qa-1, a non-canonical MHC Class I protein displayed by mistargeted RGC axons (Marin, Gutman-Wei et al. 2022). Microglia express the Complement Receptor 3 (CR3) which recognizes C1q through Complement 3 (C3), which allows microglia to recognize and eliminate RGC terminals. (Schafer, Lehrman et al. 2012). C1q can additionally be recognized by astrocytes through the MERTK and MEGF10 receptors and that recognition can lead to synaptic pruning (Schafer, Lehrman et al. 2012, Chung, Clarke et al. 2013, Iram, Ramirez-Ortiz et al. 2016). Disruption of either ligand (Qa-1, C1q, or C3) or receptor (CD94/NKG2C, CR3, MERTK, or MEGF10) results in less robust RGC terminal segregation. In the case of C1q, blocking this key glial signaling pathway led to the retention of excess functional synapses (Stevens, Allen et al. 2007). Collectively these data indicate neuron-glia communication can help actively promote developmental synapse/axon elimination.

The diversity of mechanisms engaged during pruning hinted that there was not one widely used mechanism that drove synaptic elimination throughout the developing brain. Examination of other regions of the brain revealed further molecular complexity. The barrel cortex in mouse relays information about whisker deflection. Like the dLGN, the barrel cortex is a sensory area that developmentally refines input axons into segregated somatosensory maps (Petersen 2019). Logically, it might make sense for the dLGN and barrel cortex to use the same mechanism to carry out refinement. However, the barrel cortex relies on fractalkine signaling between neurons and microglia, and complement signaling—important in the dLGN—is dispensable (Gunner, Cheadle et al. 2019).

In some brain regions the mechanisms for neuronal refinement may depend on the organism's age or developmental stage. In the hippocampus, fractalkine signaling drives developmental synapse elimination, while complement signaling seems to drive age-related synaptic loss (Paolicelli, Bolasco et al. 2011, Shi, Colodner et al. 2015, Hong, Beja-Glasser et al. 2016). Aberrant developmental neurite pruning in regions involved in neurodevelopmental disorders like schizophrenia are thought to be due to microglia dysfunction based on human gene association studies, however, the molecules that drive neurodevelopmentally necessary pruning in many areas are still unknown (Kopec, Smith et al. 2018, Mallya, Wang et al. 2019).

Much of the work on glial control of sculpting developing neuronal circuits has focused on microglia. How widely astrocytes engage specifically in neurite pruning as

part of their role in neurodevelopment—or if they use any mechanism besides the previously described MEGF10/MERTK-dependent detection of Complement signals in the visual system—remains unclear. Much of the work on understanding astrocyte and neuron communication during development has focused on how astrocytes can promote synaptogenesis or how they can fine-tune circuits through Hebbian and homeostatic plasticity instead of asking if/ how astrocytes engage in neuronal structural plasticity (Perez-Catalan, Doe et al. 2021). Work in *Drosophila* and mouse have demonstrated a role for astrocytes in phagocytic clearance of neuronal debris but have not widely implicated the cell type in actively refining circuits during development (Chung, Clarke et al. 2013, Tasdemir-Yilmaz and Freeman 2014, Lee, Kim et al. 2021).

Recently a few studies have proposed that oligodendrocyte precursor cells may participate in axon or synapse refinement during neurodevelopmental remodeling (Buchanan, Elabbady et al. 2022, Xiao, Petrucco et al. 2022). These studies provide good evidence that OPCs can internalize neurite debris and suggest that depleting OPCs during development can disrupt circuit formation but have not proposed molecular mechanisms that drive this refinement.

1.5 *Drosophila* as a model to understand neuronal remodeling

The mechanisms that drive cell death and local pruning are diverse and context-dependent. *Drosophila* offer a tractable system to precisely characterize neuronal remodeling at well-defined time points in small populations of uniquely-identifiable

neurons, and *Drosophila* genetics allow for screens and complex manipulations of molecular pathways to understand the mechanistic basis of neuronal remodeling *in vivo*. *Drosophila* have a sufficiently complex nervous system that remodels over a defined period as the animal progresses from the larval to the adult stage during metamorphosis. The restructuring of the *Drosophila* nervous system can be broken down roughly into two time periods during metamorphosis—the first 48 hours in which many cells die, neurites prune and glia clear debris, and the final 48 hours when circuits are rebuilt (Figure 1). Within the first 48 hours, cell death and neurite pruning are tightly controlled through the response of neurons, glia, and other cells to hormonal cues (Thummel 1996).

Figure 1 Neuronal remodeling in Drosophila

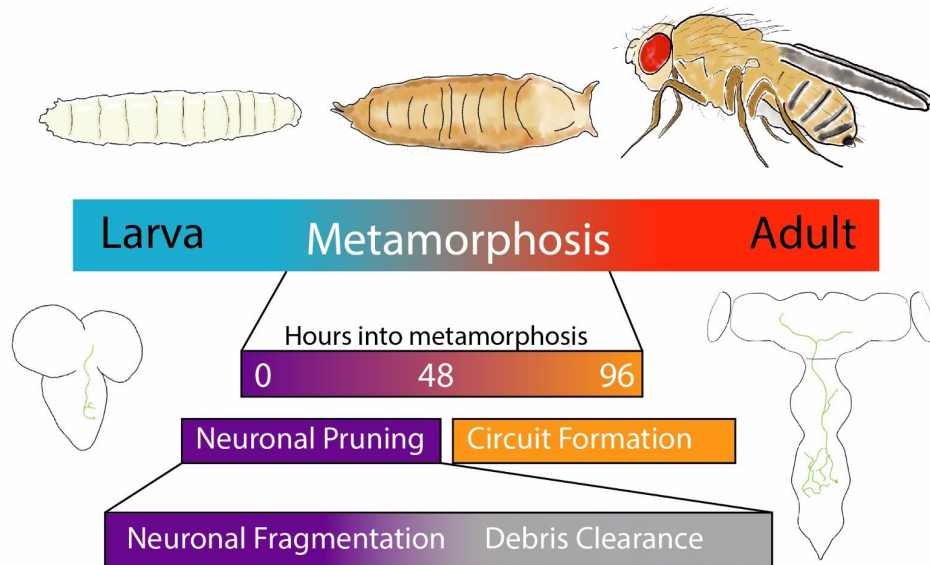


Figure 1: Timeline of neuronal development from the 3rd instar larval stage, where an animal has a fully formed juvenile nervous system, to metamorphosis, when that nervous system breaks down and reforms into the adult nervous system. Drawing of a larval and adult brain are to scale, with a single neuron sketched to demonstrate changes a neuron might undergo during this process.

Metamorphosis, a recent evolutionary innovation, allows for the precise timing of developmental transitions through broad hormonal control (Truman and Riddiford 2019). Although many animals do not undergo metamorphosis, many use steroid-mediated timing mechanisms to drive neurodevelopment. For example, thyroid hormones drive normal human brain development, and disruption of thyroid hormonal signaling can cause neurological impairment (Friesema, Jansen et al. 2006). Microglia and astrocytes express Nuclear Receptor Subfamily 1 group H member 2 (NR1H2)—a homolog to the *Drosophila* hormone receptor *EcR*— and conditional knockout of the gene in rodents leads to anxiety behavior (Friesema, Jansen et al. 2006, Pathak and Sriram 2023). The homolog of *usp* (another *Drosophila* hormone receptor), Retinoid X Receptor Alpha (RXRA), belongs to a larger protein family, the retinoic acid receptors that are critical for precisely timing cell death in the mammalian brain, and disruptions of retinoic acid signaling in humans have been linked to schizophrenia (Schug, Berry et al. 2007, Reay and Cairns 2020). A better understanding of how hormonal signaling drives neuronal remodeling in *Drosophila* may also inform our understanding of how orthologous processes work in mammals

In insects, the steroid hormone 20-hydroxyecdysone drives all neuronal remodeling events studied thus far. Immediately before the onset of metamorphosis, there is a pulse of the steroid hormone 20-hydroxyecdysone, (which I will herein call ecdysone), which binds to a heterodimeric complex of Ecdysone Receptor (EcR) and Ultraspiracle (Usp) (Lee, Marticke et al. 2000). Disrupting this binding event in neurons

that typically undergo pruning, causes a failure to prune (Lee, Marticke et al. 2000). Disruption of this binding in cells that normally undergo cell death leads to cell survival (Choi 2006). Ecdysone/receptor binding that drives neuronal remodeling depends on the B isoforms of the ecdysone receptor (EcR-B1 and EcR-B2) which can active downstream pathways that drive cell death or neurite pruning (Figure 2) (Schubiger, Wade et al. 1998, Lee, Marticke et al. 2000).

Figure 2 Ecdysone signaling in Drosophila metamorphosis

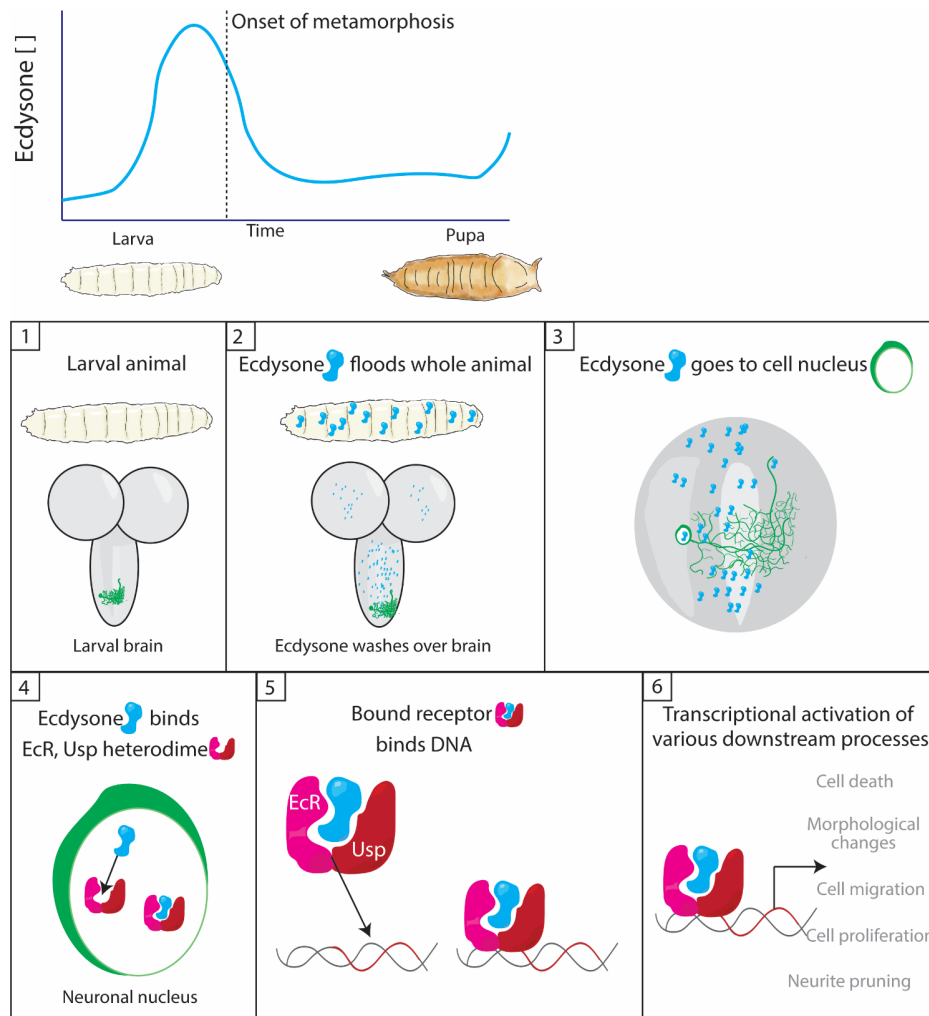


Figure 2: Illustration of the steps of ecdysone hormone/ receptor binding at the onset of metamorphosis that initiates cell death, local neurite pruning and many other physiological processes.

1.6 Cell death during *Drosophila* metamorphosis

All characterized neuronal cell death events during metamorphosis use caspase driven apoptosis and depend on EcR-B1 mediated ecdysone signaling (Figure 3) (Hara, Hirai et al. 2013, Lee, Sehgal et al. 2019).

Figure 3 Ecdysone-driven, caspase-mediated apoptosis

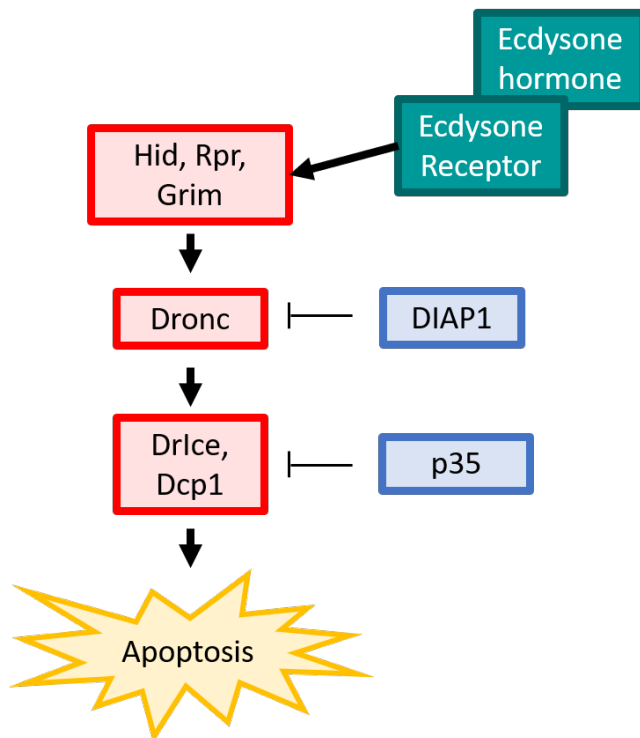


Figure 3: Simplified schematic of ecdysone driven, caspase mediated cell death during neuronal death in metamorphosis. Briefly, ecdysone binds the ecdysone receptor, activating the caspase pathway (red) which eventually leads to neuronal apoptosis. The caspase pathway can be

repressed through either endogenous proteins like DIAP1 or exogenous proteins like P35 (both in blue).

Peptidergic Corazonin (Crz) containing neurons in the *Drosophila* larvae provide a model for studying neuronal cell death in metamorphosis. The *Crz-Gal4* driver labels 16 Corazonin containing neurons in the ventral nerve chord and 6 neurons in the brain lobes (Choi, Lee et al. 2005, Choi 2006). In the first 6-8 hours of metamorphosis all 16 neurons in the VNC (vCrz neurons) die and are cleared by glia (Choi 2006, Tasdemir-Yilmaz and Freeman 2014). This cell death depends on activation of caspases *grim* and *reaper*, initiated by the EcR/ecdysone binding event (Choi 2006, Lee, Wang et al. 2011, Lee, Sehgal et al. 2013, Lee, Sehgal et al. 2019, Wang, Lee et al. 2019). The bound EcR-B1/Usp heterodimer can directly bind the promoter for *Drosophila* caspase *dronc* in other tissues like the salivary glands (Cakouros, Daish et al. 2004). Direct binding of bound EcR-B1/Usp to promoters for other molecules in the caspase pathway could also drive caspase activation in the vCrz neurons. vCrz cell death can be blocked through expression of *Crz-Gal4* driven expression of either a dominant negative version of EcR-B1 or P35, a baculoviral caspase inhibitor (Hay, Wolff et al. 1994, Choi 2006). Blocking cell death has also been reported to also save all neurites on the vCrz neurons, suggesting that in cells that die, death and pruning are executed through the same mechanism.

In addition to vCrz neurons, RP2 motor neurons in the CNS and several classes of dendritic arborization neurons in the PNS die during metamorphosis and depend on ecdysone signaling to initiate caspase induced cell death. dHb9 motoneurons die during metamorphosis as well, but the mechanisms of that elimination are unknown (Table 1)

(Banerjee, Toral et al. 2016). Notably, the timing of cell death differs between populations, suggesting that other molecules probably regulate the execution of cell death.

Anti-apoptotic dIAP proteins do not block vCrz or RP2 neuron death, although work in other tissues has suggested that these proteins can block *grim* and *reaper* induced apoptosis. This seemingly contradictory data demonstrates the complexity of cell death, and neuronal cell death at the onset of metamorphosis could be mediated by neuron specific mechanisms (Truman and Riddiford 2023). Understanding what causes differential timing in cell death, how different caspase molecules interact to drive death, and what other molecules may dictate survival or death during metamorphosis may inform our understanding more broadly of how neuronal death in the developing nervous system.

Table 1 Neurons that die during metamorphosis

Neuron name	Neuron description	Time of cell death	EcR isoform	Caspases involved
Corazonin neurons	Sixteen neurons (8/side) in the VNC undergo cell death. Six neurons in the brain lobes (3/side) survive (Choi, Lee et al. 2005).	6-8 hours after puparium formation (APF) (Choi, Lee et al. 2005)	EcR-B (Wang, Lee et al. 2019)	Grim, Reaper, Sickle (Choi, Lee et al. 2006) Dronc, drICE, Dcp-1 (Lee, Sehgal et al. 2013)
RP2 motoneurons	1 per hemisegment (Sink and Whittington 1991). Neurons in A2-A7 undergo cell death during metamorphosis (Winbush and Weeks 2011)	15-20 APF (Winbush and Weeks 2011)	EcR-B (Winbush and Weeks 2011)	Dark, Dronc, Reaper (Winbush and Weeks 2011)
dHb9 expressing Motoneurons	Motoneurons that innervate larval abdominal muscles, some die during metamorphosis, and some survive to adulthood and target adult muscles (Banerjee, Toral et al. 2016)	Two waves. First wave between 0-20APF (Banerjee, Toral et al. 2016)	N/A	N/A
ddaB class II da, ddaF, and ddaA C3da neurons	PNS neurons in the larval wall. Different classes sense different stimuli (Kanamori, Togashi et al. 2015)	Neurites degenerate around 3-4APF, cell death by 10APF (Williams and Truman 2005)	EcR-B (Williams and Truman 2005)	Caspase-dependent (blocked by P35) (Williams and Truman 2005)

1.7 Local neurite pruning during *Drosophila* metamorphosis

Hormonal ecdysone signaling also activates neuronal pruning during metamorphosis. The MB γ neurons, located in the brain lobes and involved in olfactory learning and memory, undergo stereotyped remodeling during the first eighteen hours of metamorphosis

(Heisenberg 1998). MB γ dendrites are entirely eliminated within the first six hours of metamorphosis and medially- and dorsally-projecting axons are pruned by 18 hours (Watts, Hoopfer et al. 2003). MB γ axons then regenerate to form the adult neuronal branching pattern (Yaniv, Issman-Zecharya et al. 2012). MB γ dendrite pruning can be blocked by inhibiting ecdysone signaling or inhibiting the ubiquitin-proteasome system (Lee, Marticke et al. 2000, Watts, Hoopfer et al. 2003). Inhibition of either of these pathways can also block MB γ axon pruning (Lee, Marticke et al. 2000, Watts, Hoopfer et al. 2003).

Regulation of *EcR* transcription can influence ecdysone induced neurite pruning, as transcriptional repression of *EcR* stops all downstream pathways. Nuclear receptor *Hr39* works to repress *EcR*-B1 transcription in MB γ , and homologous nuclear receptor *ftz-f1* can relieve *Hr39* repression (Boulanger, Clouet-Redt et al. 2011). MicroRNA induced posttranscriptional modifications and epigenetic methylation can further regulate *EcR* protein expression levels and influence hormone signaling (Lai, Chu et al. 2016, Latcheva, Viveiros et al. 2019).

Downstream of ecdysone signaling, cell adhesion and the endo-lysosome pathway contribute to MB γ axon pruning. MB γ are a highly fasciculated structure with many axons projecting together in close proximity. During development the axons bundle are kept in a tight configuration by a NCAM1 homolog, transmembrane protein, FasII. At the onset of metamorphosis the JNK pathway facilitates the degradation of FasII (Bornstein, Zahavi et al. 2015). Degradation of FasII causes the axons to lose cell adhesion and fall apart or become more sensitive to other mechanisms that induce fragmentation

(Bornstein, Zahavi et al. 2015) In MB γ dendrites FasII is dispensable for pruning, suggesting that different neuronal compartments could execute pruning differently in some instances (Bornstein, Zahavi et al. 2015). The transmembrane protein Patched (Ptc) somehow inhibits both axon and dendrite pruning (Issman-Zecharya and Schuldiner 2014). Interestingly, mammalian astrocytes and a subset of cortical neurons express the Ptc homolog PTCH1 during development and PTCH1 participates in cortical synaptic development (Xie, Kuan et al. 2022).

Dendritic arborization sensory neurons in the PNS have provided a useful model for uncovering mechanisms of dendritic pruning during metamorphosis. Class IV ddaC neurons in the larval body wall prune their larval dendrites but leave their cell bodies and axons intact, and regrow adult-specific dendrites that infiltrate the body wall (Kuo, Jan et al. 2005, Williams and Truman 2005). Excellent genetic tools and simple morphology have made them an attractive model for studying dendritic pruning. A few hours into metamorphosis dendrites that are proximal to the soma display transient calcium activity and then fragment due to microtubule severing (Williams and Truman 2005, Lee, Jan et al. 2009, Kanamori, Kanai et al. 2013). The initial calcium transients and the pathways that initiate microtubule destruction are regulated by ecdysone signaling (Kuo, Jan et al. 2005, Williams and Truman 2005, Kanamori, Kanai et al. 2013). To execute microtubule severing, bound EcR-B1 activates transcription factor Sox14 which can then bind the promoter for *mical*, inducing expression of this microtubule severing enzyme, leading to microtubule destruction (Kirilly, Gu et al. 2009). Other classes of dendritic arborization neurons undergo cell death, through EcR-B1 activation of Sox-14 which then drives cell

death instead of neurite pruning (Osterloh and Freeman 2009). Interestingly, ddaC neurons use caspase signaling for dendrite pruning. Caspase activation is spatially restricted to ddaC dendrites, likely through targeted degradation of caspase inhibitor DIAP1 dendrites (Rumpf, Lee et al. 2011). Despite its key role in dendrite pruning, caspase activation does not appear to be needed for MB γ axon pruning (Watts, Hoopfer et al. 2003).

Two other populations, CCAP and Tv neurons, also prune during metamorphosis but have been technically challenging to study (Table 2). Tv neurons still undergo pruning—although less than normal—when dominant-negative versions of EcR are genetically expressed (Brown, Cherbas et al. 2006), suggesting that there may be hormone-independent mechanisms of remodeling that are used by some but not all neurons, and also highlighting the need to study a diverse population of neurons to more fully characterize remodeling.

Table 2 Neurons that undergo neurite pruning during metamorphosis

Neuron name	Neuron description	Time of remodeling	EcR isoform	Mechanisms involved
ddaC C4da, ddaD/ddaE C1da	Sensory neurons in the larval body wall undergo dendritic pruning (Kuo, Jan et al. 2005)	Most dendrites are severed from the cell body by 10APF and then degenerate over the next 10 hours (Kuo, Jan et al. 2005)	EcR-B1 (Kuo, Jan et al. 2005)	Extracellular Mmp and ubiquitination for dendrite severing (Kuo, Jan et al. 2005) Caspase block does not block dendrite severing (Kuo, Jan et al. 2005) Actin disassembly (Kirilly, Gu et al. 2009) Endocytosis (Zhang, Wang et al. 2014) Ca ⁺⁺ transients (Kanamori, Togashi et al. 2015) Epigenetic repression of Hox genes (Bu, Lau et al. 2023) Mechanical severing (Krämer, Wolterhoff et al. 2023)
Mushroom body	Involved in olfactory learning and memory	4 APF- dendrite fragmentation 8 APF- axon fragmentation (Lee and Luo 1999)	EcR-B (Lee, Marticke et al. 2000)	Ubiquitin-proteasome (Watts, Hoopfer et al. 2003) Cell adhesion initiated by the JNK pathway (Bornstein, Zahavi et al. 2015) mircoRNA-34 regulation of EcR (Lai, Chu et al. 2016) TGFβ signaling (Yu, Gutman et al. 2013) PI3K-lysosome pathway (Issman-Zecharya and Schuldiner 2014) GABA-dependent activity silencing (Mayselless, Shapira et al. 2023)
CCAP neurons	Involved in pupal development and maturation. In addition to pruning some neurons also migrate (Luan, Lemon et al. 2006, Zhao, Gu et al. 2008)	3-12 APF (Zhao, Gu et al. 2008)	NA	Difficult to study as CCAP neurons are involved in initiating ecdysis
TV neurosecretory cells	Paired neurosecretory cells make up the neurohemal organ (Brown, Cherbas et al. 2006)	Dendrite 5-6APF Axon 10APF (Brown, Cherbas et al. 2006)	EcR-B But notably still see some pruning when EcR is blocked (Brown, Cherbas et al. 2006)	NA

The aforementioned studies focus on either axon or dendrite pruning but do not make specific mention of synapses. Electron microscopy and IHC for synaptic markers throughout metamorphosis has shown that synapses are largely gone by 18-48 hours into metamorphosis indicating they are eliminated extensively (Muthukumar, Stork et al. 2014, Tasdemir-Yilmaz and Freeman 2014). Whether any neurons retain synapses or the mechanisms by which synapses are removed from neurites that do not prune are unstudied and would be an exciting area for future research.

1.8 Glia in *Drosophila* neuronal remodeling

Like in other organisms, glia participate in remodeling the *Drosophila* nervous system. During metamorphosis cortex glia and astrocytes engulf dead cell bodies and neuronal debris, respectively, using a Draper (a cell surface receptor homologous to mammalian MEGF10) dependent mechanism (Tasdemir-Yilmaz and Freeman 2014). Fly glia are crucial for remodeling from the very initiation of the process. Just prior to metamorphosis, glia release a TGF β ligand Myoglianin, which binds extracellularly on neurons to IgSF receptor Plum and TGF β receptor Babo. That binding induces *EcR* transcription, which makes neurons competent to respond to ecdysone and initiate various remodeling programs (Awasaki, Huang et al. 2011, Yu, Gutman et al. 2013, Hakim, Yaniv et al. 2014). This seems to be a broad timing mechanism used to control *EcR* protein production levels across the entire *Drosophila* nervous system at the onset of metamorphosis rather than providing instructions to neurons about how to remodel.

Recently, a screen in MB γ to discover molecules that drive neuronal remodeling identified a new, neuronally secreted molecule, Orion, that may signal to astrocytes during pruning (Boulanger, Thinat et al. 2021). Orion bears similarity to a CxC3 protein, which facilitates synaptic pruning in mammals (Paolicelli, Bisht et al. 2014, Arnoux and Audinat 2015, Werneburg, Feinberg et al. 2017). Astrocytes typically infiltrate into the MB γ axon bundle at the beginning of metamorphosis, but neuronal Orion depletion leads to an infiltration failure. This lack of infiltration coincides with failed axon pruning and debris clearance. The current model suggest that neurons secrete Orion as a “find me” cue, astrocytes and potentially cortex glia, sense that cue, and infiltrate an area to execute remodeling (Boulanger, Thinat et al. 2021, Perron, Carme et al. 2023). The astrocytic receptor of Orion has yet to be identified but an obvious candidate would be Draper. Whether glial Draper senses neuronally secreted Orion in the MB γ neurons has yet to be studied. In the PNS in ddaC neurons, Orion has been proposed to act as a bridging molecule between neuronally expressed phosphatidylserine and glial Draper to enable the engulfment of neuronal debris (Ji, Wang et al. 2023). Orion and Draper have clear roles in multiple context where glial cells engulf neuronal debris, but whether *Drosophila* glia can actively participate in driving neuronal death or fragmentation remains unknown (Doherty, Logan et al. 2009, Tung, Nagaosa et al. 2013, Hakim, Yaniv et al. 2014, Tasdemir-Yilmaz and Freeman 2014, Alyagor, Berkun et al. 2018, Boulanger, Thinat et al. 2021, Ji, Wang et al. 2023).

1.9 Thesis Overview

In this thesis, I will describe how I identified new cell types in *Drosophila* that undergo neuronal remodeling, and then studied the mechanisms by which they execute remodeling programs. I focus primarily on the Beat-Va neurons, which are composed of two subtypes and undergo cell death (Beat-Va_L) or local pruning (Beat-Va_M). I show that regionally specific Hox gene expression drives apoptotic cell death in Beat-Va_L neurons. I will also describe how, using tools to gain single-cell morphological resolution of complex neurons, I discovered that Beat-Va_M neurons undergo local neurite pruning. By exploring the biology of Beat-Va_M neurons during metamorphosis, I show ecdysone-mediated transformation of astrocytes into phagocytes drives Beat-Va_M neuron remodeling in the first six hours of metamorphosis. We used TRAP-Seq experiments to identify actively translated genes during astrocyte transformation. I then screened those molecules by knocking them down in astrocytes and evaluating Beat-Va_M neurite remodeling. This allowed us understand how astrocyte transformation influences neurite fragmentation and clearance. By screening through genes from the TRAP-Seq experiment, I identified multiple genes that were important for either neurite fragmentation or clearance and found that early steps in astrocyte transformation likely drive neurite fragmentation

Chapter 2 Beat-Va neurons reveal mechanisms driving segment-dependent cell death and astrocyte-dependent neurite pruning

This work was started by Amy Sheehan who did much of the initial screening to identify new populations of neurons from the FlyLight website and then validated interesting lines in our laboratory. It was a massive effort and I'm incredibly grateful for the work that she did. Yunsik Kang, Amanda Jefferson Kang, and Ya-Chen Cheng continued this validation process and further narrowed the scope of the study by testing known regulators of remodeling. Yunsik and Amanda also collected the animals for the translomics I present here and prepared that data in collaboration with Paul Meraner. Leire Abalde-Atristain assisted with the astrocyte screen that I will present. Madie Hupp carried out some of the Abd-A and Abd-B experiments when she worked with me as a rotation student. I would also like to acknowledge Adele Avetisyan for suggesting that I examine the role of Hox genes like Abd-A and Abd-B after I talked about the patterning of cell death in a lab meeting. All figures are at the end of the results section.

This chapter is adapted from:

Astrocyte-dependent local neurite pruning and Hox gene-mediated cell death in Beat-Va neurons

Katherine S Lehmann, Madison T Hupp, Amanda Jefferson, Ya-Chen Cheng, Amy E Sheehan, Yunsik Kang*, Marc Freeman*

2.1 Introduction

During development, the nervous system is initially populated by too many neurons that form an excessive number of synaptic connections. This neural circuitry is subsequently refined through the elimination of exuberant synapses (Stevens, Allen et al. 2007), neurites (Williams and Truman 2005, Stanfield, O'Leary et al. 1982), or entire neurons (Karcavich and Doe 2005), often in response to activity-dependent signaling mechanisms. While neuronal remodeling occurs in all complex metazoans and provides a mechanism for optimization of neuronal numbers and neural circuit connectivity, aberrant neuronal remodeling is associated with neurological conditions like autism spectrum disorders, schizophrenia and epilepsy (Atz, Rollins et al. 2007, Feinberg 1982, Ishizuka, Fujita et al. 2017, Neniskyte and Gross 2017, Sekar, Bialas et al. 2016, Selemon, Rajkowska et al. 1995, Selemon, Rajkowska et al. 1998, Winchester, Ohzeki et al. 2012, Dorothy, Emily et al. 2012).

How much neuronal remodeling occurs across the mammalian nervous system remains unclear, but it is thought to be extensive and has profound effects on the final wiring diagram (Luo and O'Leary 2005, Neukomm and Freeman 2014, Riccomagno and Kolodkin 2015). Rewiring primarily occurs through changes in the number of neurons, or the pruning of parts of neurons. Axonal and synaptic connectivity can be radically altered through local pruning of axons or individual synaptic connections. For instance, retinal ganglion cells (RGCs) initially project axons to the dorsal lateral geniculate nucleus (dLGN) of the thalamus and form an excessive number of synapses on target cells, but later these are refined and exuberant RGC axons and synapses are eliminated (Dorothy,

Emily et al. 2012, Stevens, Allen et al. 2007). Large-scale changes in circuit wiring can also be driven by selective cell death (Hutchins and Barger 1998, Oppenheim 1985). 40% of mouse GABAergic inhibitory neurons in the developing postnatal cortex are culled by a wave of caspase-driven cell death in the first 20 days of life (Southwell, Paredes et al. 2012). Many of these changes occur long after the neurons have integrated into neural circuits and fired for weeks. Precisely how specific neurons are selected for elimination remains unclear.

Glial cells help sculpt developing neural circuits through participating in the selective elimination of neurites, synapses, or entire neurons, although the mechanisms by which this happens remain poorly defined. In the dLGN, C1q is believed to opsonize synapses that are destined for removal, and C1q bound synapses are then recognized and phagocytosed by complement receptor 3 (CR3)-bearing microglia (Schafer et al., 2012). Astrocytes can also contribute via the MERTK and MEGF10 receptors (Chung et al., 2013). Disruption of C1q signaling leads to less robust RGC terminal segregation and the retention of excess functional synapses (Stevens, Allen et al. 2007), arguing that glia somehow play a role in promoting the final execution of synapse/axon elimination. Interestingly, C1q is not required in all brain areas that undergo developmental neural refinement. In the mouse barrel cortex, innervating axons are extensively refined into segregated somatosensory maps (Petersen 2019). In this context, however, refinement relies on fractalkine signaling between neurons and microglia, and C1q signaling is dispensable (Gunner, Cheadle et al. 2019). Finally, phagocytic cells can actively drive cells toward final execution of cell death. In developing *C. elegans*, cell death requires

both cell intrinsic initiation of apoptotic pathways, and signals from the engulfing hypodermal cells, with engulfing hypodermal cells signaling to partially dead cells to help execute apoptosis (Hoepfner, Hengartner et al. 2001, Reddien, Cameron et al. 2001). While not widely explored in the mammalian brain, similar roles for microglia have been identified in promoting the final execution of cell death in a subset of developing Purkinje neurons (Marín-Teva, Dusart et al. 2004).

Drosophila has served as an excellent system in which to explore the molecular basis of neuronal remodeling events in vivo (Lee, Lee et al. 1999, Lee, Marticke et al. 2000, Choi 2006, Watts, Hoopfer et al. 2003, Kirilly, Gu et al. 2009, Zhang, Wang et al. 2014, Williams and Truman 2005). At pupariation, a burst of the steroid hormone 20-hydroxyecdysone (ecdysone) drives activation of neuronal remodeling programs across the nervous system, most of which are executed during the first 12-18 hours of metamorphosis (Truman, Talbot et al. 1994, Schubiger, Wade et al. 1998, Schubiger, Tomita et al. 2003). Ecdysone binds to the Ecdysone Receptor (EcR) nuclear hormone receptor and this event acts as a timing mechanism to coordinate the initiation of animal-wide metamorphic changes (Thummel 1996, Talbot, Swyryd et al. 1993, Riddiford and Truman 1993, Koelle, Talbot et al. 1991, Pinto-Teixeira, Konstantinides et al.). Cell-autonomous blockade of EcR signaling appears to inhibit all known neuronal cell death and local pruning events in the *Drosophila* nervous system (Yamaguchi and Miura 2015, Choi 2006, Schubiger, Wade et al. 1998, Marchetti and Tavosanis 2017, Hara, Hirai et al. 2013, Winbush and Weeks 2011, Kuo, Jan et al. 2005, Schubiger, Tomita et al. 2003). For instance, in the first 6-8 hours of metamorphosis in the central nervous system

(CNS), Corazonin neurons in the ventral nerve cord (VNC) activate apoptotic death through EcR (Choi 2006, Lee, Sehgal et al. 2013, Lee, Sehgal et al. 2019, Lee, Wang et al. 2011, Wang, Lee et al. 2019). Likewise, mushroom body (MB) γ neurons, located in the brain lobes and involved in olfactory learning and memory, undergo stereotyped axonal and dendritic pruning (Heisenberg 1998) that can be blocked by inhibiting EcR (Lee, Marticke et al. 2000, Watts, Hoopfer et al. 2003). To our knowledge, neuronal cell types that undergo developmental remodeling independently of EcR have not been identified.

Like their mammalian counterparts, *Drosophila* glial cells play a crucial role in neuronal remodeling. First, most remodeling events occur by the initial release of the Transforming Growth Factor- β (TGF β) family member Myoglianin from glia, which activates expression of EcR via TGF β receptors on target neurons, thereby establishing their competence to prune upon receipt of steroid hormonal signals (Awasaki, Huang et al. 2011, Hakim, Yaniv et al. 2014, Wang, Lee et al. 2019, Yu, Gutman et al. 2013). After cell death or neurite/synapse degeneration has occurred, glial cells act as phagocytes to recognize and phagocytose neuronal debris through conserved signaling pathways like Draper/MEGF10 (MacDonald, Beach et al. 2006, Doherty, Logan et al. 2009, Hakim, Yaniv et al. 2014) or Fractalkine/Orion (Boulanger, Thinat et al. 2021, Ji, Wang et al. 2023, Perron, Carme et al. 2023). Whether there are other, novel mechanisms by which glial cells coordinate neuronal remodeling during metamorphosis is an open question.

A growing body of evidence implies that the signaling pathways engaged to drive neuronal remodeling are diverse and context-dependent and we lack a deep

understanding of the molecular basis of neuronal remodeling in any context (Schafer, Lehrman et al. 2012, Yaniv and Schuldiner 2016, Boulanger and Dura 2022). In this study, we sought to identify new neuronal subtypes that remodel in the *Drosophila* pupal nervous system, and especially those that use novel mechanisms to regulate of remodeling. We characterize two populations of neurons labeled by the *BeatVa-Gal4* driver—medial (Beat-Va_M) and lateral (Beat-Va_L) neurons—that undergo complete local neurite pruning or segment-specific apoptotic cell death, respectively. We show that local pruning in Beat-Va_M neurons can happen independently of EcR, but requires signaling from astrocytes, while segment-specific cell death of Beat-Va_L neurons is downstream of EcR and governed by spatially restricted expression of the Hox gene Abd-B. Our work establishes Beat-Va neurons as a new model to explore neuronal remodeling in vivo and identifies new mechanisms for regulation of developmental pruning and cell death in *Drosophila*.

2.2 Results

2.2.1 *Beat-Va neurons undergo cell death or local pruning during metamorphosis*

We wished to identify neuronal cell types that undergo developmental remodeling, but use genetic programs that differ from previously characterized neurons in *Drosophila*. We therefore screened ~5,500 Gal4 lines on the open source Janelia FlyLight website (Pfeiffer, Jenett et al. 2008) to identify Gal4 driver lines that were active in sparse populations of ventral nerve cord (VNC) neurons during the wandering 3rd instar larval stage (wL3), the developmental stage that directly precedes metamorphosis (Figure 4A).

From these, we selected 87 lines and validated their wL3 expression patterns by crossing each line to membrane-tethered GFP (UAS-mCD8::GFP) (Appendix G). We chose 28 lines to study further and visualized their morphologies during metamorphosis. We examined them at wL3, 6 hours after puparium formation (APF) and head eversion (HE, ~12 hrs APF), the time point by which most known cell types have completed remodeling, and 18 hrs APF (Figure 4A, Appendix H). Among all of these lines, we chose to focus on *GMR92H04-Gal4*, which appeared to label a combination of cells undergoing cell death or local pruning.

GMR92H04-Gal4 was constructed by fusing an enhancer element for the *Beat-Va* gene to the DSCP and Gal4 promoters (Jenett, Gerald et al. 2012). We refer to this line as *BeatVa-Gal4* and the neurons labeled as *Beat-Va* neurons. To define the segmental patterns of neurons labeled by the *BeatVa-Gal4* driver, we used antibody staining for the transcription factors Even-skipped (Eve) and Engrailed (En), which act as convenient landmarks for the identification of individual cells in the VNC (Manoukian and Krause 1992). We found that the *BeatVa-Gal4* driver labeled one lateral neuron (referred to as *Beat-Va_L*) and one medial neuron (referred to as *Beat-Va_M*) per hemisegment in abdominal segments A3-7 (Supplemental Figure 4A-B). This driver also weakly labeled neurons in A8 and A1-2 segments, as well as a handful of cells in the brain lobes. The total number of cells labeled by this *BeatVa-Gal4* driver decreased prior to HE in the VNC, suggesting that a subset of neurons underwent cell death during metamorphosis. In addition, the complexity of neurite projections in the synaptic neuropil decreased, indicating that some of these neurons underwent pruning. (Figure 4B-B’’).

To examine the morphology of these cells in segments A3-7, we used the MultiColorFlpOut (MCFO) approach. MCFO is based on the use of UAS-regulated expression of spaghetti monster GFP transgenes (smGFP) (Nern, Pfeiffer et al. 2015). Stochastic expression of one of four UAS-regulated versions of fluorescently-dead smGFP, each with a unique epitope tag (OLLAS, V5, HA, or Flag), is activated stochastically within the population of Gal4 expressing neurons (Viswanathan, Williams et al. 2015, Nern, Pfeiffer et al. 2015). Individual neurons are then visualized by staining for each epitope (Figure 5C). By examining single-cells, we found that at 3rd instar larval stages, Beat-Va_L cells cross the midline, project anteriorly, and terminate within the VNC. Anterior Beat-Va_L neurons in segments A3-4 persisted through HE (Figure 4C) while posterior lateral Beat-Va_L neurons in segments A5-7 underwent cell death by 6 hrs APF (Figure 4D, Figure 5D). In contrast, we found that Beat-Va_M neurons extend a dense network of fine projections through multiple segments in the synaptic neuropil, totaling >1000 μm in total length. These fine processes begin fragmenting by 6 hrs APF and are cleared from the CNS by HE (Figure 4E-G). These observations reveal that *BeatVa-Gal4* labels at least two cell types, one that undergoes apoptotic death and the other local axon pruning.

2.2.2 Local pruning in Beat-Va_M neurons is not driven by Ecdysone receptor (EcR)

In all other neuronal subtypes studied, local neurite pruning during *Drosophila* metamorphosis depends on ecdysone signaling mediated through the Ecdysone receptor B1 (EcR-B1) (Zhu, Chen et al. 2019, Yu, Gutman et al. 2013, Kuo, Jan et al. 2005, Lee,

Marticke et al. 2000). Consistent with the notion that EcR signaling also regulated Beat- V_{AM} neuron pruning, we found EcR-B1 was expressed in all Beat- V_{AM} neurons in segments A3-7 (Figure 7A). To determine whether ecdysone signaling drove Beat- V_{AM} remodeling through EcR, we used a UAS-EcR^{DN} construct to cell-autonomously block EcR signaling in all Beat-Va neurons. We found that expression of EcR^{DN} appeared to reduce the total number of cells eliminated in posterior abdominal segments but did not block the pruning of Beat- V_{AM} neurite fine processes (Figure 6A-B). To visualize individual cells more precisely, we generated single-cell clones in Beat- V_{AM} neurons and quantified neuronal complexity in wL3 stages and HE using the MCFO approach. At wL3 stages, we found no differences in Beat- V_{AM} neuron morphology and neurite complexity when we compared controls to EcR^{DN} expressing cells, regardless of the segment (A3-7), arguing that EcR^{DN} expression throughout larval stages does not alter Beat- V_{AM} neuron development (Figure 6C-H). Surprisingly, we also found that expression of EcR^{DN} did not block the local pruning of Beat- V_{AM} neurites by HE (Figure 6A-D), as measured by total neurite length or total number of branch points (Figure 6E-F).

Given that EcR signaling has been shown to be required for every other pruning event described to date, we sought to explore the possibility that EcR^{DN} could be failing to block pruning due to insufficiently high levels of endogenous EcR expression in Beat- V_{AM} neurons. We first stained for the EcR^{DN} protein and observed robust expression of EcR^{DN} in all Beat- V_{AM} neurons at 6 hrs APF when endogenous EcR levels are low (Figure 7B), suggesting we had sufficient EcR^{DN} expression. It was also possible that

EcR^{DN} might have sufficient inherent activity to induce pruning in Beat-Va_M neurons (Cherbas, Hu et al. 2003), so we sought to devise alternative strategies to block EcR signaling in Beat-Va_M neurons. Because EcR mutants are lethal at late embryonic or early larval stages and the EcR locus is proximal to FRT sites used for mosaic analysis, we used CRISPR/Cas9 technology to selectively eliminate genes required for EcR signaling in Beat-Va neurons (Meltzer, Marom et al. 2019). Briefly, we used lines that ubiquitously express guide RNAs (gRNAs) to EcR, its obligate heterodimer, ultraspiracle(usp) (Yao, Forman et al. 1993), or plum, an IgSF molecule that activates EcR transcription (Yu, Gutman et al. 2013), and then expressed UAS-Cas9 selectively in Beat-Va neurons with Beat-Va-Gal4. Targeting EcR and plum using gRNAs/Cas9 led to a significant reduction in EcR expression as expected, while targeting usp did not change EcR expression (Figure 7C-D). When we examined refinement of Beat-Va_M neurons at HE, we observed only minor preservation or regrowth of small projections in usp, EcR, and plum gRNA backgrounds. (Figure 6G-N). Together these data suggest that Beat-Va_M neurons activate local pruning in a manner that does not depend primarily on EcR, although the small preservation we see suggests EcR may have a minor role.

Finally, we used RNAi to concurrently knock down BaboA and plum, two transmembrane proteins that work together to induce EcR transcription, using UAS-driven RNAi constructs in *BeatVa-Gal4* animals (Figure 8A-D) (Zheng, Wang et al. 2003, Yu, Gutman et al. 2013, Wang, Lee et al. 2019). This strategy caused a strong depletion of EcR protein as determined by antibody stains (Figure 8E). We then assessed neuronal pruning in the BaboA/plum double knockdown condition with MFCO and

found that Beat- V_{aM} neurons continued to prune neurites (Figure 8G-K). These data, coupled with our observations using EcR^{DN} and guide RNAs/Cas9, support the notion that neurite pruning in Beat- V_{aM} neurons occurs largely independently of EcR signaling.

2.2.3 Astrocytes non-cell-autonomously regulate Beat- V_{aM} neuron pruning

Beat- V_{aM} neurite fragmentation and clearance occur during the EcR-dependent transformation of larval astrocytes into phagocytic glia (Tasdemir-Yilmaz and Freeman 2014, Kang 2023). To determine what role astrocytes might play in driving Beat- V_{aM} neuron remodeling, we generated a LexAop-EcR^{DN} line which we could drive with alm-LexA to selectively block the transformation of astrocytes into phagocytes while allowing all other EcR-mediated neuronal signaling events to proceed normally. We first confirmed that our LexA/LexAop constructs efficiently blocked astrocyte transformation into phagocytes at 6 hrs APF (Figure 9G-J). Indeed, expression of this EcR^{DN} construct in astrocytes resulted in astrocytes retaining their bushy larval morphology (Figure 9A-F) (Hakim, Yaniv et al. 2014, Tasdemir-Yilmaz and Freeman 2014). We then used the MCFO approach to examine Beat- V_{aM} neuron architecture at wL3, 6APF and HE after blocking EcR-mediated signaling selectively in astrocytes. Strikingly, we found that blockade of EcR signaling in astrocytes strongly suppressed local pruning of Beat- V_{aM} neurons at 6APF, and this suppression persisted even to HE, where we observed significantly less neurite remodeling in Beat- V_{aM} neurons (Figure 10A-F).

Given that inhibition of EcR signaling in Beat- V_{aM} neurons had a minor effect on local pruning, we reasoned that remodeling of Beat- V_{aM} neurons might be driven by a

combination of EcR signaling in Beat-V_M neurons and EcR-dependent signaling from astrocytes. To test this directly, we blocked both astrocyte and neuronal ecdysone signaling by driving a UAS-EcR^{DN} simultaneously in both astrocytes and Beat-Va neurons (using *Alrm-Gal4* and *BeatVa-Gal4*). We found that the combination of blocking astrocyte transformation and blocking neuronal ecdysone signaling led to a complete inhibition of local pruning in Beat-V_M neurons (Figure 10G-L). Together, these data, coupled with those above, indicate that local Beat-V_M neurite pruning occurs in response to EcR-dependent signaling in both Beat-V_M neurons and astrocytes, with astrocytic EcR signaling playing the primary role. Finally, we note that at wL3 stages before local pruning of Beat-V_M neurons, neurites in animals expressing astrocytic EcR^{DN} were simplified to a small degree in total neurite length and number of branch points compared to controls (Figure 10E-F, K-L). This observation argues that EcR-dependent signaling in astrocytes is important for a small fraction of Beat-V_M neurite growth during embryonic or larval stages. However, these differences are minor compared to the effects of blocking EcR signaling on neurite remodeling during metamorphosis.

2.2.4 The TGF β molecule Myoglianin activates EcR expression in astrocytes to drive Beat-V_M neuron local pruning

In previously studied *Drosophila* neuronal subtypes, glial release of the TGF β molecule Myoglianin (Myo), which signals through the two TGF β receptors BaboA and Plum, results in upregulation of EcR in neurons so they are competent to remodel in response to

ecdysone (Yu, Gutman et al. 2013, Awasaki, Huang et al. 2011). RNAi knockdown of Myo in all glia using repo-Gal4 suppresses remodeling of these neurons in the *Drosophila* CNS (Awasaki, Huang et al. 2011). To explore the possibility that astrocytic Myo might be the factor regulating Beat-V_{aM} neuron pruning, we first generated a *BeatVa-LexA* line which we used to drive LexAop-Jupiter.sfGFP, which is designed to visualize neuronal processes by labeling microtubules with GFP (Poe, Tang et al. 2017). We generated lines to both visualize Beat-Va neurons with this tool and also drive UAS-Myo^{RNAi} in glia. We confirmed the expression pattern of *BeatVa-LexA* line by comparing its overlap with *BeatVa-Gal4*, UAS-mCD8::GFP (Figure 11). When we drove expression of Myo^{RNAi} in all glia, we observed a strong suppression of Beat-V_{aM} neuron local pruning compared to controls (Figure 12A-D). However, when we drove Myo^{RNAi} only in astrocytes, it did not affect Beat-V_{aM} neuron local pruning (Figure 12I). This could indicate that Myo is supplied to Beat-V_{aM} neurons by non-astrocytic glial subtypes, but this would not explain why EcR^{DN} expression in astrocytes alone could potentially block Beat-V_{aM} neuron local pruning if Myo was a key factor. Surprisingly, when we examined astrocyte morphology in a background where Myo^{RNAi} was expressed in all glia, we found astrocytes failed to transform, but did so normally if we drove Myo^{RNAi} only in astrocytes (Figure 12F-K). Furthermore, we found that EcR-B1 staining was absent from astrocytes when Myo^{RNAi} was driven in all glia, but normal when driven in astrocytes alone (Figure 12L-O). We interpret these data to mean that non-astrocytic glial subtypes provide astrocytes with Myo to activate EcR expression, which then drives astrocyte transformation into phagocytes and enables astrocyte regulation of Beat-V_{aM}

neuron local pruning. Given that Myo knockdown in astrocytes alone did not block Beat- V_{aM} neuron local pruning, other astrocyte-derived factors likely regulate activation of Beat- V_{aM} neuron local pruning.

2.2.5 Translation profiling of astrocytes identified candidate astrocyte-derived activators of Beat- V_{aM} neuron local pruning

Identifying astrocytic molecules that were actively translated during early metamorphosis in an EcR-dependent way could allow us to identify how astrocytes signal to Beat- V_{aM} neurons to initiate local pruning. We therefore performed translating ribosome affinity purification (TRAP), followed by RNA-seq at WL3, 2 APF and 6 APF animals in two backgrounds: controls and animals expressing EcR^{DN} selectively in astrocytes. Principal component analysis (PCA)—an analysis that reveals the dimensionality of datasets and then unbiasedly clusters individual groups based on that dimensionality—revealed that control and experimental condition time points clustered together (Figure 13A). We used the R program DESeq2 to identify genes that were differentially expressed between each timepoint and conditions (Figure 13B). 231 genes that showed at least a 60% reduction in reads between the 6APF WT and 6APF EcR^{DN} condition, the time point where we suspected we should find expression of astrocyte signaling molecules that might drive Beat- V_{aM} neurite fragmentation. We further analyzed this dataset for genes normally increased in translation during the first six hours of metamorphosis in the WT condition; and eliminated genes that did not increase at least 25% in reads between WL3 and 2APF, or 2APF and 6APF; which left us with 198 genes

(Appendix I). We then prioritized genes that were predicted to encode cell-cell signaling molecules (i.e. transmembrane and secreted proteins) leaving us with 46 candidates. Finally, to further increase the depth and coverage of our screen, we performed a literature search to identify any other molecule that have been previously suggested to play a role in astrocyte – neuron communication in *Drosophila* or mammals, and selected 100 additional genes (Carrillo, Özkan et al. 2015, Cosmanescu, Katsamba et al. 2018, Bornstein, Meltzer et al. 2021).

To functionally characterize these genes, we screened 146 genes using RNAi to knock each gene down in astrocytes (using *Alrm-Gal4*) and visualized the condition of the Beat-V_{AM} neurites (using *BeatVa-LexA, LexAop-GFP*) (Figure 13C). Of greatest interest were genes that, when knocked down in astrocytes, left Beat-V_{AM} neurites intact, but we also expected to find many that might play a role in astrocyte clearance of Beat-Va neuron debris. Indeed, we found many in both categories and binned each RNAi line into three groups: (1) those that resulted in intact Beat-V_{AM} neurites at HE (*CG3164, CG40485, Dpr17, DIP-ζ, LSD-1, Sallimus*); (2) those where Beat-V_{AM} neurites fragmented but were not cleared by HE (*CG15744, Dpr19, ImpL2, Kek5, Htl, Mnm*); and (3) those that gave intermediate phenotypes (examples include: *Fas3, LSD-2, Cg13784, Sema2a*) (Figure 16). Of the 146 genes assayed, 29 showed either a failure to clear neuronal debris or a failure to fragment neurites (Figure 13D, Figure 14). We next assayed astrocyte transformation into phagocytes in each of these lines and found a striking correlation: if astrocytes successfully transformed into phagocytes, Beat-V_{AM} neurons fragmented; however, if astrocytes failed to transform morphologically into

phagocytes, Beat-V_{aM} neurons remained intact (Figure 15). These data argue for a tight correlation between astrocyte transformation into phagocytes and fragmentation of Beat-V_{aM} neurons during local pruning.

2.2.6 Beat-Va_L neurons are eliminated through segment-specific, steroid-dependent apoptotic cell death

While neurite remodeling in the Beat-Va_M neurons was not blocked by cell intrinsic blockade of EcR signaling, expression of EcR^{DN} suppressed Beat-Va_L apoptosis (Figure 16A-C, E), similar to most other populations of *Drosophila* neurons that are eliminated by cell death during early metamorphosis (Lee, Wang et al. 2011, Winbush and Weeks , Denton, Shrivage et al. 2010, Zirin, Cheng et al. 2013). To determine whether this cell death occurred by canonical apoptotic signaling mechanisms, we stained for activated caspases using an antibody that recognized a cleaved version of Dcp-1 (Peterson, Barkett et al. 2003). Posterior Beat-Va_L cells (A5-7) became positive for activated caspases during early metamorphosis while cells in anterior segments that survived (A3-4) were not caspase positive (Figure 16F-H). We then expressed P35, a baculovirus caspase inhibitor that blocks many caspase-dependent cell death events (Clem, Fechheimer et al. 1991) using *BeatVa-Gal4* . We found that P35 strongly blocked cell death through HE in segments A5-6 and more weakly blocked death in A7 (Figure 16D-E) (likely due to driver strength variability), arguing posterior Beat-Va_L apoptosis is driven through caspase activation (Figure 16D-F, H).

2.2.7 Abdominal-B regulates segment-specific cell death in Beat-Va_L neurons

We next wanted to determine what led to the segment-specific initiation of caspase signaling in the posterior Beat-Va_L neurons. By morphological criteria and common

expression of EcR-B1, Beat-Va_L neurons in segments A3-7 appeared similar. We speculated that positional identity and differences in survival could be regulated by differential expression of homeobox (Hox) genes. The boundary between the anterior and posterior lateral cells (A4/5) is defined by the Abdominal-B (Abd-B) Hox gene in developing embryos (Delorenzi and Bienz 1990), and during embryonic development Abd-B can either promote or inhibit apoptotic cell death of neuronal progenitors depending on developmental context (Bakshi, Sipani et al. 2020, Clarembaux-Badell, Baladrón-de-Juan et al. 2022, Monedero Cobeta, Salmani et al. 2017). To explore the role of Abd-B in cell death of A5-7 neurons, we used antibodies to determine its larval expression pattern. We found that surviving A3-4 Beat-Va_L cells did not express Abd-B while Beat-Va_L cells in segments A5-7 strongly expressed Abd-B at wL3 and for as long as Beat-Va_L cells survived (Figure 17A, Figure 18A). We then knocked down Abd-B expression specifically in the Beat-Va neurons by driving a UAS-Abd-B RNAi construct with *BeatVa-Gal4*. This led to a strong suppression of caspase activation in posterior Beat-Va_L neurons (detected by cleaved Dcp-1 staining) through 6 hrs APF (Figure 17B-D), and partially suppressed lateral cell death compared with controls at HE (Figure 17E-G, Figure 17I). This incomplete but strong blockade of cell death is likely due to a partial knockdown effect by the RNAi construct targeting Abd-B as staining for Abd-B revealed partial rather than complete knockdown of protein levels in some cells. We note that Beat-Va_L cells retained expression of EcR-B1 even when Abd-B was depleted from these cells (Figure 18B), arguing that the suppression of cell death could not be explained by changes in EcR expression. Finally, when we performed the reciprocal experiment and

expressed Abd-B in all Beat-Va_L neurons by driving UAS-Abd-B with *BeatVa-Gal4* (Figure 18C), we found that A3-A4 lateral cells underwent cell death by HE (Figure 17H, 7I), indicating that expression of Abd-B in Beat-Va_L neurons is sufficient to induce cell death during metamorphosis.

2.3 Figures

Figure 4 *Beat-Va* neurons undergo neurite pruning and cell death during metamorphosis

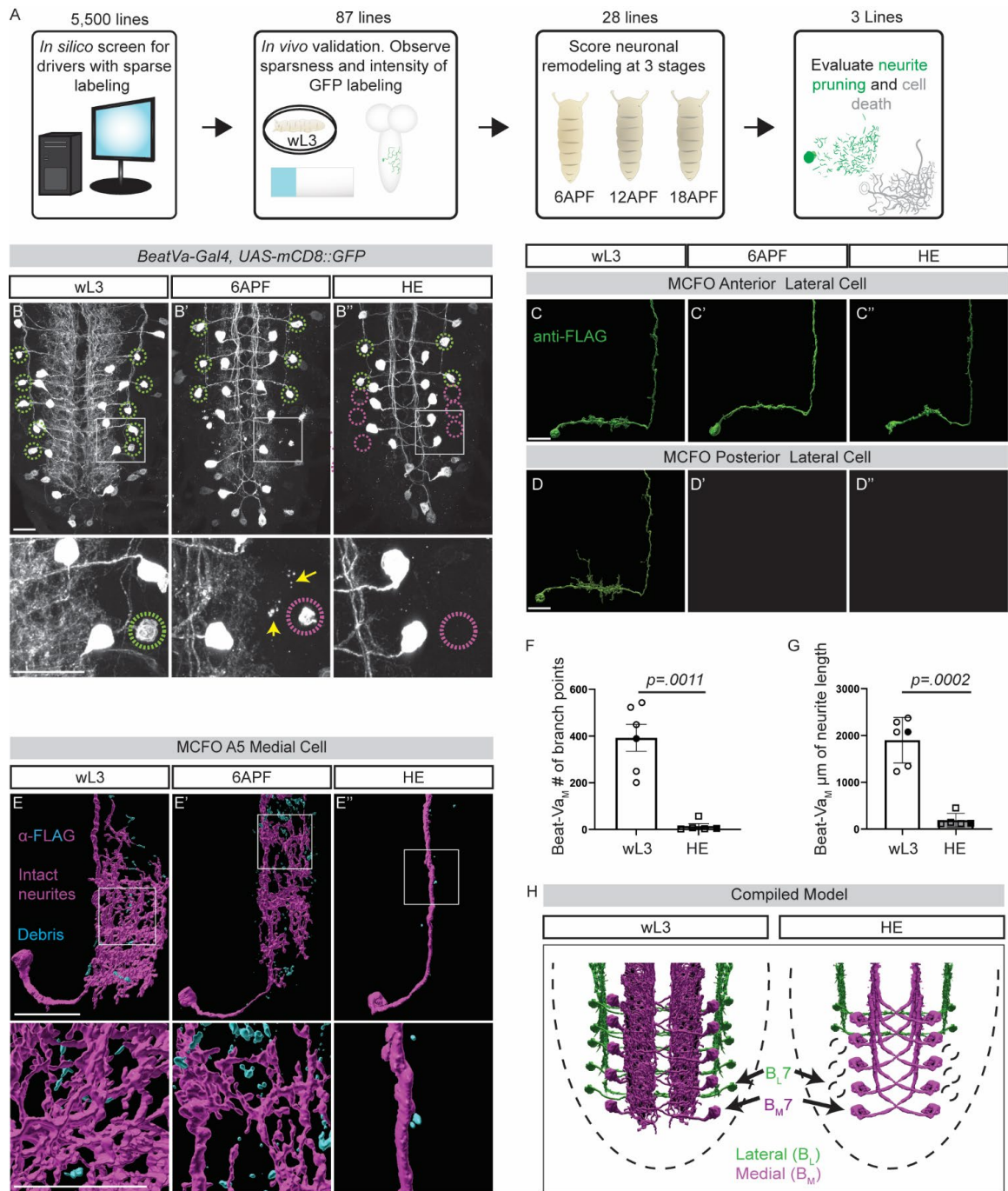


Figure 4

A) Gal4 lines generated by *Janelia* were screened in silico, 87 drivers that label sparse populations were verified for consistency and driver strength and 28 of those were chosen for further evaluation at 6APF, 12APF (HE), and 18APF.

B) Z-projection of ventral nerve cords labeled by *BeatVa-Gal4* driving an UAS-mCD8::GFP transgene at wL3 (B), 6APF (B'), and HE (B''). Surviving lateral neurons are noted by green circles, and dead or dying lateral neurons are pink. Yellow arrows denote neurite debris.

C) Single cell morphology of the anterior Beat-Va lateral cell (Beat-Va_L) at wL3 (C), 6APF (C'), and (C'') HE.

D) Posterior lateral cells at wL3 (D), 6APF (D'), and HE (D'').

E) Beat-Va medial cells (Beat-Va_M) at wL3 (E), 6APF (E'), and HE (E''). Intact neurites in magenta and fragmented neurites in cyan.

F) Quantification of the number of branch points in Beat-Va_M cells.

G) Quantification of the total combined length of all filaments in Beat-Va_M cells.

H) Composite model of both Beat-Va_L and Beat-Va_M neurons.

Comparisons by student t-test

Scale bar is 20 microns. Boxed region is magnified below each panel.

Figure 5 *Beat-Va* neurons undergo neurite pruning and cell death during metamorphosis

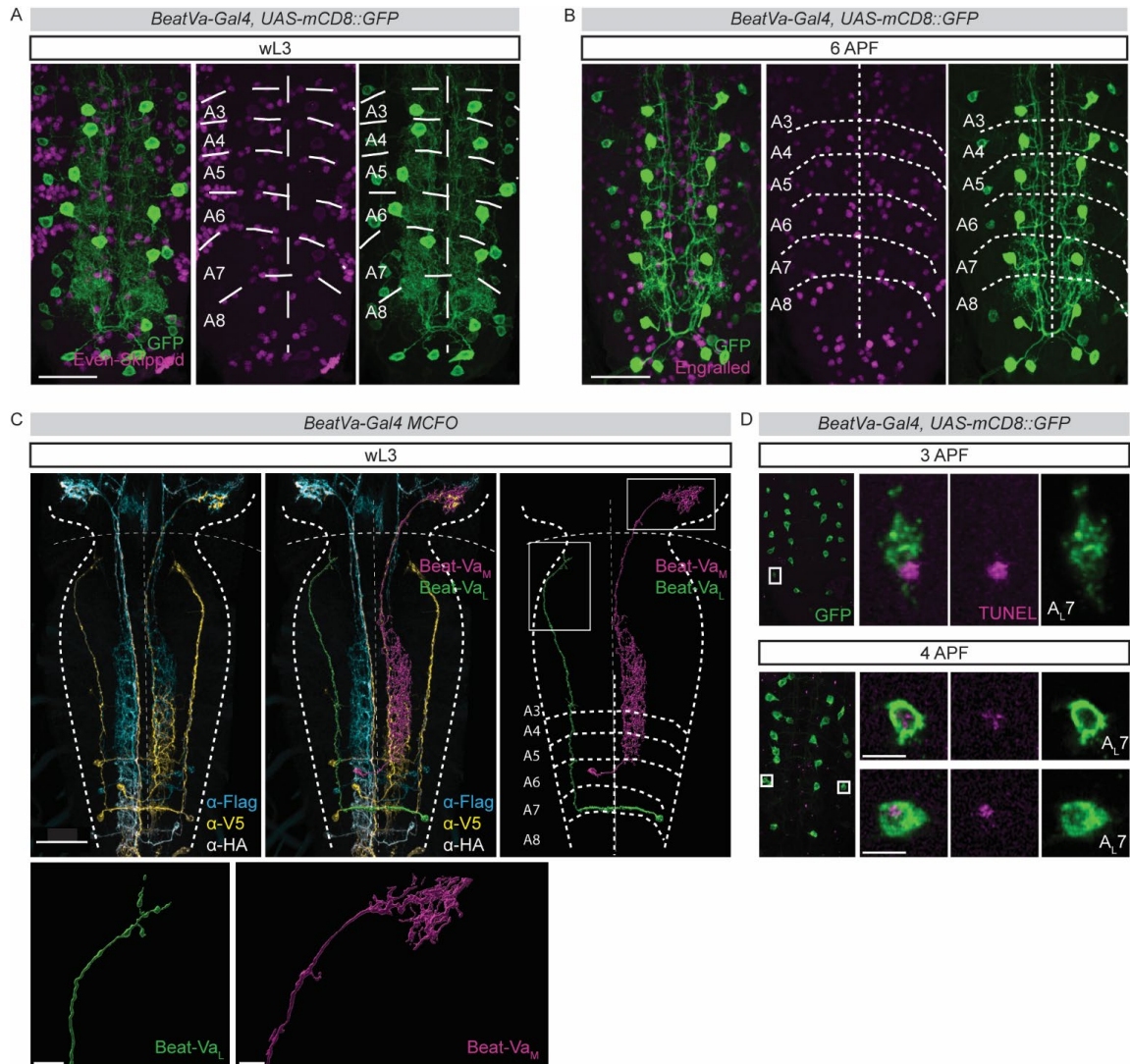


Figure 5

A) VNC at WL3 with genetic GFP labeling of *Beat-Va* neurons (green) and anti-Even-Skipped staining (magenta) to label the segments of the ventral nerve cord. Segments A3-A8 are denoted by tracing the Even-skipped staining and then superimposing traces onto *Beat-Va* neurons to define segmental positions. Scale bar is 20 microns

B) VNC at 6APF with genetic GFP labeling of Beat-Va neurons (green) and anti-Engrailed staining (magenta) to label the segments of the ventral nerve cord, showing the segmental positions persist into metamorphosis. Scale bar is 20 microns

C) Using segmental information and the MCFO approach we can render single cells in Imaris and overlay positional information. Boxed areas are Beat-Va_L and Beat-Va_M termini and are displayed at high magnification. CNS is outlined and boundary between VNC and brain lobes is marked with a dashed line. Scale bar for whole brain is 30 microns and for magnification is 10 microns **D)** Z-projection of ventral nerve cords with Beat-Va neurons labeled genetically with mCD8::GFP (green) and then subjected to TUNEL staining (magenta) to detect cells undergoing apoptotic cell death at 3APF and 4APF. Boxed areas containing TUNEL positive lateral cells are blown up and segmental position is noted. Scale bar is 5 microns.

Figure 6 *Beat-Va_M neurons remodel when EcR signaling or expression is inhibited*

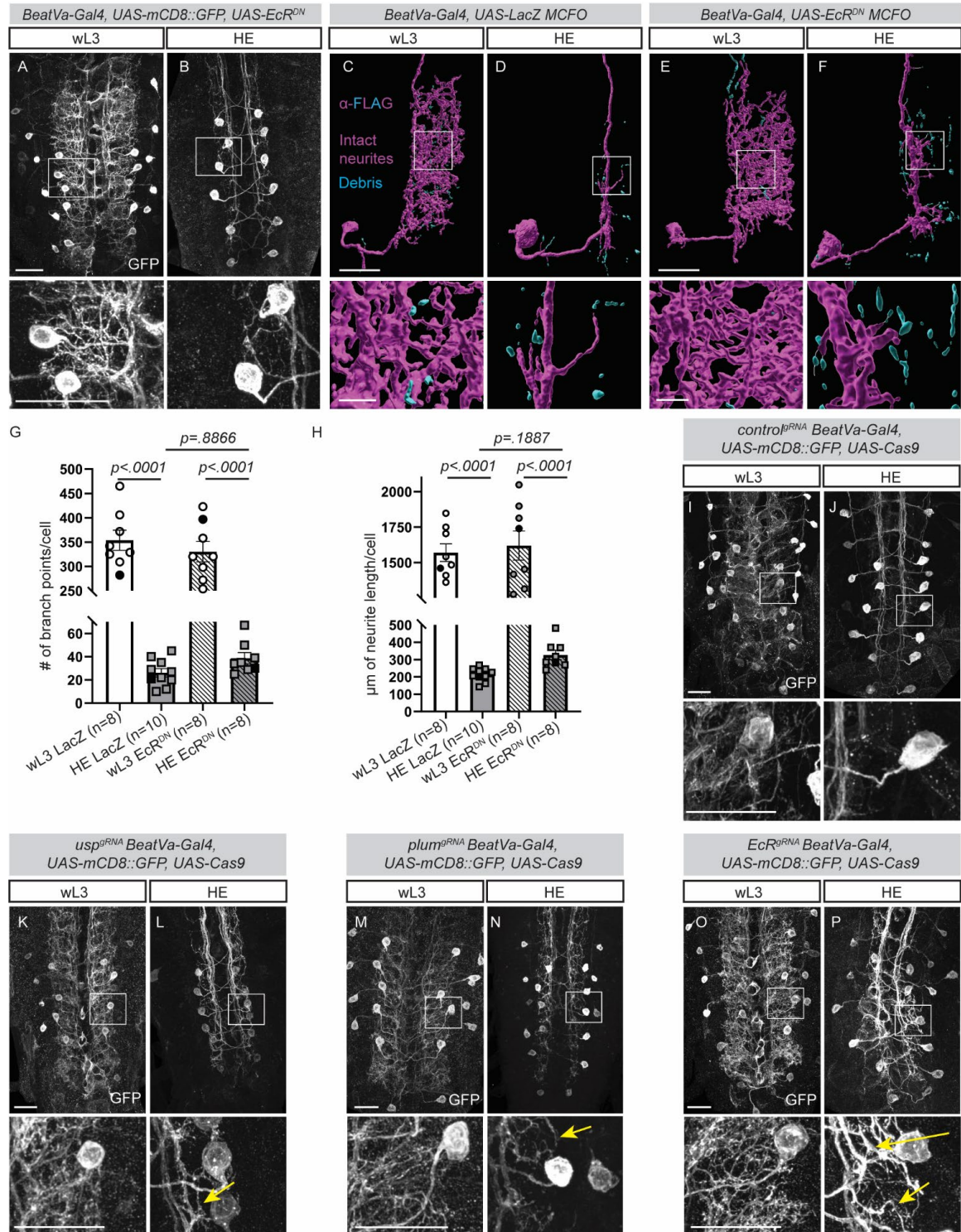


Figure 6

- A)** Beat-Va neurons genetically labeled with mCD8::GFP at wL3, expressing UAS-EcRDN.
- B)** Beat-Va_M neurons expressing EcRDN at HE.
- C)** Control Beat-Va_M neuron driving UAS-LacZ using the MCFO technique at wL3 and HE (**D**). Intact neurites, magenta; fragmented neurites, cyan. Boxed area is shown in high magnification below each image.
- E)** Beat-Va_M neuron expressing EcRDN labeled with the MCFO technique at wL3 and HE (**F**).
- G)** Quantification of Beat-Va_M branch point number at HE in EcRDN background.
- H)** Quantification of Beat-Va_M total neurite length in EcRDN background.
- I)** Beat-Va neurons genetically labeled with mCD8::GFP and expressing Cas9 under UAS control. Guide RNAs (gRNAs) are expressed ubiquitously. Cell-specific knockout of control guide RNAs at wL3 (**I**) and HE (**J**).
- K)** Targeting Ultraspiracle (*usp*) with gRNAs in Beat-Va_M neurons at wL3 (**K**) or at HE (**L**). Fine neurites, yellow arrow. Boxed areas are displayed in high magnification below each image.
- M)** plum gRNAs in Beat-Va_M neurons at wL3 (**M**) or HE (**N**). Fine neurites, yellow arrow.
- O)** Expression of EcR gRNAs in wL3 neurons (**O**) and HE (**P**). Fine neurites, yellow arrow.
- Comparisons with Two-Way ANOVA and Sidak test for multiple comparisons.
- (A-B, I-P) Scale bars are 20 microns.
- (C-F) Scale bars are 20 microns in single cell images and 5 microns in the magnified view.

Figure 7 Manipulation of EcR-B1 expression in Beat-Va neurons

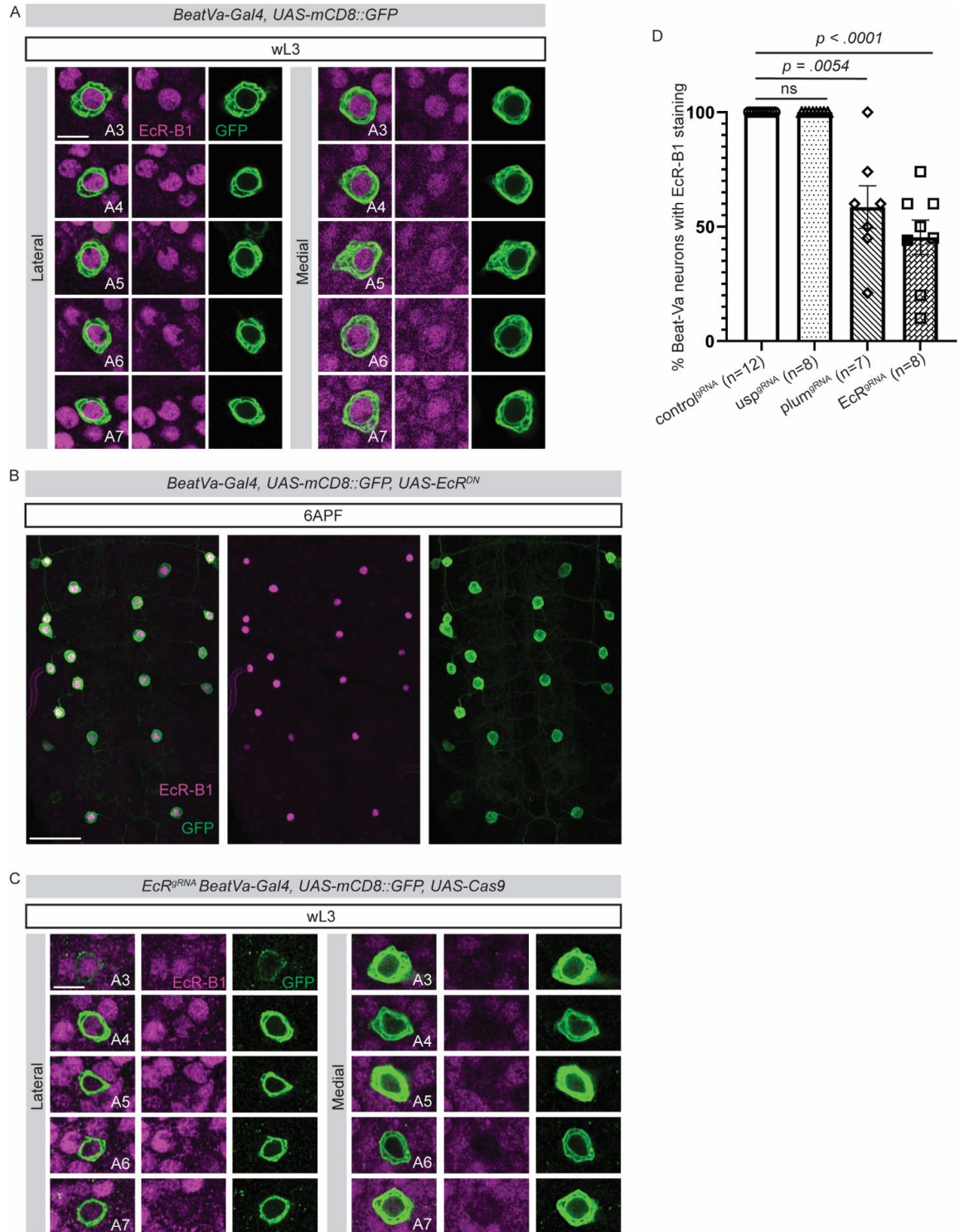


Figure 7

A) Beat-Va neurons at wL3 labeled CD8::GFP (green) stained with the EcR B1 Receptor (magenta) showing the colocalization of all lateral and medial cell bodies with the receptor.

B) Beat-Va neurons at 6APF labeled CD8::GFP (green) and expressing a UAS drive EcRDN. Stained with the EcR B1 Receptor (magenta) to identify cells that are expressing the UAS-EcRDN. There are typically not EcR-B1 positive cells at this time.

C) Beat-Va neurons at wL3 labeled CD8::GFP (green) and expressing UAS-Cas9 in a gRNA EcR animal. Stained with the EcR-B1 Receptor (magenta) to evaluate if cells lose EcR-B1 expression. **D)** Quantification of gRNA against *usp*, *plum*, *EcR* on Beat-Va EcR-B1 expression when compared with control. One-Way ANOVA, Kruskal-Wallis test for multiple comparisons.

Figure 8 Genetic depletion of EcR by targeting upstream regulators does not block Beat-VaM neuron remodeling

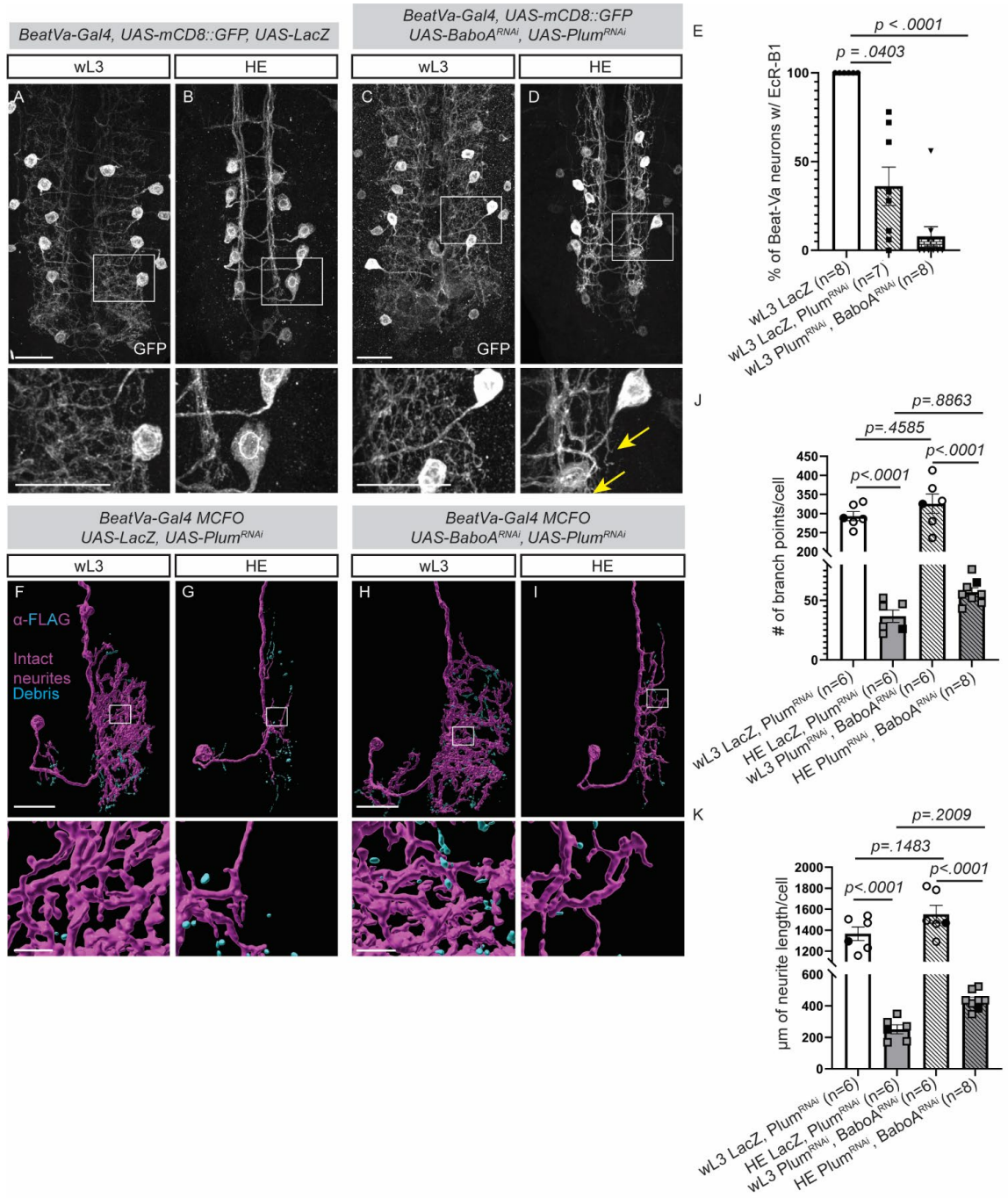


Figure 8

A) Beat-Va neurons labeled with mCD8::GFP at wL3 or HE **(B)** while driving a UAS-LacZ as a control construct. Boxed area shown at higher magnification below.

C) Beat-Va neurons expressing UAS-Plum^{RNAi} and UAS-BaboA^{RNAi} to suppress EcR-B1 expression at wL3 and HE **(D)**. Remaining projections, yellow arrow. Scale bars are 20 microns.

E) Dual expression of UAS-BaboA^{RNAi} and UAS-Plum^{RNAi} results in substantial loss of EcR protein by antibody staining. One-way ANOVA, Kruskal-Wallis test for multiple comparisons.

F) Beat-Va_M neurons driving UAS-LacZ and UAS-Plum^{RNAi} labeled using MCFO at wL3 **(F)** and HE **(G)**.

H) Beat-Va_M neurons driving UAS-BaboA^{RNAi} and UAS-Plum^{RNAi} labeled using MCFO at wL3 **(H)** and HE **(I)**. Intact neurites, magenta; fragmented neurites, cyan. Boxed areas are shown in high magnification below the image.

J) Quantification of branch point number and **(K)** neurite length for (F-I). Comparison with Two-Way ANOVA and Sidak test for multiple comparisons.

(A-D) Scale bars are 20 microns.

(F-I) Scale bars are 20 microns in single cell images and 5 microns in the magnified view.

Figure 9 Cell specific expression of *EcR^{DN}* blocks astrocyte transformation

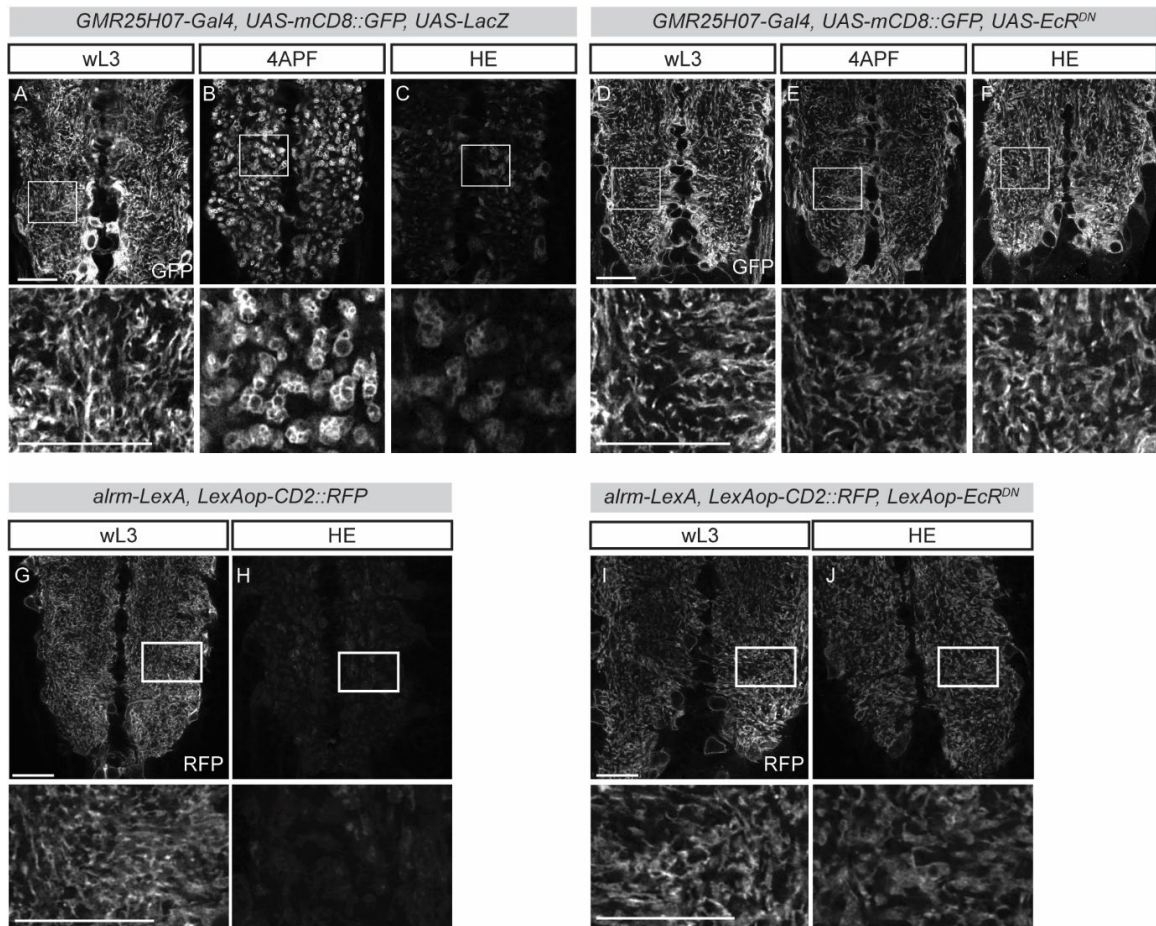


Figure 9

- A)** Astrocytes labeled with *GMR25H07-Gal4* (a strong astrocyte Gal4 line) crossed to *CD8::GFP* at wL3 showing their “wispy” morphology,
- B)** 4APF showing the phagolysomes that astrocytes display (Kang 2023), and
- C)** HE where astrocytes are normally only faintly detectable.
- D)** Astrocytes expressing a *UAS-EcR^{DN}*, labeled with *mCD8::GFP* at wL3 showing their “wispy” morphology, which is retained at
- E)** 4APF, and **F)** HE, indicating a failure to transform.
- G)** *Alrm-LexA*, *LexAop-mCD8::RFP* at wL3 where normal astrocyte morphology is apparent, and

H) HE when astrocytes are no longer visible.

I) When *Alrm-LexA* drives a LexAop-EcR^{DN} in addition to LexAop-mCD8::RFP, the astrocytes appear normal at wL3, **J)** but then fail to transform at HE.

Scale bars are 20 microns.

Figure 10 Astrocyte-derived signals converge with intrinsic Beat-Va_M neuron EcR signaling to execute local pruning

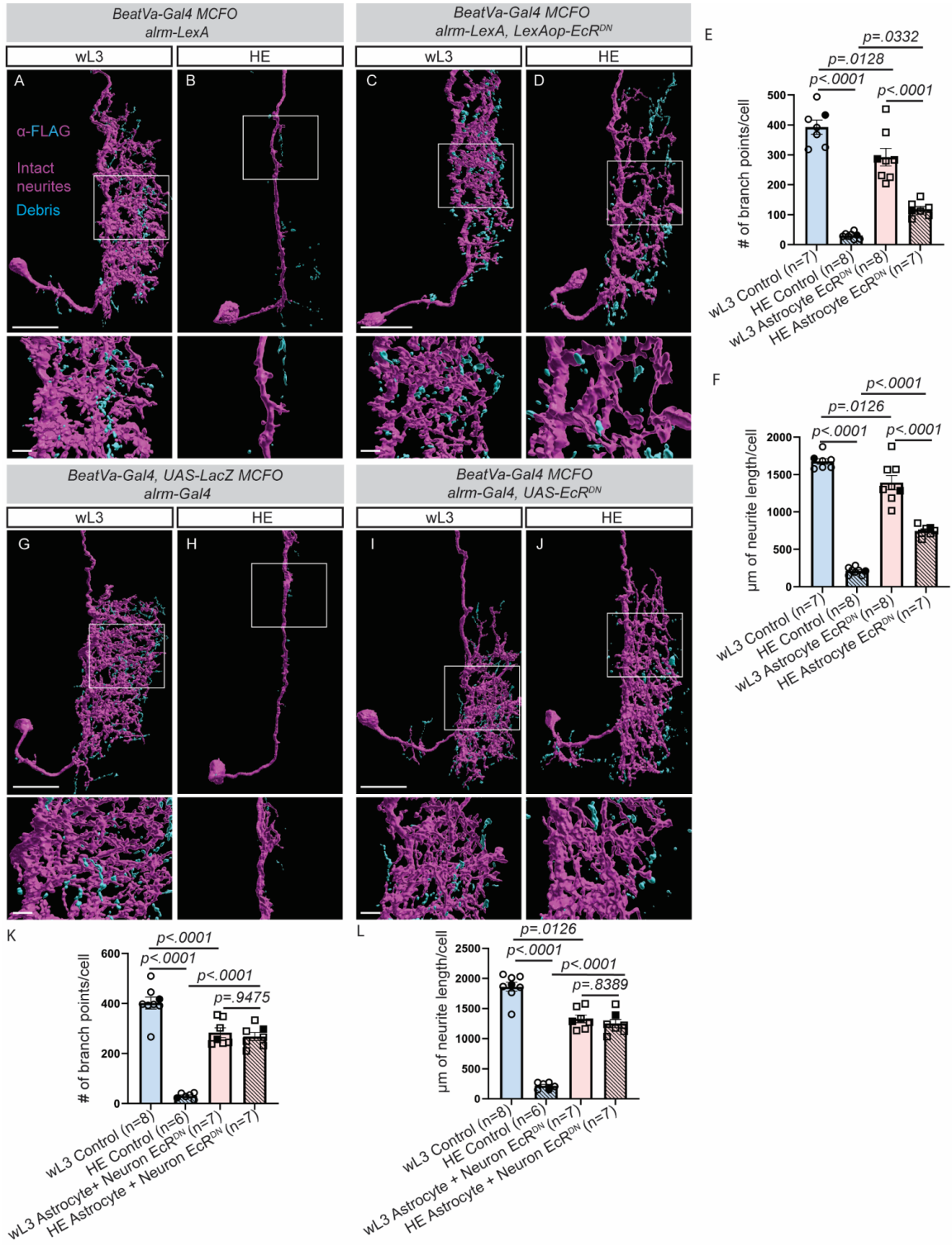


Figure 10

A) Beat- V_{aM} neurons labeled with MCFO in an *alm-LexA* background (control) at wL3 or HE **(B)**.

C) *alm-LexA*, *LexAOp-EcR^{DN}* background labeled with the MCFO technique at wL3 **(C)** or HE **(D)**.

E) Quantification of point number **(E)** or total neurite length **(F)** of (A-D)

G) Beat- V_{aM} neurons in an *alm-Gal4* background (control) at wL3 **(G)** HE **(H)**.

D) Beat- V_{aM} neurons in an *alm-Gal4*, *UAS-EcR^{DN}* background at wL3 **(I)** or HE **(J)**.

K) Quantification of point number **(K)** or total neurite length **(L)** of (G-J).

All comparisons are done with Two-way ANOVA with the Sidak test for multiple comparisons. Intact neurites, magenta; fragmented neurites, cyan.

Scale bars are 20 microns for whole neuron images and 5 microns for magnified images

Figure 11 Supplemental: Verification of newly constructed *BeatVa-LexA* line

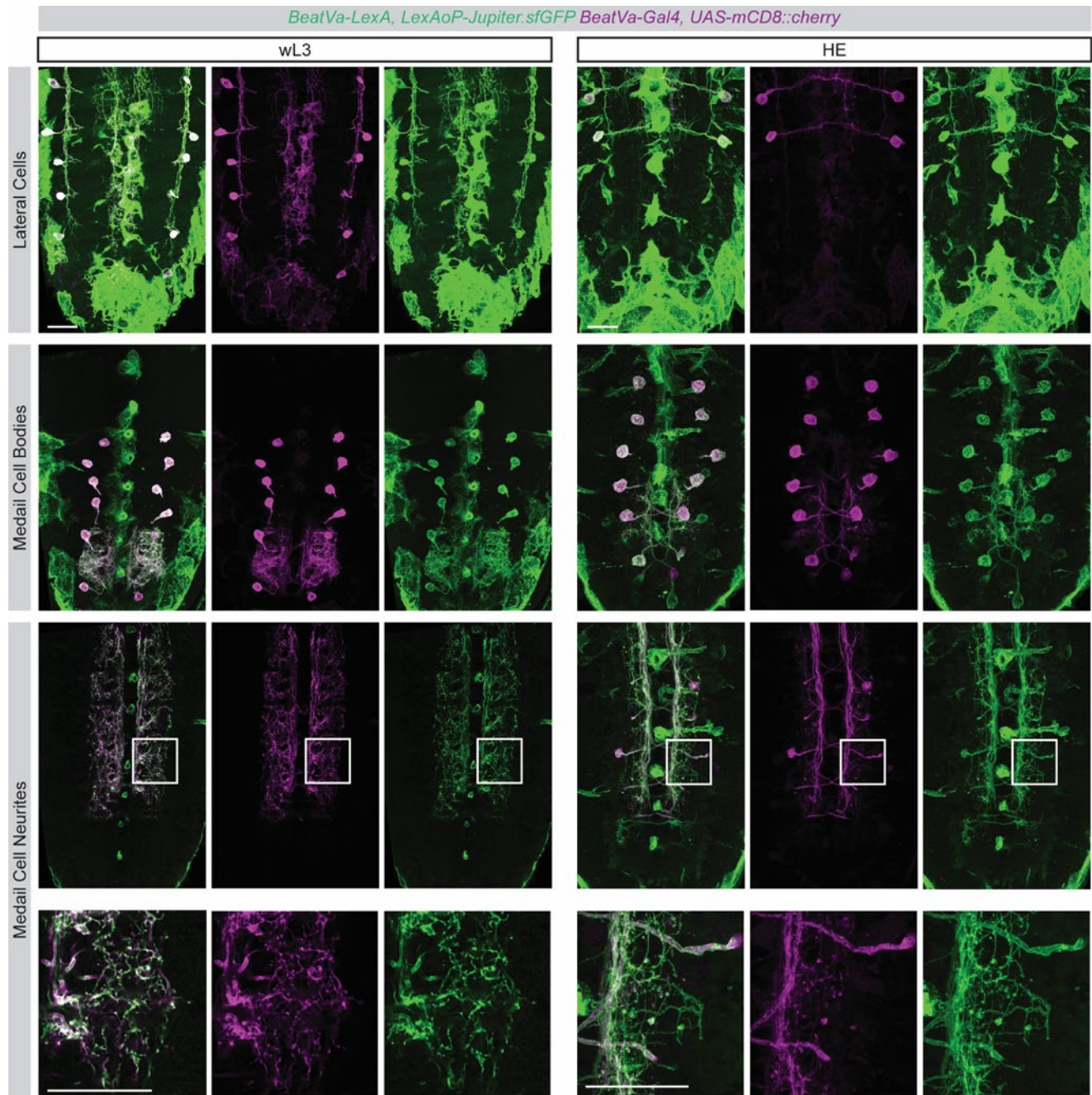


Figure 11 Animals carrying the *BeatVa-LexA* construct were crossed to animals carrying a LexAop-Jupiter.sfGFP (a GFP construct that localized to microtubule networks and had been reported to label neurite processes well (Karpova, Bobindec et al. 2006)) to genetically label any cells where the *BeatVa-LexA* line was expressed. These animals

were then crossed to an existing stock that carried both the original *BeatVa-Gal4* construct and a UAS-mCD8::cherry. Good signal overlap between the GFP and Cherry fluorophores indicates the *BeatVa-LexA* and *BeatVa-Gal4* lines labeled the same population of neurons in addition to labeling a second population of non-neuronal cells (likely surface glia). Scale bars are 20 microns.

Figure 12 Pan-glial Myoglianin expression drives phagocytic astrocyte transformation

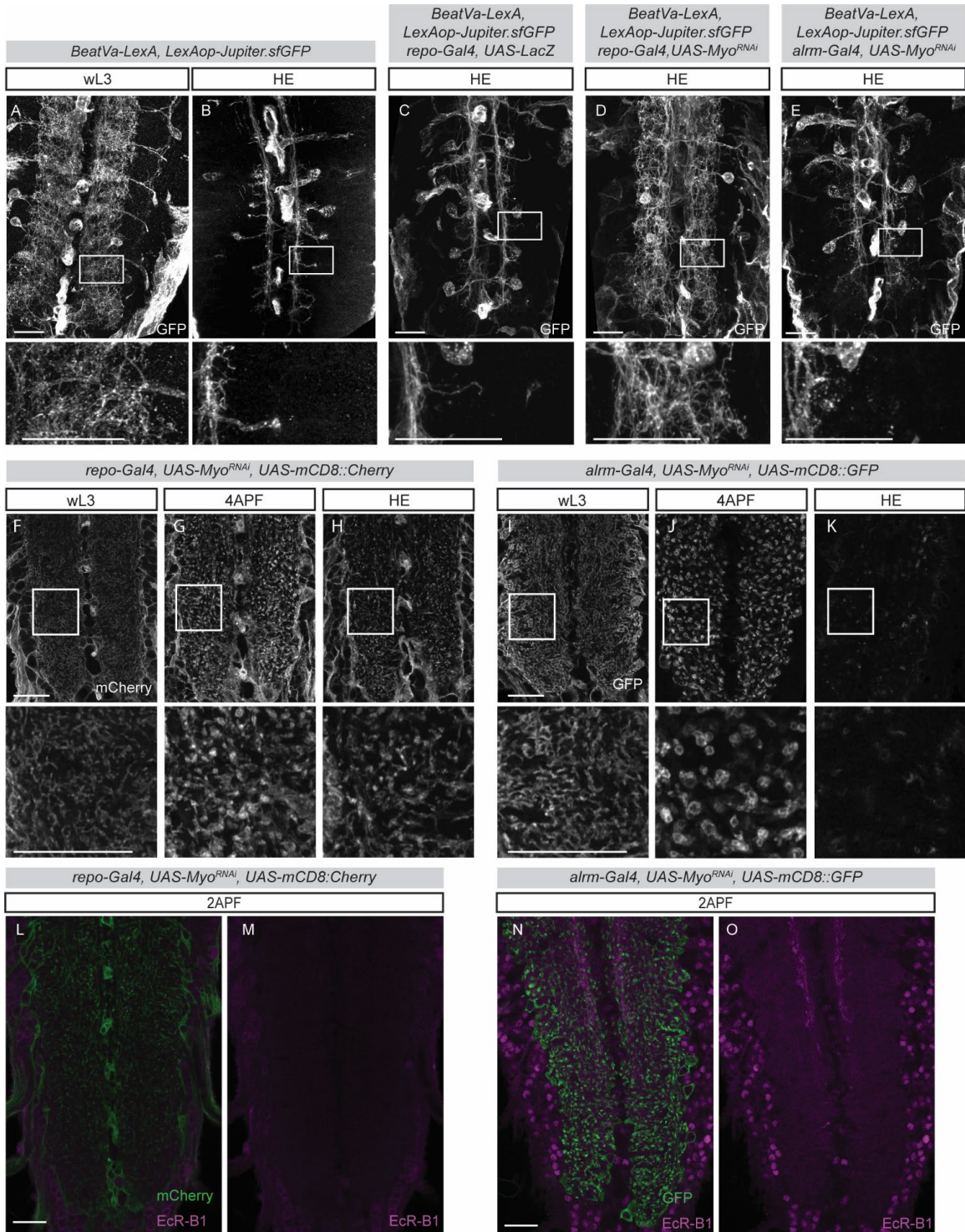


Figure 12

A) Beat-Va neurons labeled with a LexAop driven, microtubule targeted, superfolder GFP (LexAop-Jupiter.sfGFP) at wL3 or HE **(B)**.

C) Beat-V_{aM} neurons at HE with repo-Gal4 and UAS-LacZ (control) in the background.

D) Myoglianin knocked down in all glia with repo-Gal4.

E) Myoglianin knocked down only in astrocytes with alrm-Gal4.

F) Visualization of astrocytes using a UAS-mCD8::Cherry when Myoglianin is knocked down in all glia at wL3, 4 APF **(G)**, and HE **(H)**.

I) Astrocytic knockdown of Myoglianin only in astrocytes at wL3, 4 APF **(J)** or HE **(K)**.

Note that by HE astrocytes are also no longer visible in controls.

L, M) Expression of UAS-MyoRNAi in all glia, EcR-B1 staining, magenta. Astrocyte membranes, green.

N, O) Expression of UAS-MyoRNAi in astrocytes, EcR-B1 staining, magenta. Astrocyte membranes, green.

All scale bars are 20um.

Figure 13 Translational profile of transforming astrocytes reveal regulators of debris clearance and neurite fragmentation

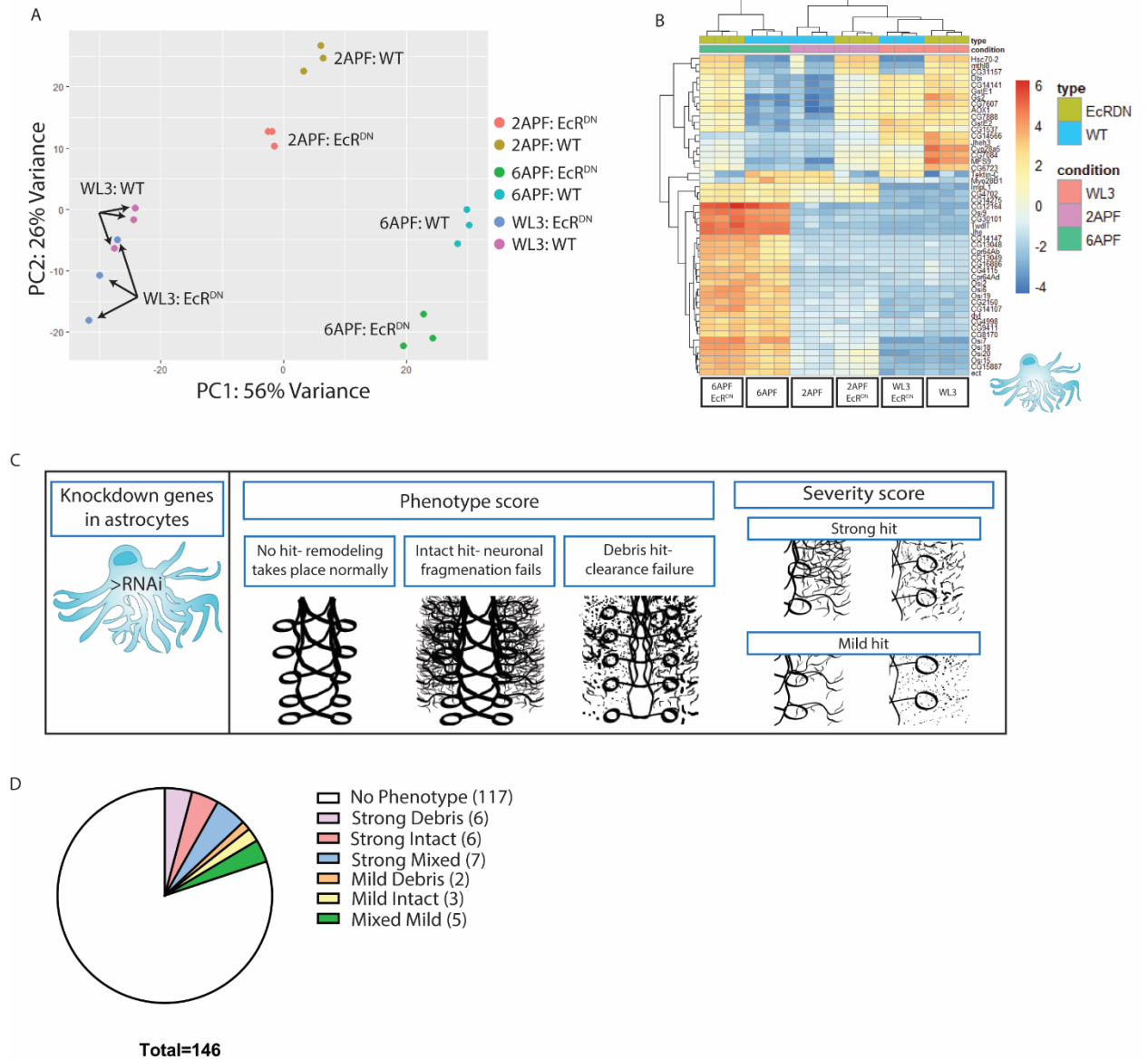


Figure 13

A) Principal component analysis (PCA) of astrocyte TRAP-seq data. Time points are WL3, 2APF and 6APF and conditions are wildtype (WT) and when astrocyte transformation is blocked with an *Alrm-Gal4* driven *UAS-EcR^{DN}* (*EcR^{DN}*).

B) Heatmap of most differentially expressed genes across time points and conditions sorted by hierarchical clustering.

C) The illustrated screen setup. We knocked down genes in astrocytes and visualized neurites at HE, when all fine neurites should be fragmented and cleared. We then scored the phenotype and severity for each gene.

D) Pie chart illustrating the results of the screen with total number of genes in each category indicated.

Figure 14 Visualization of Beat- V_{AM} neurons from all hits in the astrocyte screen

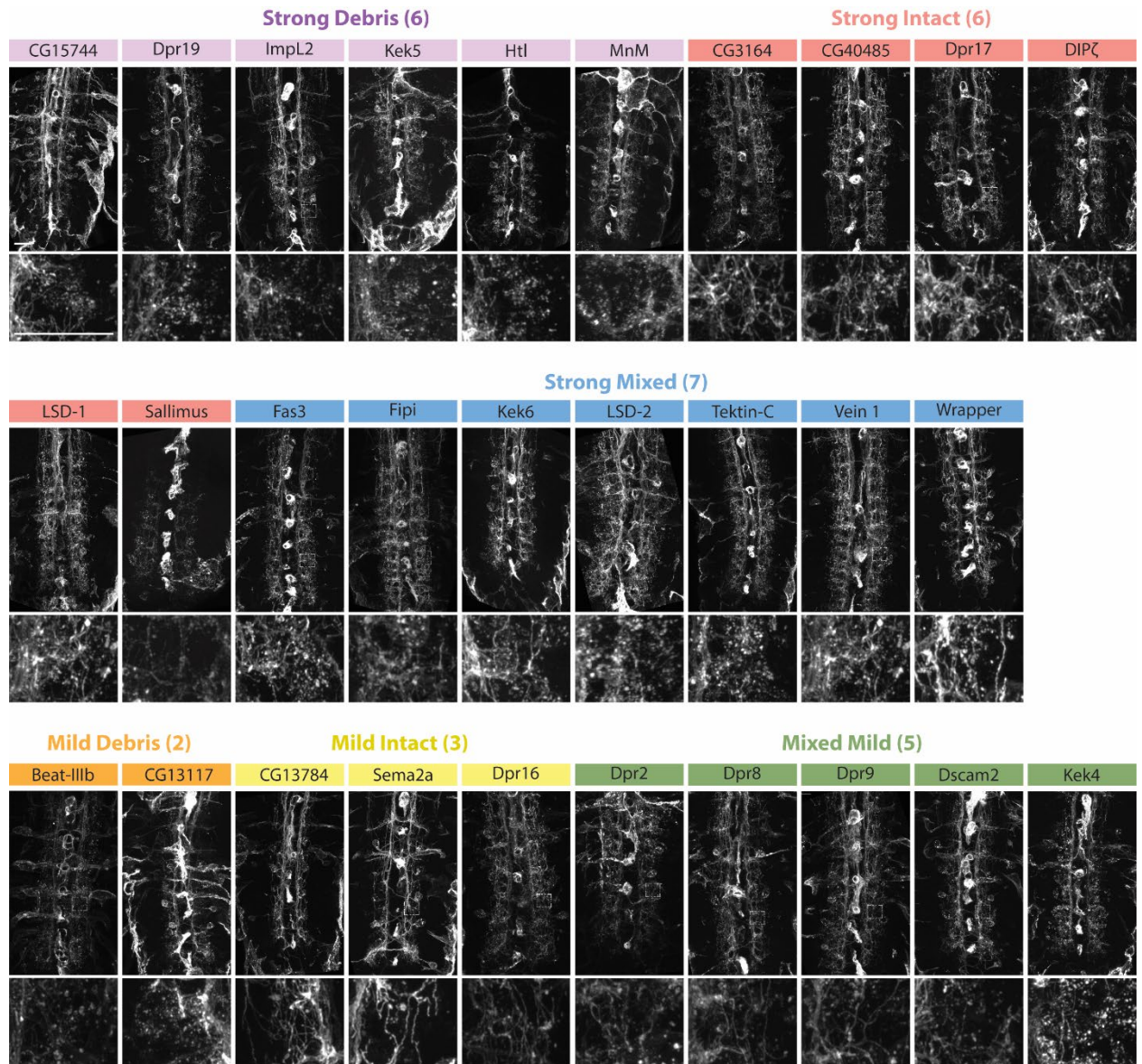


Figure 14: Visualization of Beat- V_{AM} neurons from all hits in the astrocyte screen that resulted in a debris clearance or debris fragmentation defect. Beat-Va neurons are labeled with a *LexAop-mCD8::GFP* and the ventral nerve chord is shown with a magnified image below. Scale bar is 20um. Genes are labeled with color corresponding to phenotype.

Figure 15 Astrocyte transformation tightly correlates with neurite remodeling pheontype categories

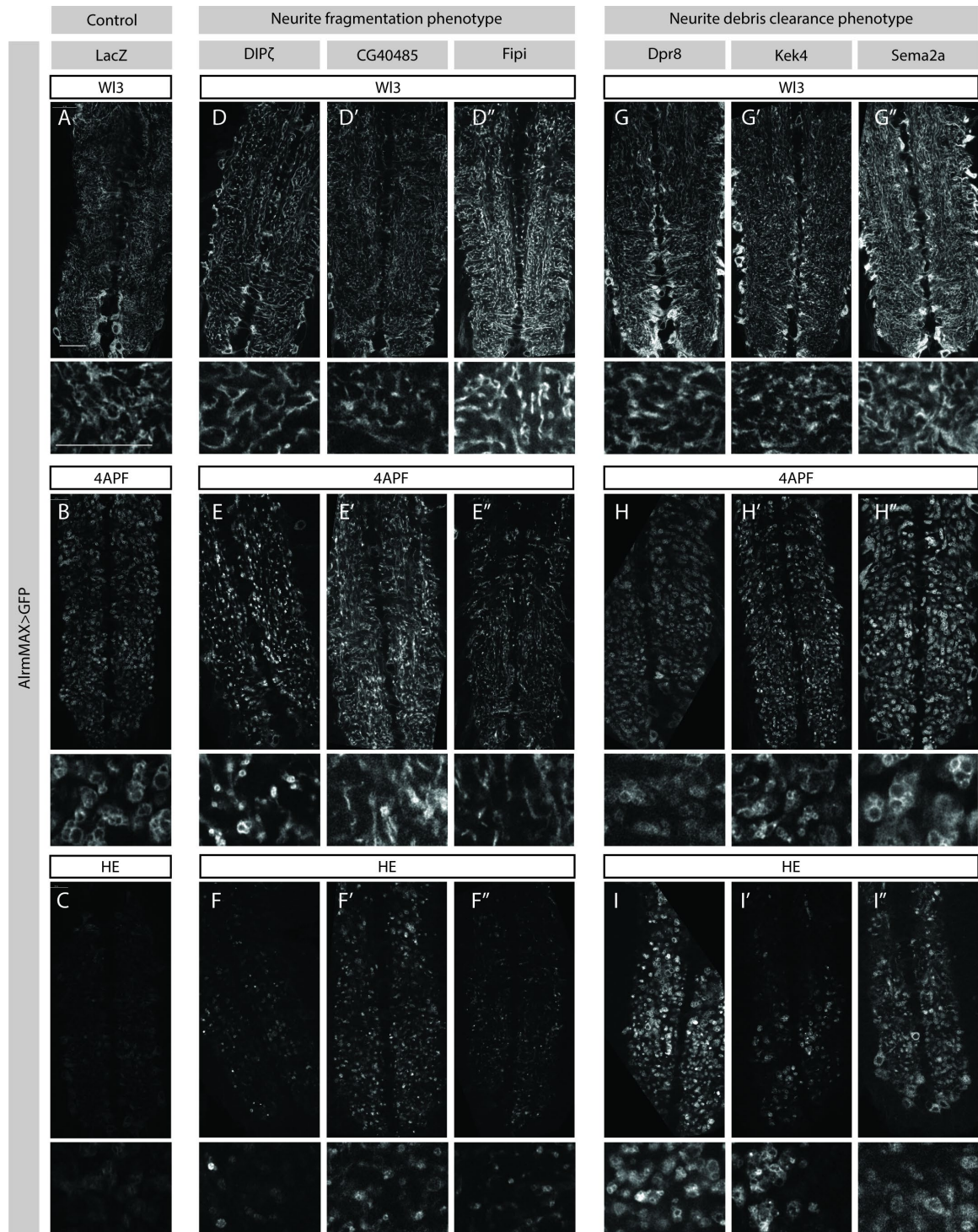


Figure 15

Astrocytes labeled with *AlrmMAX-Gal4, UAS-mCD8::GFP* in control conditions (*UAS-LacZ*) at

A) WL3, **B)** 4APF when phagocytic vesicles become obvious **C)** and HE when astrocytic labeling typically disappears.

D-D'') Molecules that when knocked down with UAS driven RNAis in astrocytes result in a lack of Beat- V_{AM} neurite fragmentation, result in normal astrocytes at WL3 but

E-E'') the astrocytes fail to transform and produce large phagocytic vesicles by 4APF.

F-F'') However astrocytic knockdown of these molecules still result in a loss of most astrocytic labeling by HE.

G-G'') Astrocytic knockdown of molecules that led to a debris clearance failure do not obviously effect astrocyte morphology at WL3 and

H-H'') the astrocytes still produce phagocytic vesicles at 4APF, however

I-I'') these astrocytes retain these phagocytic vesicles at HE and fail to lose their labeling. All scale bars are 20 microns.

Figure 16 *Beat-Va_L* neurons undergo hormone-dependent, caspase-activated apoptosis

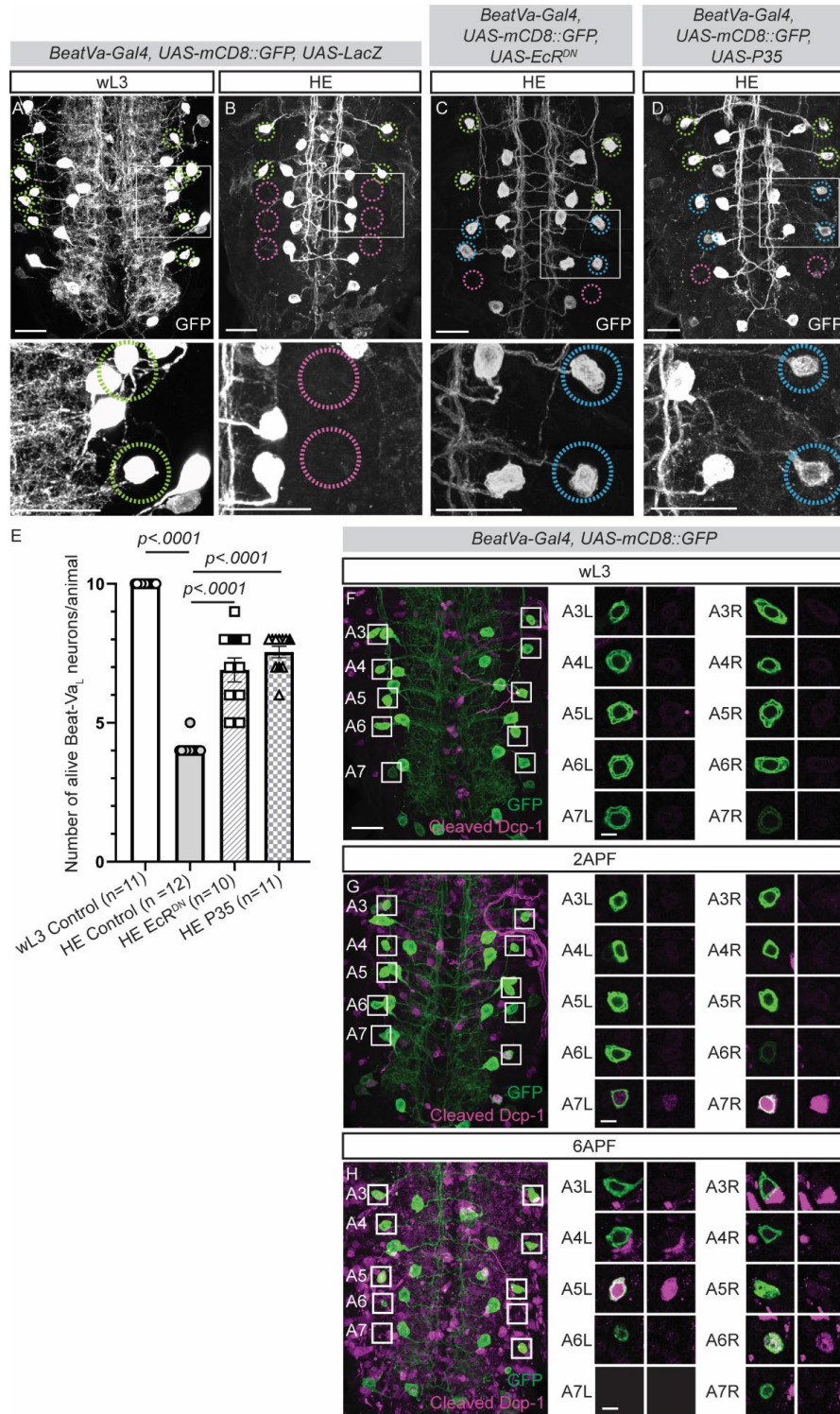


Figure 16

(A) Beat-Va neurons at wL3 (A), and HE (B) labeled with mCD8::GFP, expressing *UAS-LacZ* (control).

(C) Beat-Va neurons at HE expressing mCD8::GFP with EcR^{DN} (C) or *UAS-P35* (D). Lime green circles indicate normal lateral cells before remodeling. Pink circles indicate the position of dead lateral cells. Blue circles indicate lateral cells surviving beyond normal time point. Scale bars, 20 microns.

(E) Quantification of the number of lateral cells at wL3, or HE in controls or animal expressing EcR^{DN} or P35. Two-way ANOVA, Sidak multiple comparison test.

(F) Beat-Va neurons genetically labeled with mCD8::GFP and stained for cleaved Dcp-1 at wL3 (F), 2 APF (G) or 6 APF (H). Right, A3-A7 lateral cells from each hemisegment (L = left and R = right hemisegment) are magnified and shown as a single plane image on the right of each full VNC image.

(A-D) Scale bars are 20 microns.

(F-H) Scale bars are 20 microns in population images and 5 microns in the magnified view.

Figure 17 Hox gene *Abd-B* dictates caspase-dependent *Beat-Va_L* neuron cell death

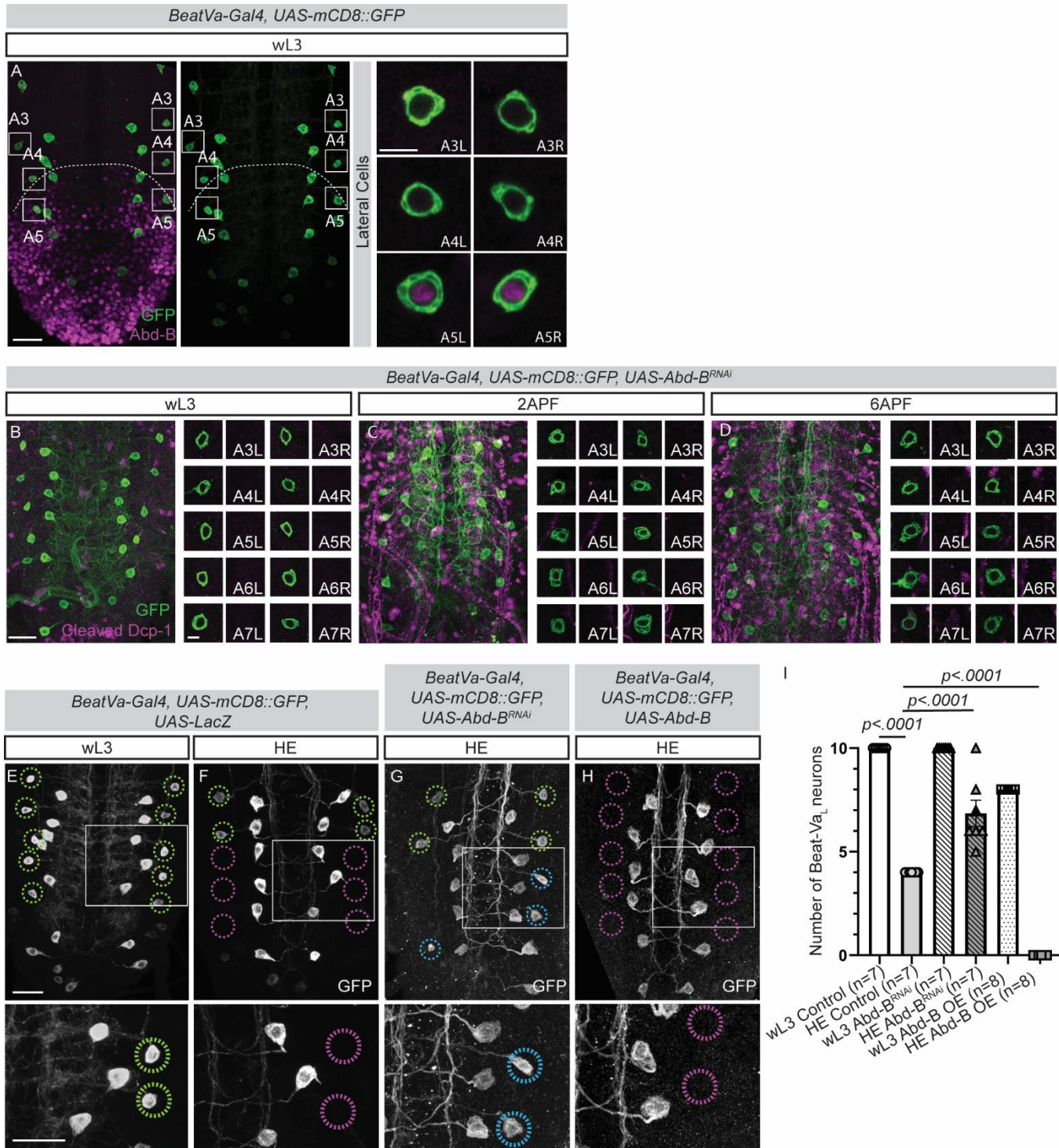


Figure 17

A) Beat-Va neurons at wL3 labeled with mCD8::GFP stained with Abdominal-B antibodies (magenta). White dashed line denotes the boundary of Abdominal B (Abd-B) expression.

B) Beat-Va neurons genetically labeled with mCD8::GFP and driving a *UAS-Abd-B^{RNAi}* at wL3 (B), 2 APF (C), and 6APF (D) stained for cleaved Dcp-1. A3-A7 lateral cells from the right and left are blown up and shown as a single plane image on the right of each image.

E) Beat-Va neurons at wL3 (E) or HE (F) genetically labeled with mCD8::GFP crossed to *UAS-LacZ* as a control. Green circles, indicate Beat-Va_L neurons. Magenta, position of dead cells.

G) Expression of *UAS-Abd-B^{RNAi}* in Beat-Va neurons. Blue circles, cells that survive inappropriately.

H) Expression of Abd-B in all lateral cells by HE leads to cell death.

D) Quantification of (E-H). Two-way ANOVA, Sidak test for multiple comparisons.

(A-D) Scale bars are 20 microns in population images and 5 microns in the magnified view.

(E-H) Scale bars are 20 microns.

Figure 18 *Abd-B* expression in *Beat-Va* neurons

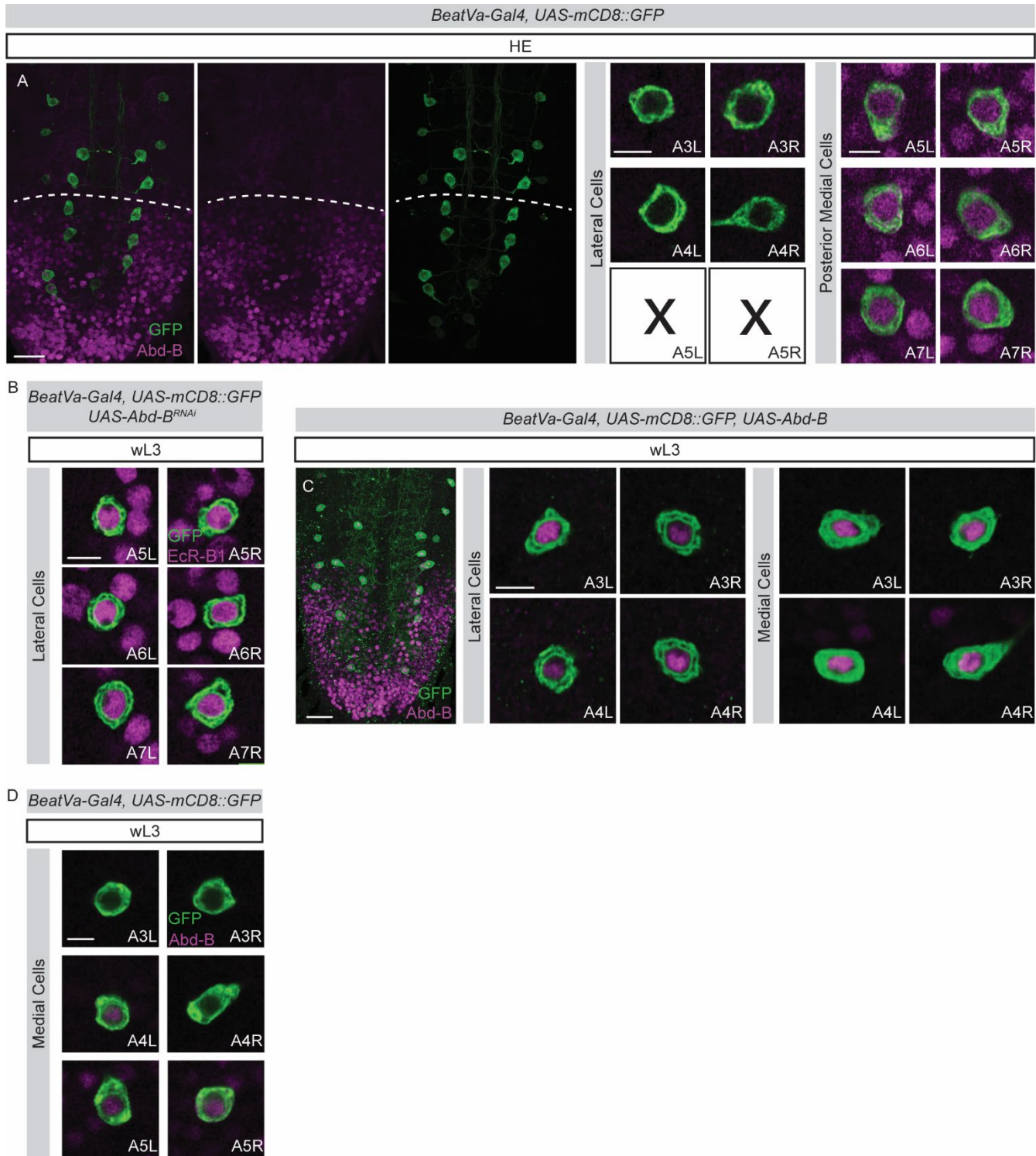


Figure 18

A) Beat-Va neurons at HE labeled with mCD8::GFP stained with anti-Abd-B. Abd-B expression persists to HE. The lateral A5 (Abd-B +) cells undergo cell death while the A3-4 cells survive and do not express Abd-B at HE. The A5-7 medial cells continue to express Abd-B at HE. Left and right hemisegment denoted by “L” and “R”. Dashed white line superimposed on Abd-B boundary.

B) Beat-Va neurons labeled with mCD8::GFP and driving *UAS-Abd-B^{RNAi}* at wL3 stained with the EcR-B1 showing the continued colocalization of EcR-B1 in the absence of Abd-B.

C) Beat-Va neurons at wL3 labeled with mCD8::GFP and crossed to *UAS-Abd-B* and stained with anti-Abd-B. The two most anterior lateral and medial cell bodies are magnified and show Abdominal- B expression, which is not usually present in these cells, confirming overexpression was successful.

D) Three most anterior medial Beat-Va neurons at wL3 labeled with CD8::GFP stained with Abd-B. Shows Abd-B is present in some medial cells even though they do not undergo cell death. Scale bar is 5 microns in all images with a single cell body and 20 microns in all other images.

2.4 Discussion

A growing collection of mechanistic studies on neuronal remodeling suggests a diversity of molecular pathways are deployed across the nervous system to accomplish remodeling in different contexts (Schafer, Lehrman et al. 2012, Yaniv and Schuldiner 2016, Neukomm and Freeman 2014, Boulanger and Dura 2022). In this study, we identified the *BeatVa-Gal4*-expressing neurons and show they remodel using mechanisms not previously reported in other heavily studied CNS cell types: mushroom body neurons (Lee, Marticke et al. 2000, Yu, Gutman et al. 2013, Lai, Chu et al. 2016) and ventral Corazonin neurons (Choi 2006, Lee, Sehgal et al. 2013, Wang, Lee et al. 2019). Beat- V_{aM} neurons exhibit EcR-independent, astrocyte activated local neurite pruning, while Beat- V_{aL} neurons die in a hox gene-mediated, segmentally restricted pattern. The unique set of mechanisms that we found to underly Beat-Va neuron remodeling – among the first new neuronal subtypes whose remodeling we have characterized in detail – supports the notion that a diversity of undiscovered remodeling mechanisms likely exist in the animal kingdom.

Beat- V_{aM} neurons undergo massive local neurite pruning during the first twelve hours of metamorphosis, which we visualized with single-cell precision. Surprisingly, unlike all other neuronal cell types studied in *Drosophila*, we found that Beat- V_{aM} neuron local pruning was not suppressed by cell-autonomous blockade of EcR signaling. Moreover, we found that blocking astrocyte developmental progression (into a

phagocytic phenotype) using EcR^{DN} reduced Beat-V_{AM} remodeling by ~50%, and when combined with simultaneous blockade of EcR signaling in Beat-V_{AM} neurons, local neurite pruning was almost entirely blocked. We interpret these data to mean that extrinsic cues from astrocytes and neuron intrinsic EcR-mediated events converge to control Beat-V_{AM} remodeling. Beat-V_{AM} neurons should therefore provide an excellent system in which to genetically dissect astrocyte to neuron signaling pathways that promote local pruning.

Astrocytes may release molecular cues onto neurites as they transform into phagocytes that promote the progression of neurite remodeling. We explored the role of the previously identified glial-secreted TGF β ligand Myoglianin in Beat-V_{AM} neuron local pruning. In other cell types, Myoglianin signaling from glia is known to activate the expression of EcR in neurons, thereby establishing their competence to prune in response to ecdysone (Awasaki, Huang et al. 2011, Yu, Gutman et al. 2013, Hakim, Yaniv et al. 2014, Wang, Lee et al. 2019). Multiple lines of evidence argue against such a role for Myoglianin in Beat-V_{AM} neuron local pruning. First, we found that while blockade of pan-glial release of Myoglianin can suppress Beat-V_{AM} neuron local pruning, depletion of Myoglianin from astrocytes did not block Beat-V_{AM} neuron local pruning. Second, we found that Myoglianin depletion led to decreased EcR expression in astrocytes and a failure of astrocytes to transform, arguing that Myoglianin from non-astrocytic glia drives astrocyte expression of EcR and in turn transformation into phagocytes. Finally, we find that blockade of EcR signaling autonomously in Beat-V_{AM} neurons has only minimal effects on Beat-V_{AM} local pruning of neurites. Why a role for

neuron-autonomous EcR signaling is more fully revealed when astrocytes are also blocked from transformation is an open question. A recent study showed that neuronal ecdysone signaling allows ddaC neurons to become competent for pruning by driving microtubule rearrangement, with subsequent physical force caused by tissue movement in the body wall during metamorphosis driving the severing and fragmentation of dendrites (Krämer, Wolterhoff et al. 2023). It is possible that neuronal ecdysone signaling may make Beat-V_{AM} neurons competent for remodeling through similar mechanisms, but execution of fragmentation requires a secondary mechanical event. Astrocytes could, for example, provide the physical force that severs small neurites during metamorphosis as they transform and become phagocytic, as we observed a tight correlation between astrocyte transformation and Beat-V_{AM} neurite fragmentation. We note that the fragmentation we observed when EcR signaling was blocked in Beat-V_{AM} neurons occurred primarily in smaller diameter Beat-V_{AM} neurites. Perhaps the architectural integrity of large versus small diameter of a neuronal process makes fine neurite processes more susceptible to remodeling, as larger processes are more likely to be microtubule rich while smaller processes are more likely actin-based. We therefore speculate that astrocytes activate Beat-V_{AM} neuron local pruning either through secretion of a different signaling factor, through the physical force astrocytes generate during transformation into phagocytes, or both.

We further demonstrated that Beat-V_{AL} neurons die in a caspase and steroid hormone-dependent fashion, similar to other neuronal cell types that undergo cell death at metamorphosis (Choi 2006, Lee, Sehgal et al. 2013). However, we found that the Hox

gene *Abd-B* controls the segment-specific patterns of Beat-Va_L neuron cell death, with the three Abd-B⁺ posterior Beat-Va_L cells undergoing cell death, while the anterior two Abd-B-negative cells survive. Knocking down *Abd-B* in Beat-Va neurons blocked caspase activation and cell death in the posterior cells, while overexpressing *Abd-B* in Beat-Va neurons drove cell death in the two, normally surviving, anterior Beat-Va_L cells. Notably, neither overexpression nor knockdown of *Abd-B* had any noticeable effect on Beat-Va_M neuron local pruning, despite their having a similar segmentally-restricted pattern of Abd-B expression in segments A5-7. We interpret these data to mean that Abd-B confers positional identity that leads to cell death in the appropriate Beat-Va_L cells.

Hox genes such as *Abd-B* can function as a pro-apoptotic or anti-apoptotic molecules. In some cases, Abd-B can drive caspase-mediated cell death through direct regulation of gene expression. Abd-B-driven chromatin remodeling can lead to exposure of activator genes *grim*, *reaper*, and *hid*, thereby enabling activation of apoptotic death (Arya, Sarkissian et al. 2015). Abd-B can also physically bind the transcription co-factor Dachshund, and these factors have been shown to work cooperatively to induce cell death in some embryonic neurons (Clarembaux-Badell, Baladrón-de-Juan et al. 2022). In other cases, for instance in Beat-Va_M neurons, Abd-B expression clearly does not regulate cell death at all, presumably because pro- or anti-apoptotic functions of Abd-B are regulated by cell type-specific co-factors. Finally, additional studies of the Abd-B ortholog, HOXA10A, have revealed that hox genes can modify cell death through production of long non-coding RNAs and other post transcriptional modifications during cancer metastasis (Chen, Kan et al. 2022). Whether and how these mechanisms might relate to

the role of Abd-B in driving segment-specific cell death is an interesting question for the future.

2.5 Methods and notes

2.5.1 Key Resource Table

REAGENT or RESOURCE	SOURCE	IDENTIFIER
Antibodies		
Chicken polyclonal anti GFP 1:500	Abcam	Ab13970 RRID: AB_300798
Mouse conjugated FITC anti GFP 1:200	Rockland	600-302 RRID:AB_218217
Rabbit polyclonal anti HA 1:250	Bethyl	A190-108P RRID:AB_162713
Rat polyclonal anti FLAG 1:200	Novus	1-06712 RRID:AB_1625982
Mouse monoclonal anti V5 1:500	Invitrogen	R960-25 RRID: AB_2556564
Mouse monoclonal anti Even-Skipped	DSHB	3C10 RRID:AB_528229
Mouse monoclonal anti Engrailed	DSHB	4D9 RRID:AB_528224
Mouse monoclonal anti EcR-B1	DSHB	AD4.4 RRID:AB_2154902
Mouse monoclonal anti Abd-A	DSHB	FP6.87 AB_10660834
Mouse monoclonal anti Abd-B	DSHB	1A2E9 AB_528061

Rabbit polyclonal cleaved Dcp-1	Cell signaling Technology	9578 RRID:AB_2721060
Rabbit polyclonal anti - Crz	Yunsik Kang	
Alexa Fluor 488 AffiniPure Donkey Anti-Chicken IgY (IgG) (H+L)	Jackson Immunoresearch	703-545-155 RRID:AB_2340375
Cy3 AffiniPure Donkey Anti-Rabbit IgG (H+L)	Jackson Immunoresearch	711-295-152 RRID:AB_2340613
Alexa Fluor 488 AffiniPure Donkey Anti-Rabbit IgG (H+L)	Jackson Immunoresearch	711-545-152 RRID:AB_2313584
Alexa Fluor 488 AffiniPure Donkey Anti-Rat IgG (H+L)	Jackson Immunoresearch	712-545-153 RRID:AB_2340684
Cy3 AffiniPure Donkey Anti-Rat IgG (H+L)	Jackson Immunoresearch	712-165-153 RRID:AB_2340667
Alexa Fluor® 488 AffiniPure Donkey Anti-Mouse IgG (H+L)	Jackson Immunoresearch	715-545-151 RRID:AB_2341099
Cy™5 AffiniPure Donkey Anti-Mouse IgG (H+L)	Jackson Immunoresearch	715-175-151 RRID:AB_2340820
Cy™3 AffiniPure Donkey Anti-Mouse IgG (H+L)	Jackson Immunoresearch	715-165-151 RRID:AB_2315777
Bacterial and virus strains		

One Shot TOP10 Chemically Competent E. coli	ThermoFisher	Cat#C404010
Experimental models: Organisms/strains		
w1118; P y+t7.7 w+mC=GMR31C03-GAL4 attP2	BDSC	#48103
w1118; P y+t7.7 w+mC=GMR77E07-GAL4 attP2	Janelia	32250
w1118; P y[+t7.7] w[+mC]=GMR92H04-GAL4 attP2	Janelia	33723
Crz-GAL4	Jae Park	
w1118 P R57C10-FLPG5.PEST attP18; P 10xUAS(FRT.stop)myr::smGdP-OLLAS attP2 PBac 10xUAS(FRT.stop)myr::smGdP-HA VK00005 P 10xUAS(FRT.stop)myr::smGdP-V5-THS-10xUAS(FRT.stop)myr::smGdP-FLAG su(Hw)attP1	BDSC	#64091
w1118 P hs-FLPG5.PEST attP3; PBac10xUAS(FRT.stop)myr::smGdP-HA VK00005 P 10xUAS(FRT.stop)myr::smGdP-V5-THS-10xUAS(FRT.stop)myr::smGdP-FLAG}su(Hw)attP1	BDSC	#64085
y[1] w[*]; betaTub60D[Pin-Yt]/CyO; P w[+mC]=UAS-mCD8::GFP.L LL6	BDSC	#5130

UAS-P35 (Second chromosome)	Thummel	
w1118; P UAS-EcR.B1-ΔC655.W650A TP1-9	BDSC	#6872
w1118; P UAS-EcR.B1-ΔC655.F645A TP1	BDSC	#6869
w1118 P UAS-bsk.DN 2	BDSC	#6409
y1 w*; P UAS-CD4-tdGFP 8M2	BDSC	#35839
w[1118]; P w[+mC]=UAS-lacZ.NZ 20b	BDSC	#3955
w1; P UAS-Abd-B.m.C 1.1	BDSC	#913
y1 sc* v1 sev21; P TRiP.GLV21012 attP2	BDSC	#35647
y[1] v[1]; P {y[+t7.7] v[+t1.8]=TRiP.JF02546} attP2	BDSC	#27258
y[1] sc[*] v[1] sev[21]; P {y[+t7.7] v[+t1.8]=TRiP.HMS02203} attP40	BDSC	#41670
UAS-Dronc ^{DN}	(Kondo, Senoo-Matsuda et al. 2006)	
y[1] v[1]; P {y[+t7.7] v[+t1.8]=TRiP.HM05120} attP2	BDSC	#28909
w1118 P {UAS-bsk.DN} 2	BDSC	#6409
UAS-Atg1 ^{DN(K38Q)}	(Scott, Juhász et al. 2007)	
y[1] v[1]; P {y[+t7.7] v[+t1.8]=TRiP.JF03248} attP2	BDSC	#29569
UAS-Wlds	(Hoopfer, McLaughlin et al. 2006)	
P {ry[+t7.2]=hsFLP} 12, y[1] w[*]; P {y[+t7.7] w[+mC]=UAS-Cas9.P2} attP40	BDSC	#58985

y[1] v[1]; P{y[+t7.7] v[+t1.8]=TKO.GS01063}attP2	BDSC	#77246
y[1] v[1]; M{v[+t1.8]=WKO.5-F2}ZH-86Fb	BDSC	#84163
y1 v1; M{WKO.1-F11}ZH-86Fb	BDSC	#83089
y1 v1; M{WKO.5-D2}ZH-86Fb/TM6B, Tb1	BDSC	#84961
y1 sc* v1 sev21; P{TRiP.HMC05055}attP40	BDSC	#60062
w[*]; P{y[+t7.7] w[+mC]=UAS- babo.a.RNAi}attP16	BDSC	#44400
Alm-Gal4	Doherty et al. 2009	
w[1118]; P{y[+t7.7] w[+mC]=GMR25H07- lexA}attP40	BDSC	#52711
w[*]; P{w[+mC]=13xLexAop2-CD4- tdTom}4/CyO, P{Wee-P.ph0}Bacc[Wee-P20]	BDSC	#52271
w[*]; PBac{y[+mDint2] w[+mC]=13xlexAop Jupiter.sfGFP}VK00033/TM6B, Tb[1]	BDSC	#77134
UAS-Myo-RNAi	(Awasaki, Huang et al. 2011)	
UAS-mCD8-cherry	Made by A. Sheehan	
drprΔ5 (draper -/-)	(Freeman, Delrow et al. 2003)	
y[1] w[*]; P{w[+mC]=UAS-drpr.RNAi}2/CyO	BDSC	#67034
w1118; P{GD14457}v40627	VDRC	#40627

w1118; P{GD14457}v27180	VDRC	#27180
y1 w*; Mi{Trojan-GAL4.1}CG3164MI10825-TG4.1 ND-15MI10825-TG4.1-X/SM6a	BDSC	#76211
w1118; P{GD777}v42734	VDRC	#42734
P{KK106749}VIE-260B	VDRC	#108413
UAS-myr-GFP-V5-P2A-H2B-mCherry-HA/TM3, Ser	Chang et al. 2019	
Alm-Lex	Yunsik Kang	
elaV-Gal80	(Yang, Rumpf et al. 2009)	
UAS-EGFP-L10a	(Huang, Ainsley et al. 2013)	
Software and algorithms		
FIJI	Schindelin et al	RRID:SCR_002285
Imaris 10.0	Bitplane	RRID:SCR_007370
Prism	Graphpad	RRID:SCR_002798
R		RRID:SCR_001905

2.5.2 *Drosophila* Genetics

Drosophila melanogaster were raised using standard laboratory conditions. All experiments were conducted at 25°C unless otherwise explicitly noted. A complete list of all fly strains used in this study can be found in the key resource table.

2.5.3 Immunohistochemistry

Dissection and immunostaining of larval fly brains were performed according to the FlyLight protocols (Jenett, Gerald et al. 2012). Larval brains were dissected in cold 1X PBST (phosphate buffered saline, Invitrogen) with 0.1% Triton X-100 and fixed at 4% paraformaldehyde (PFA, Electron Microscopy Sciences) for 20 minutes at room temperature. Fixed brains were washed three times with 1X PBS while nutating at room temperature for 10-15 minutes per wash. Primary and secondary antibodies were diluted in PBST (0.1% Triton X-100) and incubated with samples at 4° C for 24-48 hours. Washes after antibody incubations were done at room temperature with 1X PBS for 3 X 15 minutes. Samples were mounted in VECTASHIELD antifade mounting medium (Vector Laboratories) and stored at 4° C until imaging

2.5.4 Translating Ribosome Affinity Purification Sequencing

Drosophila Strains: To generate flies in which ribosomes were tagged in astrocytes, flies with *elaV-Gal80* were crossed with *Alrm-Gal4*. Larval brains were dissected at the WL3 stage pupa brains at 2 hours and 6 hours into metamorphosis. 100 animals were pooled for each sample and 3 samples were evaluated at each time point.

Sample Preparation: Brains were transferred into an RNase free Eppendorf tube and kept on ice until 5 larvae or pupae were collected, no longer than 20 minutes. Samples were then stored at -80° C.

Lysate preparation: Samples were homogenized in lysis buffer (20 mM HEPES KOH pH 7.4, 5 mM $MgCl_2$, 150 mM KCl, protease inhibitor, with 0.5 mM DTT, 100 μ g/mL cycloheximide, 50 μ g/mL emetine, 10 μ l/mL SUPERase-in RNase inhibitor and 10 μ l/mL RNase OUT ribonuclease inhibitor added right before use). 250 μ l buffer was added to each tube of 50 samples. Samples were then placed on ice and homogenized for 20-30 seconds using pestles (Biomasher II, Kimble). 1 mL supernatant was transferred into a new tube. To each sample, 111 μ l NP-40 was added and was mixed gently by inversion. Then, 123 μ l DHPC was added and mixed gently by inversion and incubated on ice for 5 minutes. Samples were centrifuged at 16,100xg at 4° C for 15 minutes.

Bead preparation: 375 μ l of Protein G Dynabeads were prepared for each sample. Beads were washed 3 times for 5 minutes with shaking in a 0.15M KCl wash buffer (20 mM HEPES-KOH pH 7.4, 150 mM KCl, 5 mM $MgCl_2$, 1% NP-40 with mM DTT, 100 μ l/mL cycloheximide and 50 μ g/mL emetine added immediately before use) and were pelleted using a magnetic stand. Stock solutions of cycloheximide were prepared in MeOH at a concentration of 10 mg/mL and emetine prepared in EtOH at a concentration of 50 mg/mL. After the third wash, beads were resuspended in 0.15 KCl and GFP antibodies (50 μ g of each of HTXGFP-19C8 HTZGFP-19F7) up to a total of 375 μ l per

sample. Beads were incubated at RT for 2 hours with end over end rotation. Unbound antibody was removed by washing 3 times for 5 minutes in the 0.15 M KCl wash buffer.

Pull-down: For each sample, 1mL supernatant was transferred to the washed GFP-bound beads. Beads were resuspended in sample lysates and incubated at 4° C with end over end rotation for 30 minutes. Beads were then washed 3 times for 5 minutes at 4° C in 0.35 M KCl wash buffer (20 mM HEPES-KOH pH 7.4, 350 mM KCl, 5 mM MgCl₂, 1% NP-40 with 0.5 mM DTT, 100 µg/mL cycloheximide and 50 µg/mL emetine added immediately before use). Samples were then placed on ice for up to 20 minutes.

RNA recovery: Buffer was removed and samples were resuspended in RLT buffer (Qiagen RNA minelute kit) with BMe added just before use. Tubes were mixed by inversion to resuspend the beads and placed on ice. RNA isolation was performed according to the instructions provided with the kit. RNA was eluted by adding 100 µL of water to the membrane, spinning for 1 minute, and the adding another 10µl of water and repeating the spin step.

RNA sequencing and analysis: RNA quality and quantity was assessed using an Aligent 2100 Bioanalyzer and and RNA 60000 PicoChip run with the eukaryotic total RNA program. Concentrations ranged from .5ng/µl -24.5ng/µl as measured with the Aligent RNA 6000 Pico Assy. RIN values ranged from 5.8-8.2. cDNAs were prepared with SmartSeq Ultra Low input kit (Takara). The cDNAs were fragmented with an S220 sonicator and sequencing libraries prepared using a TruSeq stranded ribosomal reduction protocol (Illumina). Libraries were prepared using a low-input protocol. cDNAs were prepared with the SmartSeq Ultra Low Input kit (Takara). The cDNAs were fragmented

with an S220 sonicator (Covaris) and sequencing libraries were prepared using the DNA Nano Prep Kit (Illumina). Libraries were profiled with a TapeStation (Agilent) and quantified using an NGS Quantification Kit (Kapa BioSystems/Roche) on a StepOnePlus Real Time PCR Workstation (Thermo/ABI). Libraries were sequenced on a HiSeq 2500 (Illumina). Fastq files were assembled using bcl2fastq (Illumina).

2.5.5 Image Analysis and Processing

Imaging of fixed larval brains was performed using a Zeiss LSM 880 with Airyscan. Confocal z-stacks were acquired using the optimal z-interval and around 0.05-0.09 μm /pixel resolution with a 40x/1.3 Plan-Apochromat oil objective. Images were Airyscan processed, images tiles stitched with a 6-8% overlap when necessary and converted into IMARIS format for 3D analysis. Images that needed to be rendered in 3-D were loaded into IMARIS; images where either a single z-stack or a z-projection was needed were loaded into ImageJ.

2.5.6 Analysis and statistics

To quantify individual neuronal morphologies, we used the Surface module in IMARIS 10 (Bitplane) with the Filament module. The module was trained on example images through iterative machine learning and then the algorithm was applied to all images. The first 100 μm of each neuron after it crossed the midline was analyzed for both total filament length and number of branch points. All statistical analyses were carried out using GraphPad Prism 9; statistical details, p values, and numbers of analyzed samples

are indicated in the figure legends. Any comparison between two parametric data sets that only had one independent variable was conducted with a student t-test. Any comparison between more than two parametric data sets that only had one independent variable was conducted with a One-way ANOVA with the Sidak test for multiple comparisons. Any comparison between more than two non-parametric data sets that only had one independent variable was conducted with a One-way ANOVA with the Kruskal-Wallis test for multiple comparisons. Any comparison between more than two parametric data sets that had two independent variable was conducted with a Two-way ANOVA with the Sidak test for multiple comparisons.

2.5.7 Generating *BeatVa-LexA* Stock

BeatVa-LexA lines were made with Gateway cloning. The 3471 base pair enhancer region was cloned with primer sequences provided on the *Janelia Flylight* page. They were cloned into the *pBPnlsLexAGADflUw* vector (#26232 Addgene) and verified through Sanger sequencing (Genewiz). Injections were site directed using the $y^1 w^{67c23}; P[CaryP attP2]$ line (BL8622), $y^1 w^{67c23} P[CaryP attP18]$ (BL 32107) line and $y^1 w^{67c23}; P[CaryP attP40]$ line. The *attP18* insertion was used in all above experiments. The line was verified by comparing GFP expression generation from the *Beat-LexA* line driving a *LexAop-GFP* to a *BeatVa-Gal4* line driving a *UAS-mCD8::cherry*.

2.5.8 Generating *LexAop-EcR^{DN}* Stock

The *LexAop-EcR^{DN}* construct was created by amplifying DNA from flies containing *UAS-EcR.B1DC655.W650A* (Bloomington Drosophila Stock Center). The amplification was carried out using the EcR^{DN} Kozak *AgeI* F primer (cccccaACCGGTcaaaacATGAAGCGGCGCTGGTCGAACA) and EcR^{DN-W650A} *XbaI* R primer (cccaatctagaCTAGATGGCATGAACGTCGGCGA). The resulting PCR product was digested with *AgeI* and *XbaI* (NEB) and then ligated into the *pattB-13xLexAop2EGFP* plasmid (Coutinho-Budd, Sheehan et al. 2017), with GFP removed via *AgeI* and *XbaI* digestion. The final construct, *pattB-13xLexAop2-EcR^{W650A}*, was generated through ligation using T4 ligase (NEB), and the transformation was carried out in *DH5a* cells (Zymo). The construct's sequence was verified through Sanger sequencing (Genewiz), and it was utilized for attP154 landing site-specific integration on the 2nd chromosome (Bestgene).

2.5.9 *BeatVa-Gal4* turns on embryonically

One early concern with this project was around the strength and duration of the *BeatVa-Gal4* driver. It was possible that the GAL4 didn't turn on until late in the larval stages, which could mean that manipulations resulted in no phenotype because the GAL4 perdurance wasn't long enough to allow for expression of whatever was downstream of the UAS. To address this, we imaged embryos and assessed expression of a UAS driven GFP under control of the *Beat-Gal4*. We found high GFP expression in the embryo, indicating to us that GAL4 turned on early (Figure 19).

Figure 19 BeatVa-Gal4 turns on in Drosophila embryos

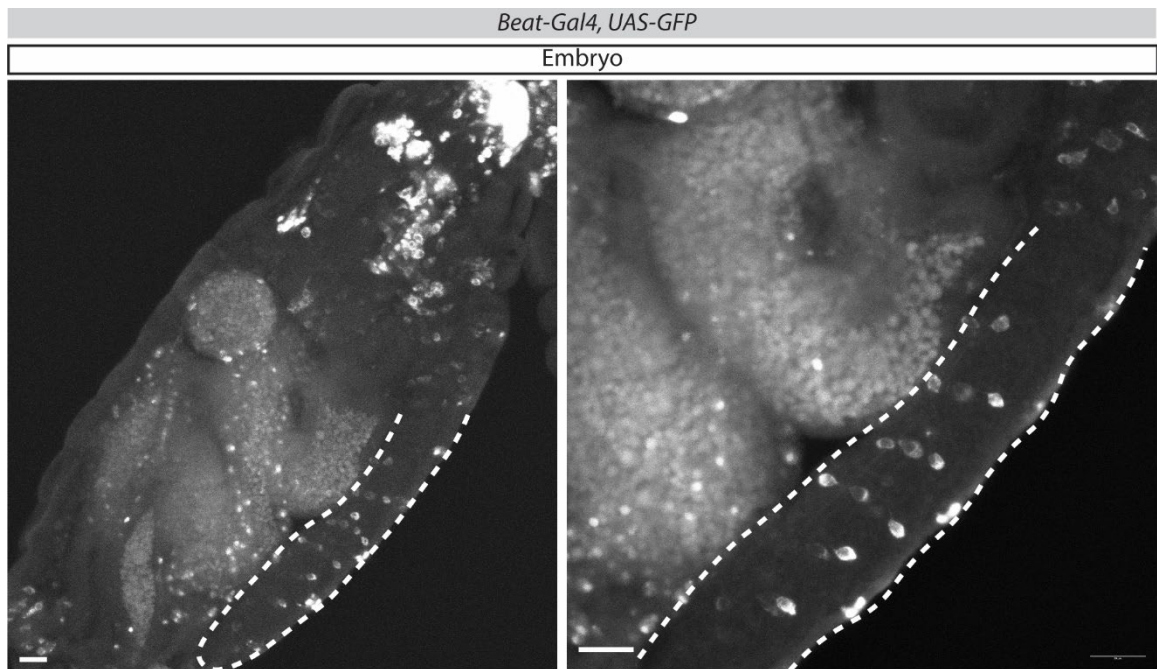


Figure 19: Confocal microscopy Z-stack of a *Drosophila* embryo with Beat-Va cells labeled via *Beat-Gal4, UAS-mCD8::GFP*. Ventral nerve cord is outlined with a dashed line and magnified to visualize Beat-Va cells in the ventral nerve cord. Scale bar is 20 microns.

Chapter 3 Discussion

3.1 Identifying new populations of neurons that remodel during metamorphosis

In this project I sought to identify and characterize new neuronal populations that either die or locally prune during *Drosophila* metamorphosis. Through screening a large collection of *Gal4* driver lines, I identified *BeatVa-Gal4*, along with *CadN-Gal4* and *Pvf3-Gal4* (characterized in Appendices A and B, respectively) which labeled five, previously uncharacterized, morphologically distinct neuronal populations (Figure 20). These neurons undergo apoptotic death or locally prune neurites over the first twelve hours of *Drosophila* metamorphosis. As described in the previous chapter, medial *BeatVa-Gal4*-expressing neurons use an exciting new mechanism that involves astrocyte to neuron signaling. Additionally, I re-examined the relationship between cell death, ecdysone signaling and neurite pruning in vCrz neurons (Appendix C). In contrast to previous reports, I found that many small neurites continue to prune even upon inhibition of ecdysone signaling or cell death, arguing that ecdysone/caspase-independent signaling events can drive remodeling.

Figure 20 New populations of neurons that remodel during metamorphosis



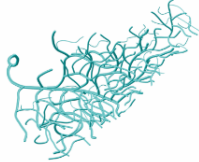


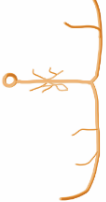


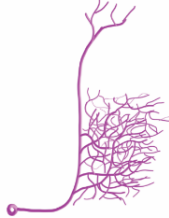

Gal4 Line	Neuron name	Expression pattern	WL3	HE
<i>CadN-Gal4</i>	CadN neuron	VNC Probably 1 cell per hemisegment		
<i>Pvf3-Gal4</i>	Fountain neuron	Lobes 1 cell per lobe		
	Stick neuron	VNC Crosses midline Probably 1 per hemisegment		
<i>Beat-Gal4</i>	Beat _L	VNC Crosses midline 1 per hemisegment		
	Beat _M	VNC Crosses midline 1 per hemisegment		

Figure 20: Summary of *Gal4* driver lines that label new populations of neurons that remodel during metamorphosis. CadN neurons are characterized in Appendix A. Pvf3 neurons are characterized in Appendix B. Beat-Va neurons are discussed extensively in Chapter 2.

3.2 The role of ecdysone signaling in *Drosophila* neurite pruning

Neuronal ecdysone signaling drives the vast majority of neuronal remodeling in *Drosophila*, including local pruning in neurites (Lee, Marticke et al. 2000, Watts, Hoopfer et al. 2003). A key step in our screen of the Gal4 collection from Janelia's

FlyLight collection entailed identifying cells that remodel even when they express EcR^{DN}, as we hoped to identify new, ecdysone independent mechanisms of remodeling. In CadN neurons, Pvf3_B cells, and Beat-Va_M neurons, fine neurites continued to prune even when ecdysone signaling was blocked. In all aforementioned cases, the fine neurite projections fragmented and disappeared by twelve hours into metamorphosis, however the large axonal projection in each cell type remained intact. Analysis of these cell types should provide new insights into the ecdysone independent signaling events that drive neuronal remodeling during metamorphosis.

To rigorously test if remodeling that I observed did not depend on ecdysone, I performed a series of experiments to evaluate the tools I used to manipulate ecdysone signaling. Through IF, I confirmed that EcR^{DN} was well expressed in all Beat-Va neurons during the first twelve hours of metamorphosis. Additionally, blocking ecdysone signaling with EcR^{DN} blocked Beat-Va_L death indicating that the construct could block ecdysone signaling in some contexts. Preliminary data also showed that driving an EcR^{DN} with *Pvf3-Gal4* blocked stick cell remodeling but not Pvf3_B remodeling, again suggesting that we could block ecdysone driven events with our tools. Finally, I directly depleted EcR from Beat-Va neurons with gRNAs/Cas9 technology or eliminated it genetically (e.g concurrently knocking down BaboA and Plum), but these did not stop Beat-Va_M remodeling. Collectively these data indicate that other mechanisms, besides neuron-specific, ecdysone-mediated signaling, drive pruning in Beat-Va_M and Pvf3_B neurons.

vCrz neurons provide the opportunity to examine how blocking apoptotic cell death, steroid signaling, or other pathways affect cell death and neurite fragmentation.

Blocking ecdysone was reported to block cell death and save neurite branches from fragmentation in vCrz neurons (Wang, Lee et al. 2019). However, we found that this was not the case. When we blocked ecdysone signaling, we did block cell death but the fine projections continued to prune. The previous authors relied largely on antibody staining and low-resolution microscopy, whereas we were fortunate to be able to use genetic tools to label cells with membrane tethered GFP, and high-resolution confocal microscopy. The vCrz data, and our observations that Beat-V_{AM}, CadN neurons, and Pvf3_B cells all continue to display local neurite pruning specifically in smaller neurites when neuronal ecdysone signaling is blocked, suggests that fine neurites use another mechanism in addition to, or in place of, ecdysone driven neurite fragmentation. Different underlying cytoskeletal architecture between fine projections and thick processes could dictate dynamic changes in the fine processes of the neurons examined in this study, as has been shown in ddaC neurons in the PNS (Wang, Rui et al. 2019).

Studies in MB γ neurons—the only well characterized model for local neurite pruning in the CNS prior to this study—have helped define some of the molecular and cellular mechanisms that drive local axon pruning in *Drosophila* (Lee, Marticke et al. 2000). MB γ neurons are somewhat unusual compared to neurons in the VNC, they are not particularly complex, with only a single dorsal- or medially-projecting axon, and they form a tightly fasciculated bundle of ~1000 neurons (Lee, Lee et al. 1999). The neurons explored in this thesis (e.g. Beat-Va and Pvf3 neurons) are quite different, in that they are not part of a large homogenous bundle, and are highly branched. These differences in morphology might change the types of pruning mechanisms engaged by neurons. To

understand if neuronal ecdysone signaling drives remodeling in neurons of varying complexity, we could examine other neurons from our initial Flylight identification screen during remodeling in the presence and absence of normal, neuronal ecdysone signaling.

Alternatively, neuronal ecdysone signaling may make some neurons more competent for remodeling, but the neuron could require a secondary process to fully execute pruning. A recent study shows that neuronal ecdysone signaling allows *ddaC* neurons to be competent for pruning by driving microtubule rearrangement, but physical force caused by tissue movement in the body wall during metamorphosis causes the severing and fragmentation of dendrites (Krämer, Wolterhoff et al. 2023). The idea that some neurites are physically broken during local pruning could explain why I consistently observed the fragmentation and clearance of small diameter neurites across neuronal populations, but not larger neurites. Maybe the architectural integrity and diameter of a neuronal process (and the potential stabilization by microtubules) makes a neurite more or less susceptible to remodeling. Smaller neurites could simply be more fragile. The previously described study took place in the PNS where large movements in the tissue correlate to *ddaC* dendrite severing. Similar efforts to track tissue movement in the CNS and neurite fragmentation have not been attempted but could be an interesting future line of investigation. For instance, it could be informative to live image *Beat-V_{AM}*, *Pvf3_B* and *Cad_N* neurons over the course of neurite fragmentation and see if fragmentation events correlate to gross tissue movement and expansion, like what has been observed in the PNS *ddaC* neurons.

Astrocytes could also induce fragmentation of small neurites through physical force as they transform into phagocytes. Astrocytes undergo a stark morphological change during the same time course that Beat, Pvf3, CadN and vCrz neurons remodel (Hakim, Yaniv et al. 2014, Stork, Sheehan et al. 2014, Tasdemir-Yilmaz and Freeman 2014). Moreover, I found that inhibition of astrocyte transformation blocks about 50% of remodeling in Beat-V_{aM} neurons and preliminary data suggest this holds true in Pvf3_B neurons (Appendix B). In Beat-V_{aM} neurons, concurrently inhibiting astrocyte transformation and neuronal ecdysone signaling fully stops neurite pruning. This could be explained by changes in physical forces as described above, or molecular signaling between neurons and astrocytes that drives fragmentation. Divorcing the physical rearrangement of astrocytic membranes from other molecular events that occur at the onset of astrocyte transformation will be difficult. Answers may be found through further investigation of the products of my screen for astrocytic signaling molecules that promote Beat-V_{aM} neuron fragmentation. Furthermore, we have recently established an *ex vivo* live imaging set up in the lab that may allow us to at least correlate astrocyte movement to neurite fragmentation.

3.3 Caspase signaling in neuronal remodeling

To test whether canonical caspase-mediated apoptotic pathways drove neurite remodeling, we cell-specifically blocked caspase activity in Beat-V_a, Pvf3, CadN and Crz neurons. In vCrz neurons and Beat-V_{aL} neurons, caspase inhibition stopped cell death, although in vCrz neurons fine projections continued to remodel. Caspase inhibition did not block neurite remodeling in Beat-V_{aM}, Pvf_B or CadN neurons but may have

inhibited remodeling in Pvf3 stick cells—the population that was also sensitive to ecdysone manipulations. This suggests that caspase activation may be used selectively to drive neurite pruning in some populations of neurons but not others. Alternatively, axons and dendrites could differentially use caspases to execute local pruning. For example, dendrites in DdaC *Drosophila* neurons display high caspase level during dendritic remodeling and inhibiting caspase activity blocks remodeling (Kuo, Jan et al. 2005). Axons in MB γ neurons do not use caspases to drive remodeling, and inhibition of the caspase pathway does not lead to any changes in axonal pruning (Watts, Hoopfer et al. 2003). By establishing new population of neurons like the Beat-Va, Pvf3 and CadN neurons that undergo neurite pruning we will be able to better understand how caspase activation governs local neurite pruning across multiple populations of neurons, thereby gaining a more wholistic picture of how developmental cell death mechanisms intersect with local neurite pruning mechanisms across the *Drosophila* CNS.

3.4 Hox genes in *Drosophila* neurodevelopment

Of the six populations of neurons I characterized, only one displayed positional differences in cell fate. CadN neurons, Pvf3_B, Pvf3 stick cells, and Beat-Va_M neurons all exhibited similar neurite pruning patterns independent of segmental position in the VNC. vCrz neurons all die, although interestingly there are Corazonin neurons in the dorsal lateral brain lobes that survive (dlCrz) (Choi, Lee et al. 2005). Beat-Va_L cells were unusual in that they underwent VNC segment dependent cell death. The two anterior cells survived whereas the three posterior cells died in the first twelve hours of metamorphosis.

We found Hox genes regulated these differences in segment-specific cell death. Hox genes are famously necessary for patterning an animal's body plan (McGinnis and Krumlauf 1992, Quinonez and Innis 2014). In neurodevelopment Hox genes can help determine neuronal identity, specify connectivity, and provide positional information to neurons before brain segmentation occurs (Philippidou and Dasen 2013). Evidence for the interplay between Hox genes and apoptosis in the CNS was first described in neuronal precursors in *C.elegans* (Kenyon 1986) and more examples of how Hox genes interact with caspases to drive or block apoptosis—typically in the embryonic brain or in neuroblasts—soon emerged in *Drosophila* (Bello, Hirth et al. 2003) and mammals (Gaufo, Flodby et al. 2000). The presence of this mechanisms across species argues for an ancient evolutionary role for Hox genes in segmentally-regulated culling of neuronal populations.

The two genes I examined, *abd-A* and *abd-B* can play anti-apoptotic and pro-apoptotic roles during *Drosophila* neurodevelopment in the embryo. *Abd-A*, which can induce neuroblast death during embryogenesis or dictate cell fate specification in the neuroblast 6-4 lineage, was expressed by Beat-Va_L and Beat-Va_M neurons but the expression pattern didn't reflect the pattern of Beat-Va_L cell death (Kang, Kim et al. 2006). Perhaps *Abd-A* plays important roles in Beat-Va neuron targeting and fate later in metamorphosis. Additionally, *Abd-A* can work combinatorically with *ubx* (another Hox gene) and maybe manipulating both *abd-A* and *ubx* concurrently would change Beat-Va_L survival (Konopova and Akam 2014).

Unlike Abd-A, Abd-B protein expression reflected the cell death boundary we observed in the Beat-Va_L cells and manipulation of Abd-B in only the Beat-Va neurons changed Beat-Va_L cell survival. When we knocked down Abd-B expression in Beat-Va neurons, the posterior Beat-Va_L cells that normally underwent cell death survived and no longer activated caspases. When we overexpressed Abd-B in Beat-Va neurons we induced cell death in the anterior Beat-Va_L cells that normally survive, indicating that in some populations Abd-B alone can induce cell death. Curiously, the Beat-Va_M neurons did not show any obvious fate changes when Abd-B was manipulated, even though the three posterior Beat-Va_M neurons had Abd-B protein and knockdown and overexpression of Abd-B worked well in the medial population (as assessed through IF with an antibody against Abd-B). Similarly manipulating Abd-B expression in vCrz neurons did not change cell death patterns (Unpublished, Rachel De La Torre). The molecular basis for these differences remains unknown, but clearly Abd-B does not necessitate cell death in all neuronal populations.

Abd-B can drive caspase mediated cell death through direct regulation of apoptotic genes. Abd-B driven chromatin remodeling can expose the locus for the *Grim*, *Reaper*, and *Hid* activator caspase genes, which enables activation of apoptotic death (Arya, Sarkissian et al. 2015). Beat-Va_M, vCrz and dlCrz neurons may have other proteins that repress the exposure of these genes, or their chromatin structure may not allow for exposure of these cell death genes. Abd-B could also work co-operatively with co-factors that are specific to the Beat-Va_L neurons. A recent study that showed Abd-B can physically bind the transcription co-factor Dachshund and Abd-B and Dachshund

work cooperatively to induce cell death in embryonic *Drosophila* neurons (Clarembaux-Badell, Baladrón-de-Juan et al. 2022). Beat-Va_M, vCrz, and dlCrz neurons may not express transcription co-factors like Dachshund, and if this was the case Abd-B alone would not be able induce cell death.

Finally, there is the question of how Abd-B intersects with ecdysone signaling during metamorphosis. Thus far, all cells that die during metamorphosis can be forced to survive by blocking ecdysone signaling, and my work on Beat-Va_L and vCrz neurons supports this phenomenon. Abd-B could control cell death by regulating EcR expression. However, when we examined EcR protein expression in Beat-Va neurons where Abd-B had been manipulated we found that the Beat-Va neurons continued to express EcR. This leads us to the model in (Figure 21) that shows Abd-B working cooperatively with EcR and a yet-to-be-identified third factor to induce caspase-dependent cell death in subset of neurons. To identify how Abd-B induces caspase drive cell death we could conduct a forward genetic screen in the *Beat-Gal4; UAS-Abd-B* overexpression background and look for mutants where the Beat-Va_L neurons, which reliably die in this background, survive.

Figure 21 *Abd-B* dependent, *EcR* mediated, caspase driven apoptotic cell death

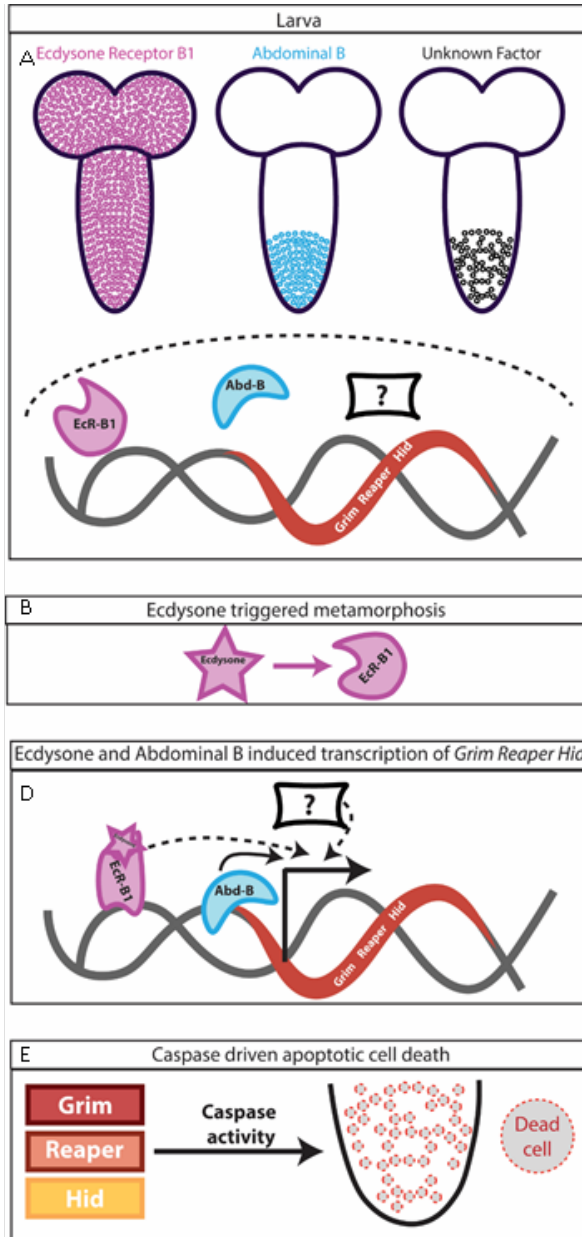


Figure 21: **A)** In a larval brain, both Abd-B and EcR proteins are present along with numerous unknown factors, but they don't activate gene transcription for cell death related genes *grim*, *reaper*, *hid* (GRH). **B)** At the onset of metamorphosis ecdysone binds EcR **C)** allowing for Abd-B to bind the GRH locus and that binding event along with modulation from an unknown factor causes GRH transcription in a subset of cells **D)** leading to caspase activation and **E)** cell death in some cells.

3.5 Hox genes in mammalian neurodevelopment and cell death

In humans, *abd-B* homolog HOXA10 has not been implicated in any neurodevelopmental disorders, but can play both an anti-apoptotic and pro-apoptotic roles in cancer, raising the possibility that better understanding of how *abd-B* either promotes or inhibits cell death could lead to a better understanding of malignant tumor progression (Wang, Liu et al. 2023). Conversely, understanding how HOXA10 drives or inhibits cell death could shed new light on how Abd-B interacts with the caspase pathway to control cell death. Long non-coding RNAs (lncRNAs) are critically important in gene regulation and a lncRNA transcript of HOXA10A was recently identified as central to oral cancer growth and metastasis (Chen, Kan et al. 2022). The lncRNA HOXA10 transcript can bind the tumor protein 63 RNA (TP63) transcript which disrupts normal cell death mechanisms (Chen, Kan et al. 2022). Currently there are no annotated lncRNA transcripts annotated at the *abd-B* locus in *Drosophila*, but future experiments could test if Abd-B mRNA can post-transcriptionally modify mRNA transcripts that are important for cell death and survival, and post-transcriptional modifications could offer insight into how Abd-B and HOXA10 play both pro and anti-apoptotic roles.

Although the homolog of Abd-B, HOXA10, does not play any direct, known, role in neurodevelopment, Hox genes broadly play critical roles in neuron progenitor fate specification in the developing mammalian hindbrain and spinal cord. Inhibition of Hox genes disrupts circuit development, likely due to incorrect neuronal subtype specification (Gonçalves, Le Boiteux et al. 2020). One of the surprising findings from my study was that manipulating Abd-B did not noticeably change cells fate or targeting, suggesting that

in Beat-Va neurons *abd-B* does not determine neuronal type specification. In mammalian neurodevelopment some Hox genes like Hoxb5, contribute to neuronal crest apoptosis during neurodevelopment (Kam, Cheung et al. 2014). Further work in *Drosophila* and other model organism may uncover new biology that informs our understanding of how Hox genes contribute to neuronal death at other stages of neurodevelopment.

3.6 Synaptic vs neurite remodeling

Understanding if single synapses are selected for pruning or if full neurite branches are pruned, could help define what questions future studies should address. Likely both of these processes occur in different contexts and may be driven by different molecular mechanisms, however the current tools used in the mammalian neuronal remodeling field struggle to address this distinction. During development, microglia contain internalized synaptic markers, suggesting that they have pruned synapses to shape circuitry (Neniskyte and Gross 2017). The studies that found this synaptic debris did not examine if microglia also had internalized axon or dendrite debris (Stevens, Allen et al. 2007, Schafer, Lehrman et al. 2012, Neniskyte and Gross 2017). Do glia actually eliminate individual synapses, or do they prune whole branches and eliminate synapses through happenstance?

Our data show that full branches are pruned away in an astrocyte-dependent manner, so, in this case, synaptic pruning along these branches would be due to full branch loss rather than glial selection of individual synapses. Previous work in the lab showed that blocking the transformation of astrocytes into phagocytes also blocked the

clearance of synapses from the VNC neuropil. That work quantified all synapses in the neuropil through IF and didn't examine whether any of the remaining synapses were functionally intact (Tasdemir-Yilmaz and Freeman 2014).

One possibility—based on work from a recent paper that shows the importance in neuronal activity in MB γ neurons—is that some synapses are stripped before neuronal fragmentation, which causes less neuronal activity, driving branch fragmentation and leading to the loss of any remaining synapses (Mayseless, Shapira et al. 2023). I did not examine this in any of the neurons I studied, but such work could provide important insight into how activity, or loss of activity through synapse elimination, drives pruning.

Beat- V_{AM} and Pvf₃ neurons retain their branches when astrocyte transformation is blocked but we don't know if they retain their synapses. With new tools, it would be interesting to evaluate synaptic labels in Beat- V_{AM} or Pvf_{3B} neurons where astrocytic pruning has been blocked and the larval branching patterns are retained. If synaptic pruning and branch elimination use same mechanism, we would expect that neurons that retain their branches will also retain their synapses. If some synapses still disappear during inhibitions of astrocyte transformation, it would indicate that synapse loss and neurite degeneration are genetically separable, and that knowledge could be used to screen neuron intrinsic mechanisms of synaptic pruning that are separable from branch pruning.

What happens to synapses on neuronal branches that don't normally undergo remodeling? In our screen for new lines that undergo remodeling early in metamorphosis, we found several lines whose projections don't change. These could be good populations

to examine synapse specific elimination. The Beat- V_{AM} neuron retains one thick branch throughout the first twelve hours of metamorphosis as do CadN neurons. We don't know if there are normally synapses on these branches, and, if there are synapses, if those synapses disappear during metamorphosis. Previous work would indicate that they should, but that work only used one, presynaptic marker to mark synapses which leaves open the possibility that some small number of synapses are retained through metamorphosis.

3.7 Identifying astrocytic molecules that drive remodeling

Glia broadly drive cell death and pruning, and astrocytes or cortex glia clear debris in the remodeling *Drosophila* brain (Awasaki, Huang et al. 2011, Yu, Gutman et al. 2013, Hakim, Yaniv et al. 2014, Tasdemir-Yilmaz and Freeman 2014). It was not known if astrocytes could actively promote neuronal remodeling. My work on Beat- V_{AM} and Pvf3 B neurons shows they both rely on ecdysone driven astrocyte transformation to execute the bulk of neurite pruning. Based on my experiments, it seems that whatever drives neurite fragmentation lies downstream of astrocytic ecdysone signaling. As previously discussed, astrocytes could induce neurite breakage through physical force when they transform into phagocytes, or astrocytes could release or display some factor that induces neurite pruning. We tried to identify astrocyte-specific factors that might drive neurite fragmentation through a targeted genetic screen. We knocked genes down in astrocytes and evaluated how that knockdown affected Beat- V_{AM} neurons.

This screen produced 29 genes that we considered “hits”. Hits either retained intact Beat-V_{aM} neurites or failed to clear Beat-V_{aM} neurite debris. An important caveat to these findings is that 21 of the 29 hits from the astrocyte screen were the result of a single RNAi knock down. Any future work should confirm these hits through use of other tools such as mutant animals or gene deletion with CRISPR/Cas9.

That said, an interesting correlation emerged from this data: all genes that—when knocked down in astrocytes—strongly stopped Beat-V_{aM} pruning, also blocked astrocyte transformation. This suggests a very tight correlation between astrocyte transformation and Beat-V_{aM} neurite pruning.

An ideal hit would have been one where astrocytes transformed into phagocytes morphologically, and then Beat-V_{aM} neurites failed to prune, but we did not find any molecules in our screen that met this criterion. When *Sema2a*, *CG13784*, or *Dpr-16* were knocked down in astrocytes, there was a weak suppression of Beat-V_{aM} fragmentation, but no debris clearance phenotype. The lack of debris indicates that astrocytes transformed properly and could clear debris as expected, which could argue these molecules are specifically necessary for astrocyte-mediated fragmentation of neurites. It would be interesting to pursue this question in double- or triple-knockdown situations. If concurrently knocking down multiple genes enhances suppression of Beat-V_{aM} fragmentation it would argue for genetic redundancy in the astrocyte-derived signal.

Ongoing work in the lab is using proteomics to identify molecules displayed on the surface of astrocytes while they transform into phagocytes early in metamorphosis. This work may provide a more targeted list of molecules to investigate. For example,

whatever astrocytic molecule that drives Beat-Va_M neurite pruning may not be differentially transcribed during astrocyte transformation but may be differentially trafficked. If this were the case, TRAP-seq would fail to identify the molecule but characterizing the surface proteome would prove more informative.

Future experiments could also re-express astrocytic genes of interest (either the aforementioned genes or proteins identified in the surface proteome) in astrocytes where ecdysone signaling has been blocked to see if particular molecules, downstream of ecdysone signaling are sufficient to either induce astrocytic transformation, induce Beat-Va_M fragmentation or both.

3.8 Identifying new molecules used in astrocyte driven debris clearance

An unintended feature of the astrocyte screen was the identification of new molecules that may be important for clearing neuronal debris during metamorphosis. Knockdown or knockout of *Draper*, the one phagocytic receptor that has been identified as important for astrocytic debris clearance, does not fully disrupt debris clearance, suggesting the existence of other molecules that help with the recognition and internalization of neuronal debris (Tasdemir-Yilmaz and Freeman 2014). Two genes of particular interest emerged from my screen: *beat-IIIb* and *CG31806* which are located in the same gene locus. Two non-overlapping RNAis in this locus produced a phenotype where Beat-Va_M neurites were not cleared. In the future, it would be informative to evaluate the role of these molecules in debris clearance, both in isolation and in combination with *Draper* depletion to explore possible redundancy with *Draper*.

Beat-Va neurons and vCrz neurons may also inform different aspects of how astrocytes clear debris. Astrocytes may recognize and clear debris from dying cells differently from debris in remodeling cells. vCrz neurites display high levels of activated caspases (detected by IF for cleaved DCP-1) before and during fragmentation, while Beat-Va_M neurons do not have detectable caspase activation (Unpublished, Rachel De La Torre), indicating that specific types of cellular debris might have different molecular tags that can be detected by different receptors on astrocytes. Evaluating Beat-Va_M debris clearance and vCrz debris clearance simultaneously could shed light on potential similarities and differences between debris from these cell types.

In closing, my work argues that identifying new populations of neurons to study the details of neuronal remodeling, will lead to discovering new mechanisms that drive cell death and local neurite pruning during metamorphosis. My data suggest that canonical ecdysone signaling works in complex ways to activate a broad array of neuronal remodeling programs, including working in concert with astrocyte-derived cues to promote local neurite pruning. Astrocyte driven pruning of Beat-Va_M neurons—and potentially Pvf3_B neurons—opens the door to incisive genetic analysis of these mechanisms, which I hope will be a line of investigation in the future for our lab and others. This area represents a new role for *Drosophila* astrocytes, previously thought to be primarily responsible for phagocytosing debris after fragmentation. My work also raises interesting questions about the intersection or divergence of mechanisms used to drive cell death and mechanisms used to drive local neurite pruning. I find that at least in some cases, inhibiting neuronal apoptosis does not block local neurite pruning during

metamorphosis further supporting the idea that we are only beginning to understand the molecular complexity of neuronal remodeling.

Appendices

Appendix A: CadN neurons

The *GMR31C03-Gal4* line, *CadN-Gal4*, was created as part of Janelia's Flylight project (Pfeiffer, Jenett et al. 2008). It was generated by fusion of an 1872 base pair fragment from an intronic region of *CadN* to *Drosophila* core synthetic promoter (DCSP) followed by a Gal4 and insertion of the construct into the *attp2* landing site on the 3L chromosome (Pfeiffer, Jenett et al. 2008). *CadN* encodes a member of the cadherin family of proteins, which are calcium-dependent cell adhesion proteins (Iwai, Usui et al. 1997) known to be involved in patterning the nervous system through homophilic interactions (Trush, Liu et al. 2019). The *CadN-Gal4* line drives in medial neurons in the ventral nerve cord (VNC) at the wandering 3rd instar larva stage (WL3). Based on morphology, these are likely motor neurons, as their terminals project out into the muscle field. At the WL3 stage, the neuron has a main branch from a very medial cell body with many fine branches more laterally. Shortly after pupariation, these fine branches bleb (2 APF), fragment (6 APF) and are cleared from the VNC HE (Figure 22). The primary branch that extends out into the periphery remains until at least HE.

Figure 22 *CadN* neurons undergo neurite pruning during metamorphosis.

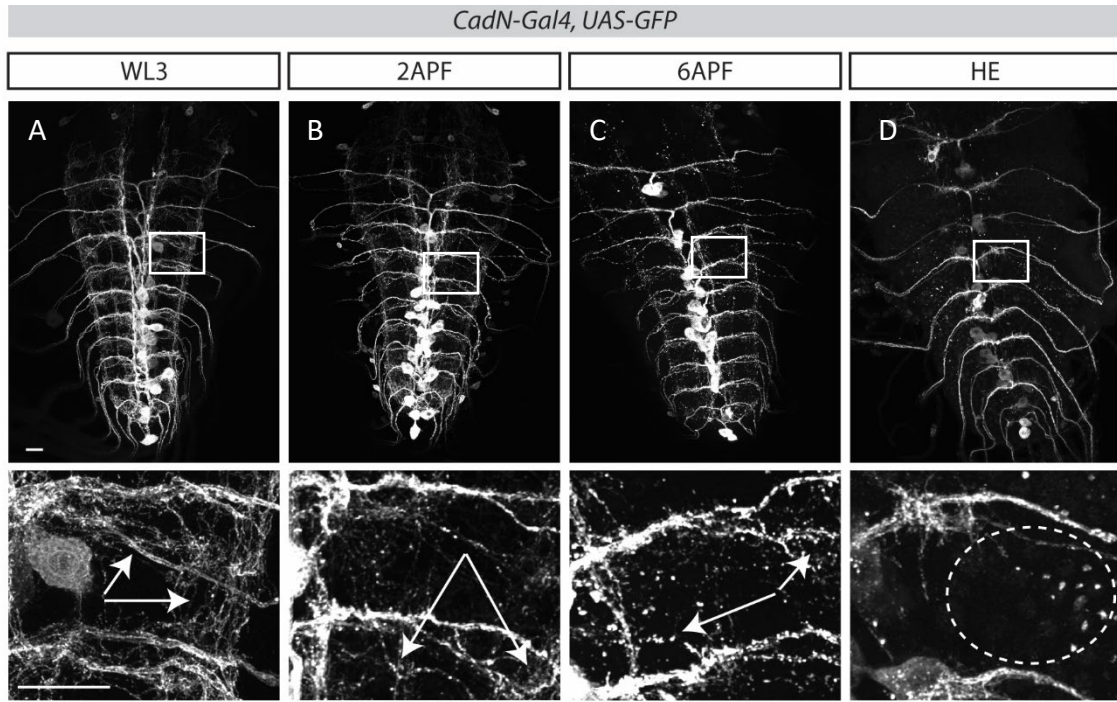


Figure 22: Z-stack of *CadN* neurons in the ventral nerve cord of larvae at indicated stages genetically labeled with *mCD8::GFP* by crossing animals carrying the *CadN-Gal4* construct to animals carrying a *UAS-mCD8::GFP*. Boxed areas are magnified below each image. Arrowheads at **A**) WL3 denote the fine neurites that project from the main branch. **B**) By 2APF, fine projections and are fragmentating and blebbing can be seen (arrows). **C**) At 6APF, most branches have been reduced to debris (arrows). **D**) which is largely cleared by HE (largely empty circle). Scale bars are 20 microns.

We explored whether blocking caspase signaling or ecdysone signaling stopped the remodeling we observed. We inhibited caspases by expressing *UAS-p35*, and ecdysone signaling using *UAS-EcR^{DN}*, using the *CadN-Gal4* driver. Interesting, we found normal pruning of the fine projections from *CadN* neurons in the CNS, suggesting that *CadN*

neurons use a new mechanism a caspase and ecdysone-independent pruning program (Figure 23).

Figure 23 Neither caspase nor ecdysone signaling drives CadN neuron pruning

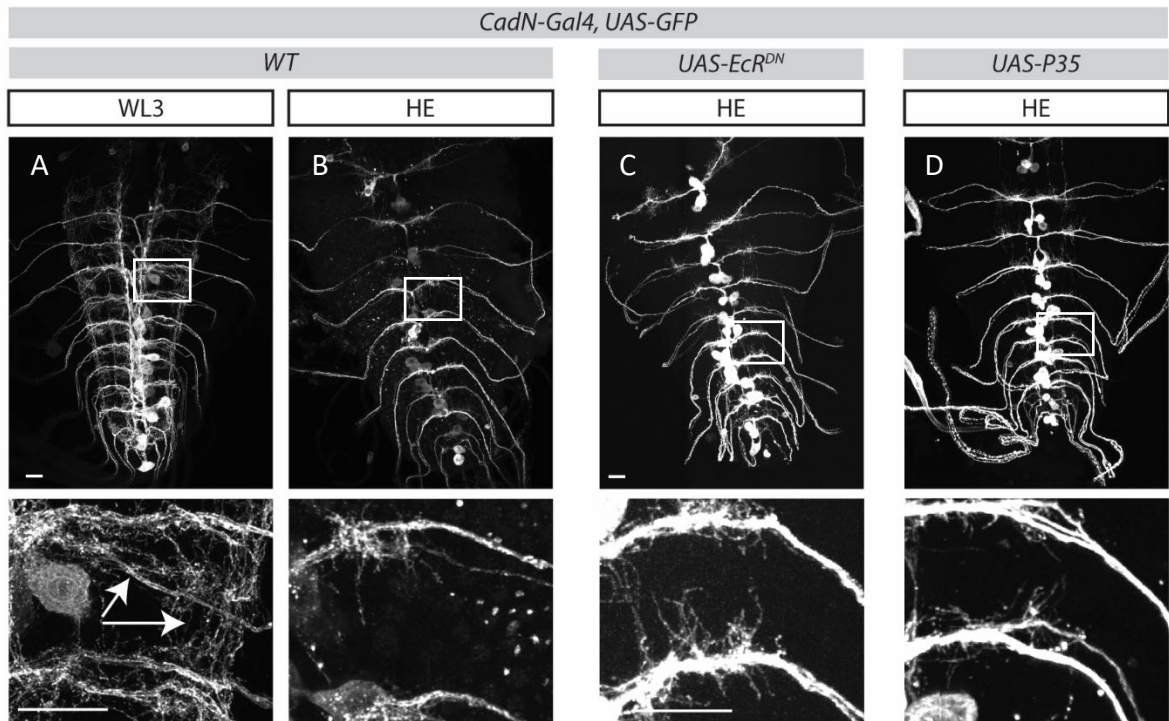


Figure 23: Z-stack of CadN neurons genetically labeled with mCD8::GFP. Boxed areas magnified below. **A)** At WL3 arrowheads indicate the fine projections that **B)** disappear by HE. We would expect that fine neurites would be preserved if their pruning depended on either ecdysone or caspase activation. However, the fine neurites disappear even when **C)** ecdysone signaling or **D)** caspase-driven apoptosis is blocked, indicating that another mechanism drive CadN fine neurite elimination. Scale bars are 20 microns.

One explanation for continued pruning during inhibition of ecdysone or caspase signaling would be that CadN neurons are not capable of undergoing ecdysone-driven caspase activation because they are not competent for receiving ecdysone signaling due to a lack of the EcR receptor. To investigate this possibility, we stained larvae for EcR protein and

examined expression in the CadN cell bodies. We found the EcR-B1 ecdysone receptor (the isoform associated with neuronal pruning) was indeed present in CadN neurons at levels comparable to other neurons at the WL3 stage, suggesting that these neurons are competent to respond to ecdysone (Figure 24).

Figure 24 CadN neurons express EcR-B1

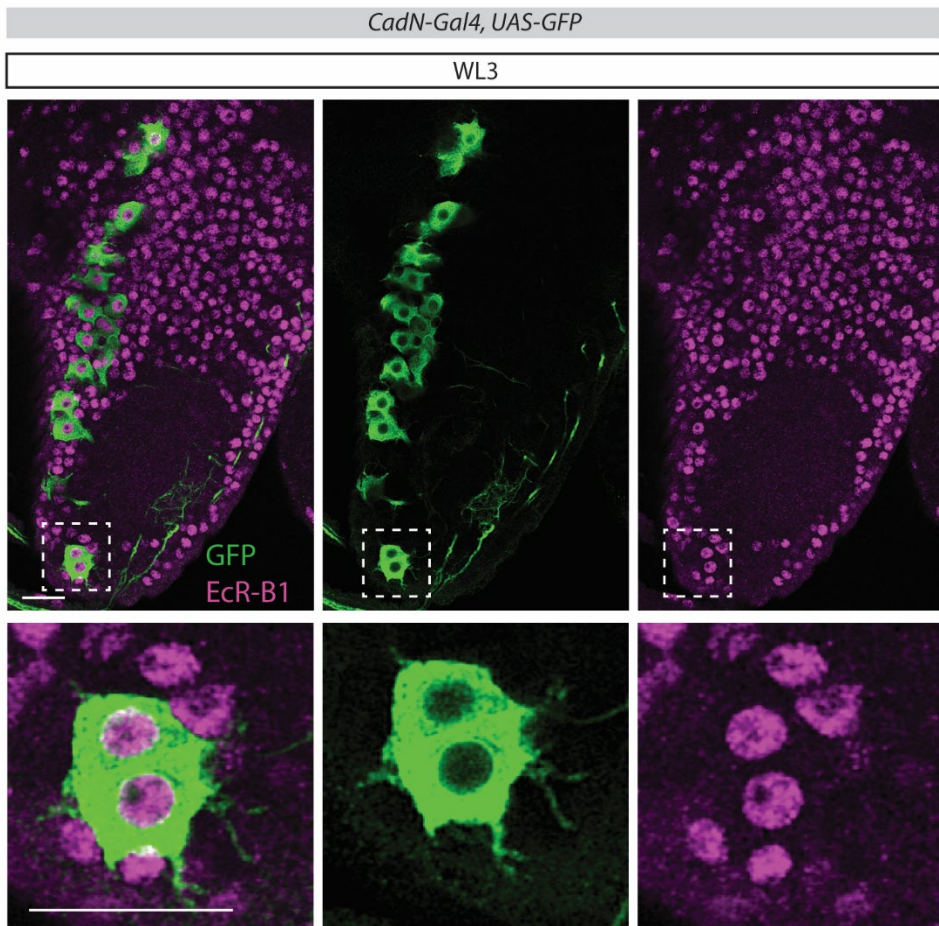


Figure 24: A single Z-plane of CadN neurons expressing mCD8::GFP (**green**) stained with EcR-B1 antibody (**magenta**) to detect nuclear ecdysone receptor presence. CadN neurons are positive for EcR-B1 at WL3. Scale bars are 20 microns.

CadN neurons may therefore be an interesting population of cells to study motor neuron remodeling. In the future, fillet preparation dissections that preserve the brain, along with the larval body wall, might help answer if these neurons project outside of the CNS and where they might project to.

Appendix B: Pvf3 neurons

The Pvf3 neurons are labeled by the *GMR77E07-Gal4* line, which was generated by fusing a 3,974-intron region of *Pvf3* to the DSCP and Gal4 promoter. Pvf3 is a ligand for the receptor tyrosine kinase Pvr, which is involved in neuron-glia signaling in embryogenesis (Read 2018). When we examined the expression pattern of this line, the most striking features were complex projections in each brain lobe that were refined by HE, and smaller complex projections near the midline of the VNC that also underwent refinement by HE (Figure 25). Given the complexity of the neurons labeled by the driver line, we used MCFO approach to track identifiable, single cells and understand which cells produced the projections we observed in the brain lobes and VNC. We found three populations of neurons each with distinct morphologies. The neuronal projections in the brain lobes were produced by a neuron in the brain lobe (Pvf3_B cells) instead of a cell that projected from the VNC. The cells that produced the medial VNC projections (which we termed stick cells) have cell bodies in the VNC and project contralaterally. A second population of cells in the VNC with a more complex morphology we termed branching ladder cells (Figure 25-28).

Figure 25 Pvf3 neuron refinement during metamorphosis

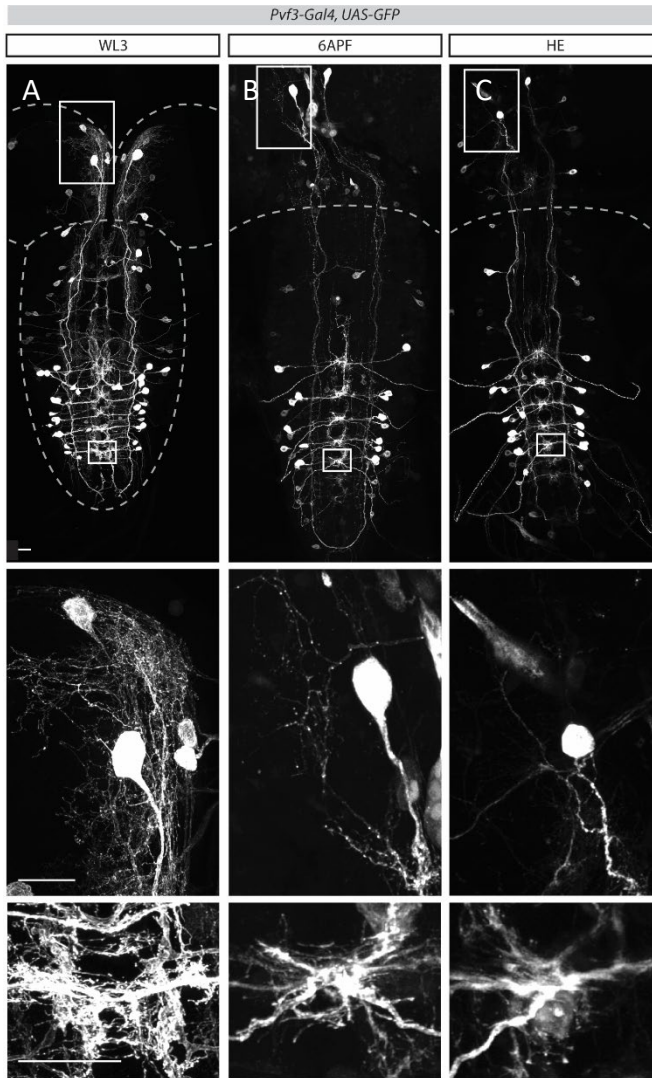


Figure 25: **A)** Z-stack of Pvf3 neurons genetically labeled with mCD8::GFP. Brain (VNC + 2 lobes) is outlined at WL3 with boxed regions shown at high magnification to show neurite structure. The boundary between the VNC and lobes is demarcated at 6APF and HE. **B)** Top projection shows clear degeneration of projections in the lobes by 6APF and **C)** almost complete elimination of most processes by HE. The bottom images show medial projections in the VNC and a loss of complexity from WL3 to HE. Scale bars are 20 microns.

Figure 26 Pvf3_B cell visualized through MCFO approach

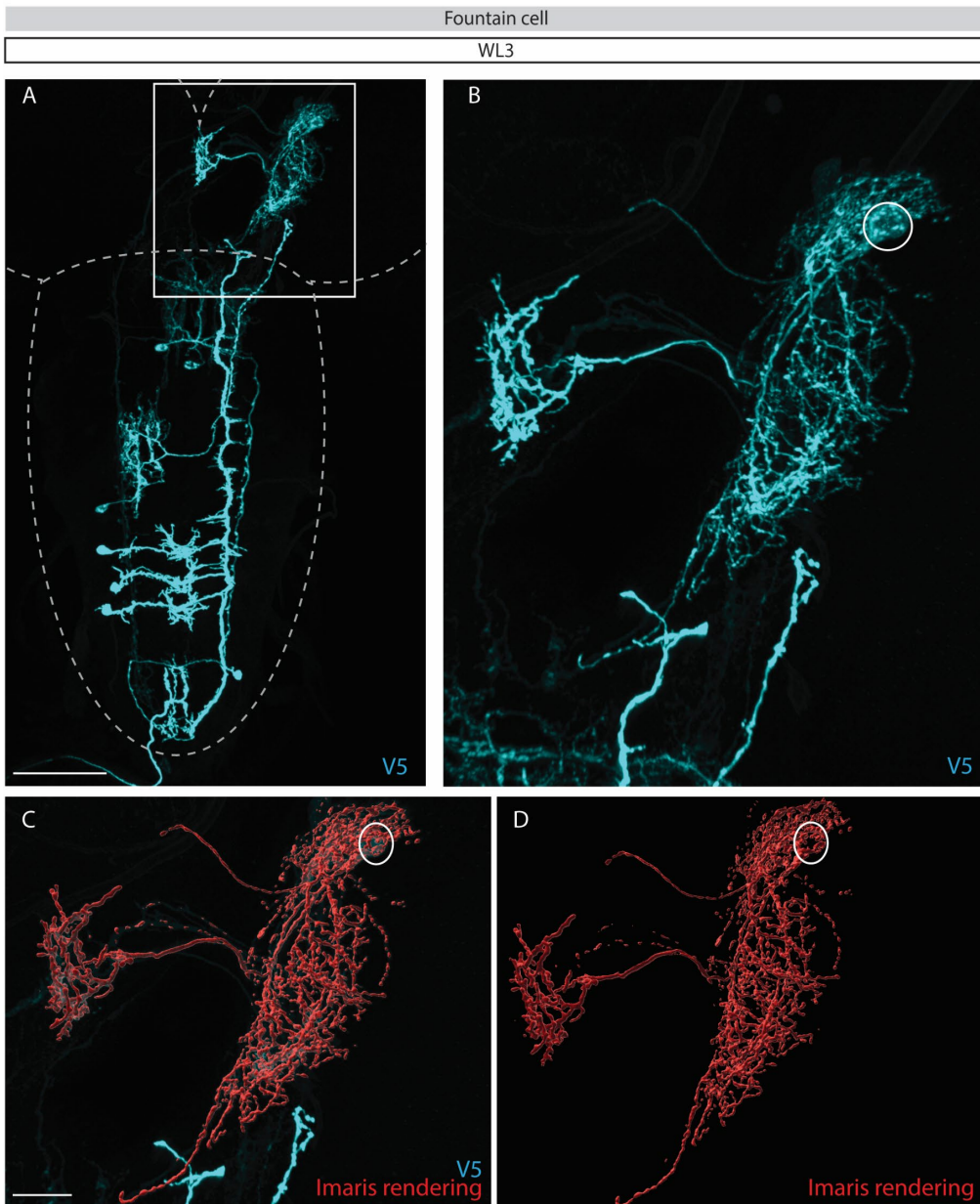


Figure 26: **A)** WL3 brain with stochastic labeling of Pvf3 neurons using the MCFO technique and antibody staining for epitopes (V5 in this case) with brain morphology outlined. Scale bar is 70 microns. **B)** A higher magnification view of the Pvf3_B (Pvf3 Brain) cell. **C)** Pvf3_B cell Imaris rendering overlain with staining. Scale bar is 20 microns, and **D)** Imaris rendering of the cell. The cell body for the Pvf3_B cell is circled in B-D.

Figure 27 Pvf3 branching ladder cell at WL3

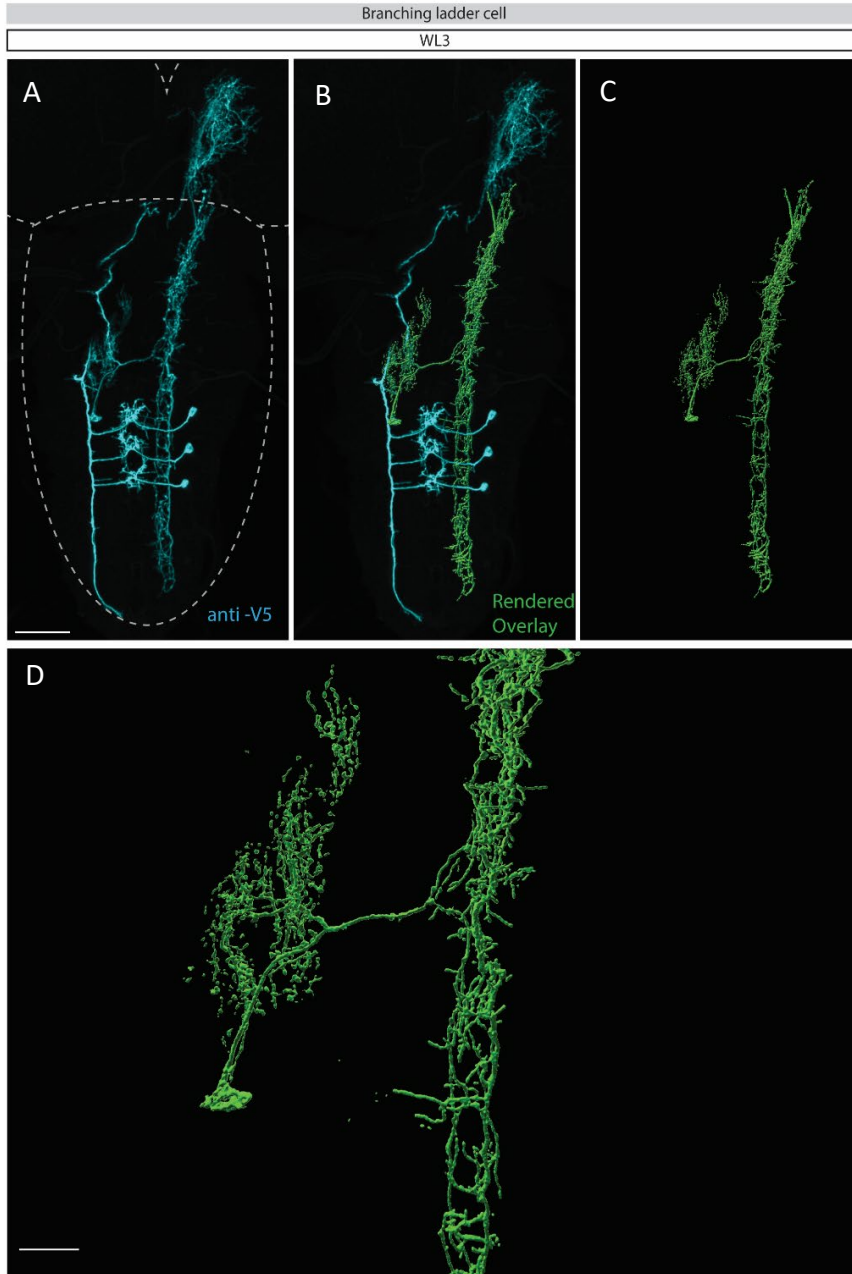


Figure 27: A) WL3 animal with stochastic labeling of Pvf3 neurons using the MCFO technique. Both stick and branching ladder cells are visible in the VNC. Scale bar is 50 microns. **B)** branching ladder cell has been rendered in Imaris and **C)** isolated using a masking program in Imaris. **D)** Higher magnification around the cell body to understand branching morphology. Scale bar is 20 microns.

Figure 28 Pvf3 stick cell at WL3

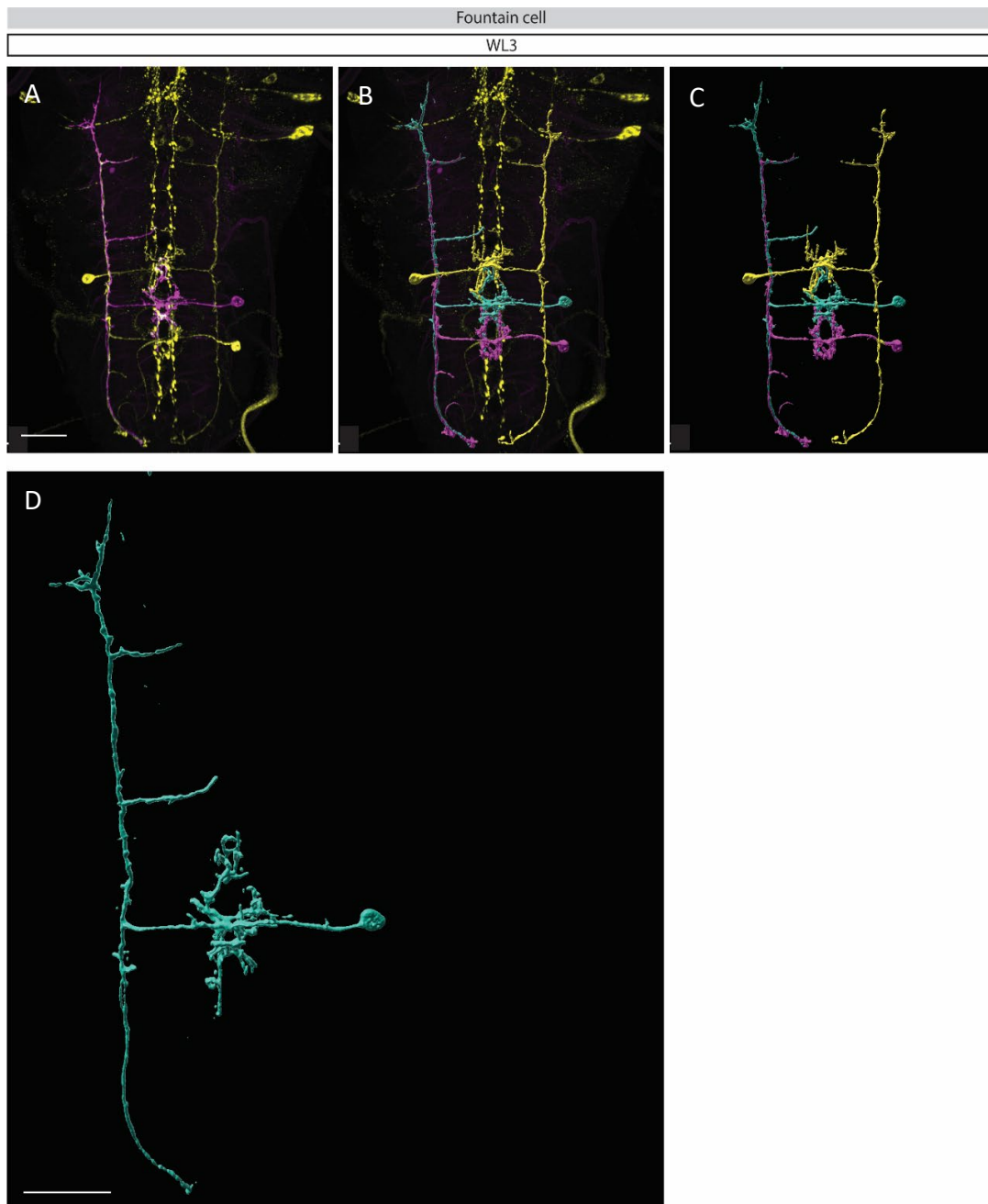


Figure 28: **A)** WL3 animal with stochastic labeling of Pvf3 neurons in the VNC using the MCFO technique. **B)** 3 stick cells have been rendered in Imaris, and **C)** isolated. **D)** A single cell is shown at higher magnification to observe morphology. Scale bars are 30 microns.

After identifying the cell morphologies that made up the labeled cells, we then asked if either caspase or ecdysone-driven refinement took place in these cells by driving either EcR^{DN} (which should block signaling by inhibiting ligand-receptor binding) or P35 (which blocks caspase-driven cell death) in just the Pvf3 neurons. We also assayed whether JNK-driven cell adhesion might play a role by expressing a dominant negative version of Basket (Bsk), which has previously been reported to disrupt neuronal remodeling programs through changes in cell adhesion-dependent (Bornstein, Zahavi et al. 2015). We found that none of these manipulations stopped Pvf3_B cell refinement in the brain lobes. However, cell-specific expression of EcR^{DN} and P35 expression did reduce the amount of refinement in the stick cell projections, suggesting that different Pvf3 cells engage unique programs to drive refinement of projections (Figure 28).

Figure 29 *Pvf3_B* and *Pvf3* stick neurons use different mechanisms to carry out neurite refinement

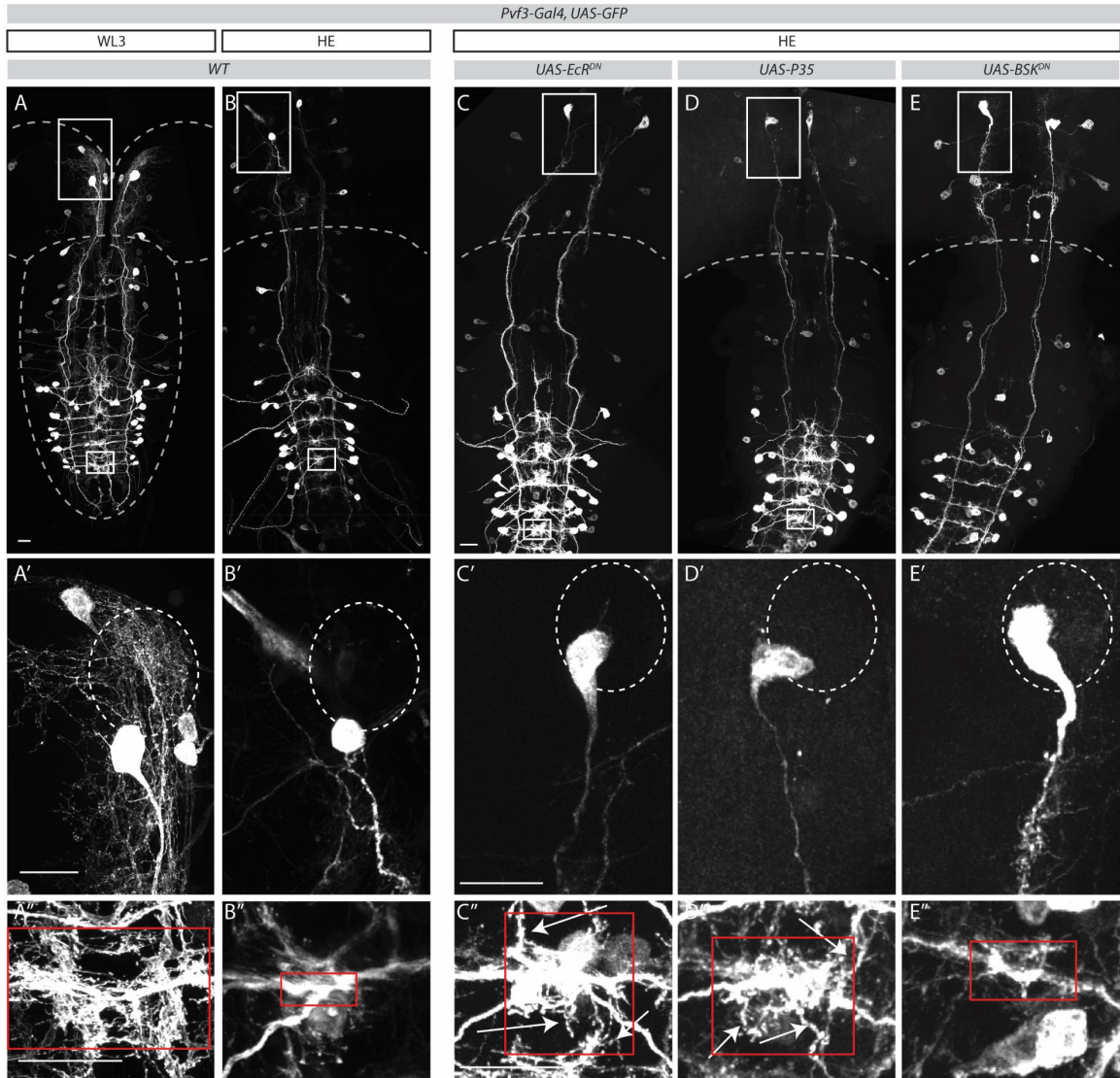


Figure 29: WT *Pvf3* neurons labeled genetically with mCD8::GFP at **A)** WL3 and **B)** HE with the *Pvf3_B* projection (**A'** and **B'**) at high magnification and area of neurite projections outlined and medial stick projections in the VNC (**A''** and **B''**) at high magnification with area of projection outlined in red. When **C)** *EcR^{DN}*, **D)** *P35* or **E)** *Bsk^{DN}* are driven in only the *Pvf3* neurons; the *Pvf3_B* cells lose projections (**C'**-**E'**). The stick cell medial projections in the VNC show a loss of complexity in the *BSK^{DN}* (**E''**) condition but not the *P35* or *EcR^{DN}* (**C''**-**D''**) animals. Scale bars are 20 microns.

Pvf3_B cells displayed nuclear localization of EcR, indicating that, like the CadN and Beat-Va neurons, Pvf3_B cells were competent to receive ecdysone signaling but it is not essential to drive their neurite pruning (Figure 29-30).

Figure 30 Pvf3 cells express the ecdysone receptor

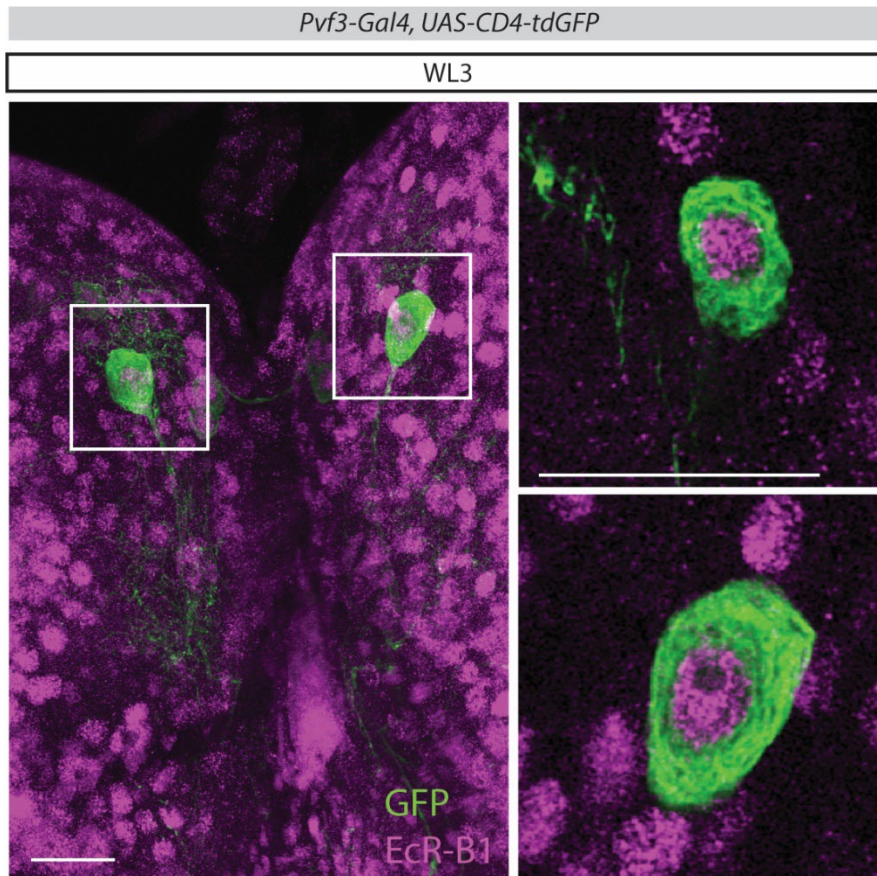


Figure 30: WL3 animals with Pvf3 neurons labeled genetically with mCD4::tdtGFP (**green**) and stained for EcR-B1 (**magenta**). A single z-plane with Pvf3_B cell bodies are blown up to the right to show colocalization of EcR and Pvf3 cell bodies. Scale bars are 20 microns.

B.1 A technical note on Pvf3 neurons

The reasons we chose to spend less time on Pvf3 neurons were: 1) the Gal4 driver seemed to turn on in other neurons during the first twelve hours of metamorphosis,

making an already complex set of neurons and projections even more complex and challenging to trace; and 2) the mCD8::GFP we used did not label the Pvf3_B cell projections well. The second problem is likely solvable by using an mCD4::GFP (which uses the human transmembrane protein CD4 instead of CD8 and can sometimes provide better neuronal labeling), which provides beautiful labeling of the Pvf3_B cells (Figure 31).

Figure 31 *Pvf3* labeled with *mCD4::GFP*

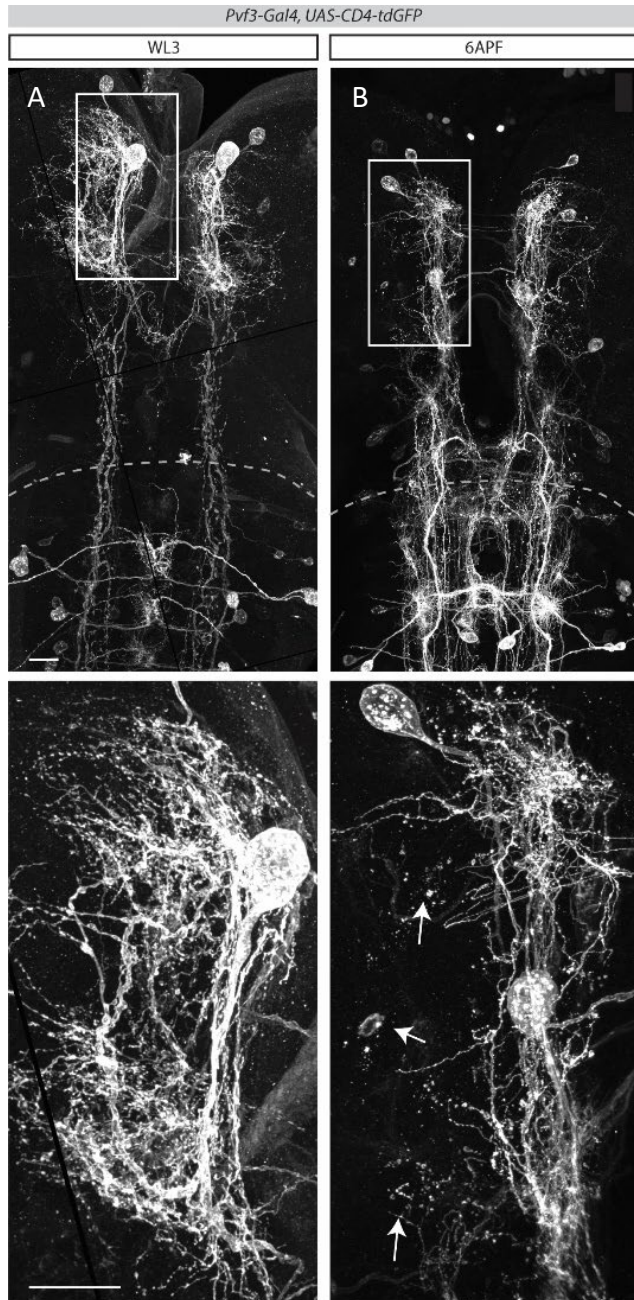


Figure 31: *Pvf3_B* cell labeling with *mcd4::GFP* at **A)** WL3 and **B)** 6APF Arrowheads indicate fragmented neurites. Scale bars are 20 microns.

Appendix C: Corazonin neurons remodel when caspase and ecdysone signaling is blocked

The general trend we observed throughout this study was that many cells undergo refinement during the first twelve hours of metamorphosis, and we discovered drivers that label neurons that continue to undergo neurite refinement when hormonal signaling is blocked. We consistently noticed that very fine projections continued to remodel. Previous evaluation of ventral nerve cord Corazonin neurons (vCrz) neuronal remodeling showed that vCrz cell death was dependent on ecdysone driven signaling and that blocking this signaling allowed the cells to survive and large neurite projections remained intact (Choi, Lee et al. 2005, Choi 2006, Lee, Wang et al. 2011). These studies used antibody staining and low magnification microscopy to examine neurite pruning which made it difficult to evaluate any fine projection remodeling that occurred. Using transgenic labeling (driving a *UAS-mCD8::GFP* with a *Crz-Gal4*) we found that Crz neurons have fine projections branching from larger axonal projections at WL3 (Figure 32A). As reported, vCrz neurons die and are cleared by HE in controls (Figure 32B). Cell death was blocked by inhibition of either ecdysone signaling (EcR^{DN}) or through expression of *P35* to block caspase activation (Figure 32C-D). However, upon close examination, we found the surviving cells lost many of their fine projections by HE, while only larger projections were maintained (Figure 32C-D).

Figure 32 Fine projection refinement persists in vCrz neurons when cell death is blocked

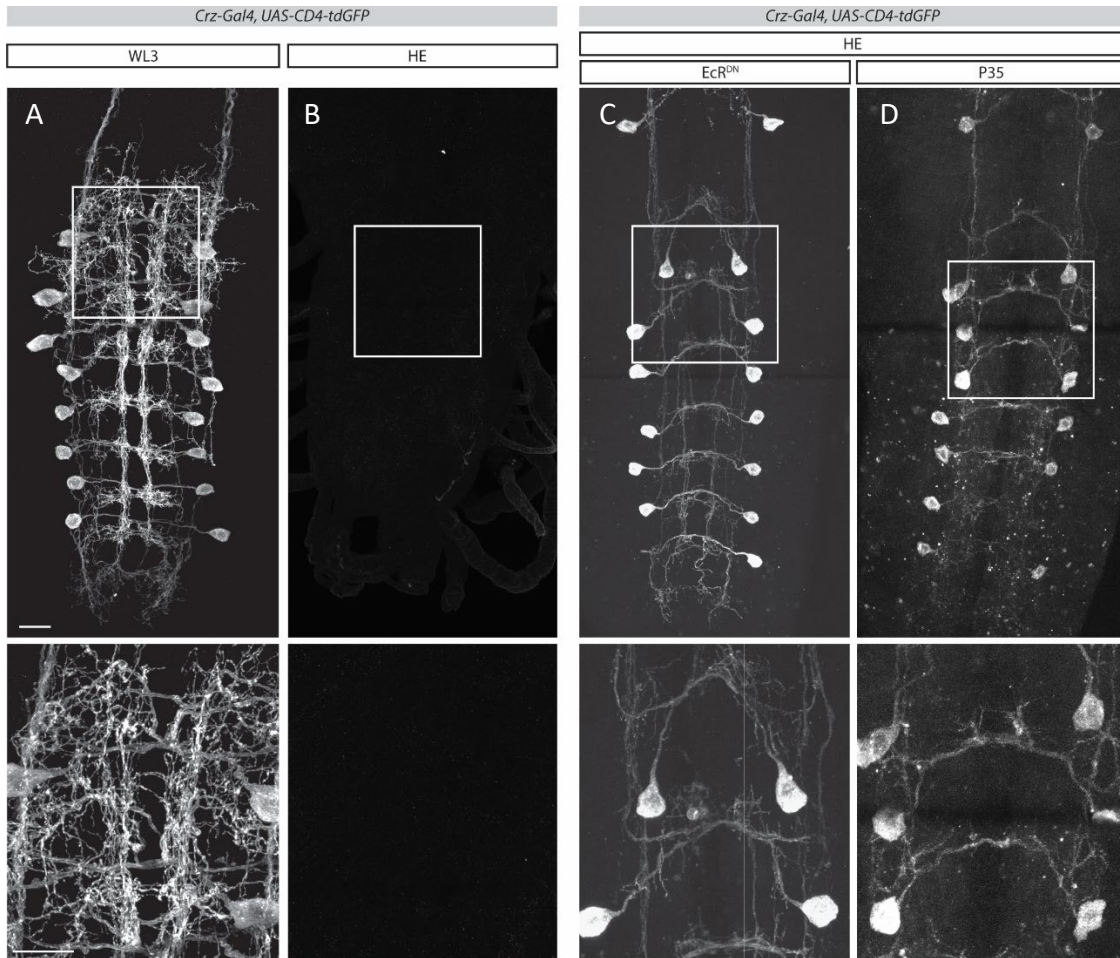


Figure 32: vCrz neurons in the VNC labeled genetically with mCD8::GFP. **A)** WL3 vCrz neurons are complex with many neurite branches and **B)** usually undergo cell death, and are cleared by HE. **C)** Cell death can be blocked by expression of *UAS-EcR^{DN}* or **D)** *UAS-p35*, but anterior fine projections still prune. Boxed areas are shown in high magnification below each image. Scale bars are 20 microns.

The continued remodeling of vCrz neurons, even when cell death was blocked via direct inhibition of caspase signaling (P35) or upstream inhibition of hormonal ecdysone signaling, strongly suggested to us that ecdysone-driven remodeling acted differently in

regulating cell death vs. neurite pruning and that simply saving a cell from death wasn't sufficient to also save neurites from remodeling, as had been previously suggested (Choi 2006, Lee, Wang et al. 2011).

Appendix D: More information on Beat-Va neurons

Beat-Va is part of the BEAT-VA family of proteins, members of the immunoglobulin superfamily (IgSF). BEAT-VA proteins can bind to SIDE proteins (another member of the IgSF) to dictate axon guidance (Li, Watson et al. 2017).

D.1 A technical note on Beat-Va_M A7 neurons

The posterior-most A7 Beat-Va_M cell displays a different branching pattern and is excluded from cell quantification (Figure 33). The A7 Beat-Va_M neurons did not strongly drive GFP in whole-population labeling. However, when we generated single-cell labeling using the MCFO technique, the neurons did not display as much neurite pruning as other medial cells. This could either be a technical limitation or represent interesting biology that may offer further insight into why some neurites prune. In the future, it may be helpful to use a Split-Gal4 approach to label this cell and better characterize its pruning pattern.

Figure 33 A7 Beat-Va_M cell morphology

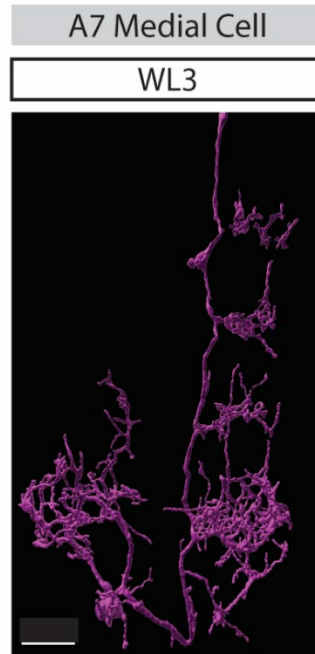


Figure 33: A7 medial cell labeled by the *BeatVa-Gal4* driver line labeled by MCFO. Scale bar is 15 microns.

Appendix E: Astrocytic Draper is necessary for proper astrocyte transformation

Draper is critical for specific steps of neuronal remodeling during the time course we examined. Draper, expressed by glia and critical for debris engulfment, is not known to be important for initiating neuronal fragmentation. In metamorphosis, this was primarily examined by analyzing the ability of glia to clear debris from Corazonin neurons, which, as discussed previously, typically die during the first eight hours of metamorphosis (Tasdemir-Yilmaz and Freeman 2014). We thought that it was possible that Draper could play a more active role in dictating pruning in surviving neurons. We found that in *draper* null animals (*draper* $-/-$), there is a lack of Beat-Va neuron debris clearance, and both cell bodies from lateral cells and neurite debris are visible at HE compared to controls (Figure 34B-C). Upon careful examination of neurites, it did appear that some Beat-Va_M neurites remained intact at HE (Figure 34C), which was also observed when we expressed astrocytic-specific Draper^{RNAi}, arguing for a role for Draper in astrocytes (Figure 34D-F).

Figure 34 Knockdown of Draper stops some Beat-VaM neurite fragmentation

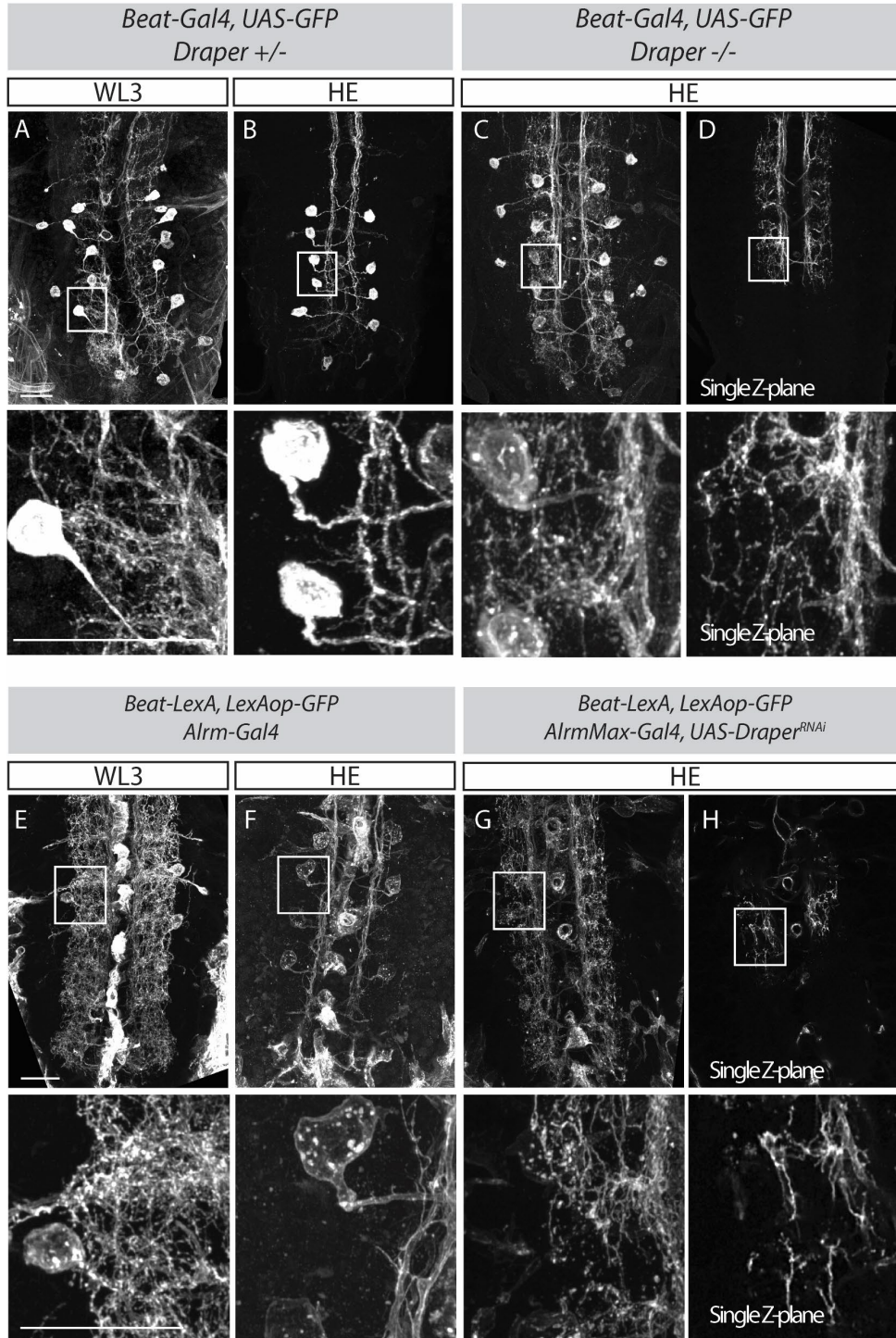


Figure 34: Beat-Va neurons genetically labeled with mCD8::GFP at **A)** WL3 with many fine processes and **B)** HE in control animals, where almost no fine neurites remain. However, in the

C) *Draper* genetic null mutant, debris, and seemingly intact neurites remain, which can be seen best in the **D)** single z-plane rendering of the *draper* null. To confirm this was due to loss of Draper in astrocytes, we compared Beat-V_{AM} neurites that had been genetically labeled using the LexA/LexAop binary system in control conditions at **E)** WL3 and **F)** HE where neurites had been pruned away and compared them to Beat-V_{AM} neurites **G)** when there is an astrocyte-specific knockdown of Draper with RNAi, again showing seemingly **H)** intact neurites when Draper is knocked down. Scalebars are 20 microns.

This suggested two possibilities: either astrocytic Draper signaled to the neurites to fragment, or Draper delayed astrocyte transformation as we had seen with the pan-glial knockdown of Myoglianin. Upon investigation of astrocyte morphology in the Draper knockdown astrocytes, we found that the astrocytes transformed more slowly and morphologically retained larval morphology at 4APF, indicating at least a partial failure of transformation (Compare Figure 34A-C to 34D-F). One interpretation of this data is that Draper depletion slowed astrocyte transformation which in turn led to delayed Beat-V_{AM} fragmentation.

Figure 35 *Draper* is necessary for proper astrocyte transformation

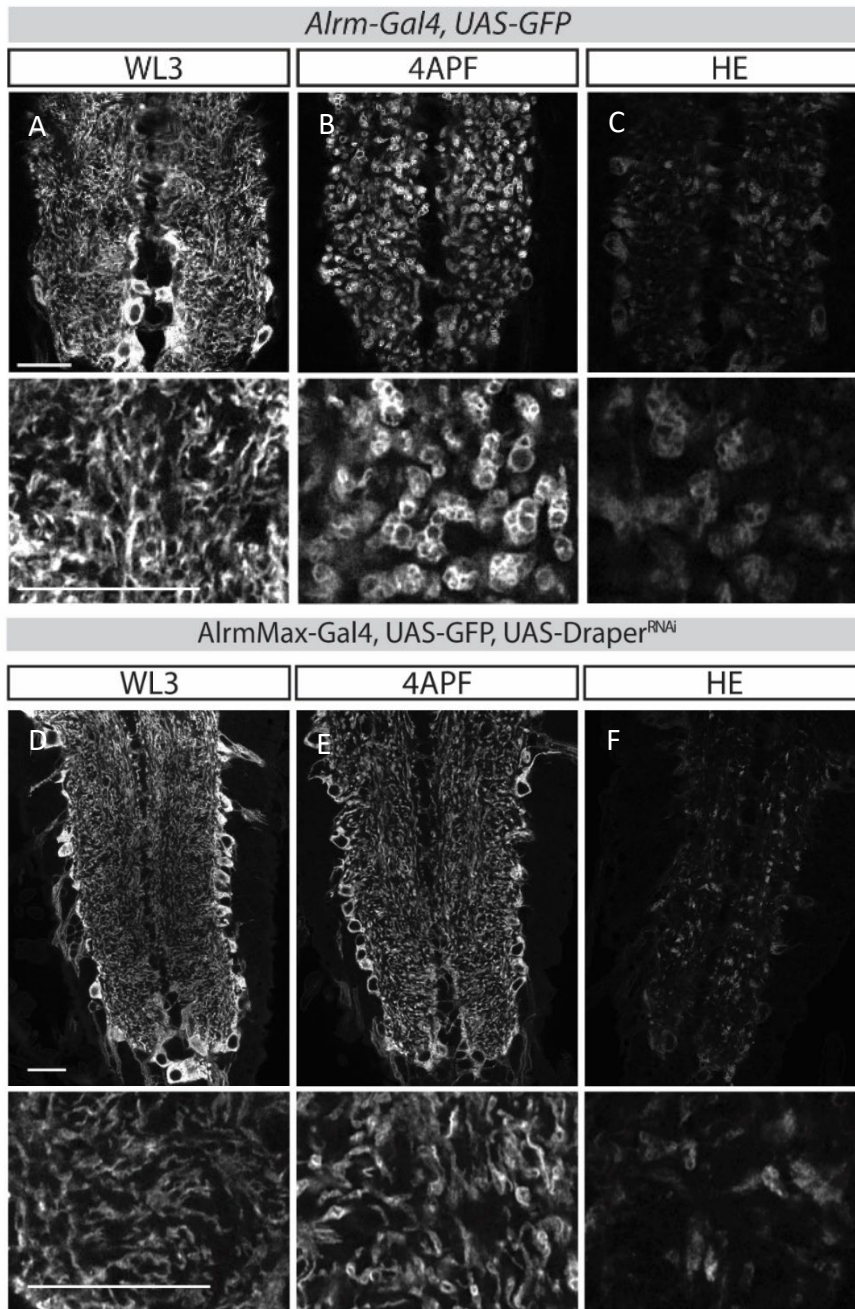


Figure 35: Visualization of astrocytes genetically labeled with GFP undergoing standard transformation from **A)** WL3, to **B)** to 4APF to **C)** HE. This transformation is disrupted when *Draper* is knocked down in only astrocytes. Although astrocytes look relatively normal at **D)**

WL3 by **E)** 4APF phagocytic vesicles fail to form and **F)** HE when some astrocytic labeling is retained. Scale bars are 20 microns.

Appendix F: Abd-A patterning does not reflect Beat-Val cell death patterns

Abdominal A (Abd-A), a *hox*, transcription factor can mark cell death during anterior/posterior patterning during embryonic development (Delorenzi and Bienz 1990, Karch, Bender et al. 1990). Abd-A does not have known roles in cell fate specification during metamorphosis, but we wondered if, given its reported expression patterns, it could play a previously undescribed role in cell fate specification during metamorphic neuronal remodeling. To determine if Abd-A dictated cell death and survival in Beat-Val neurons we first needed to assess if the A4/A5 boundary that is present in the embryo—and that defined our cell death boundary—was present in the late larval stage and into metamorphosis. We found Abd-A was expressed with varying intensity throughout the larval VNC with the most notable change in intensity between segments A3 and A2, and by HE much of the posterior expression had been lost but A2/A3 still defined the boundary between high and low expression (Figure 36).

Figure 36 *Abd-B* does not define the *Beat-Va_L* cell death pattern

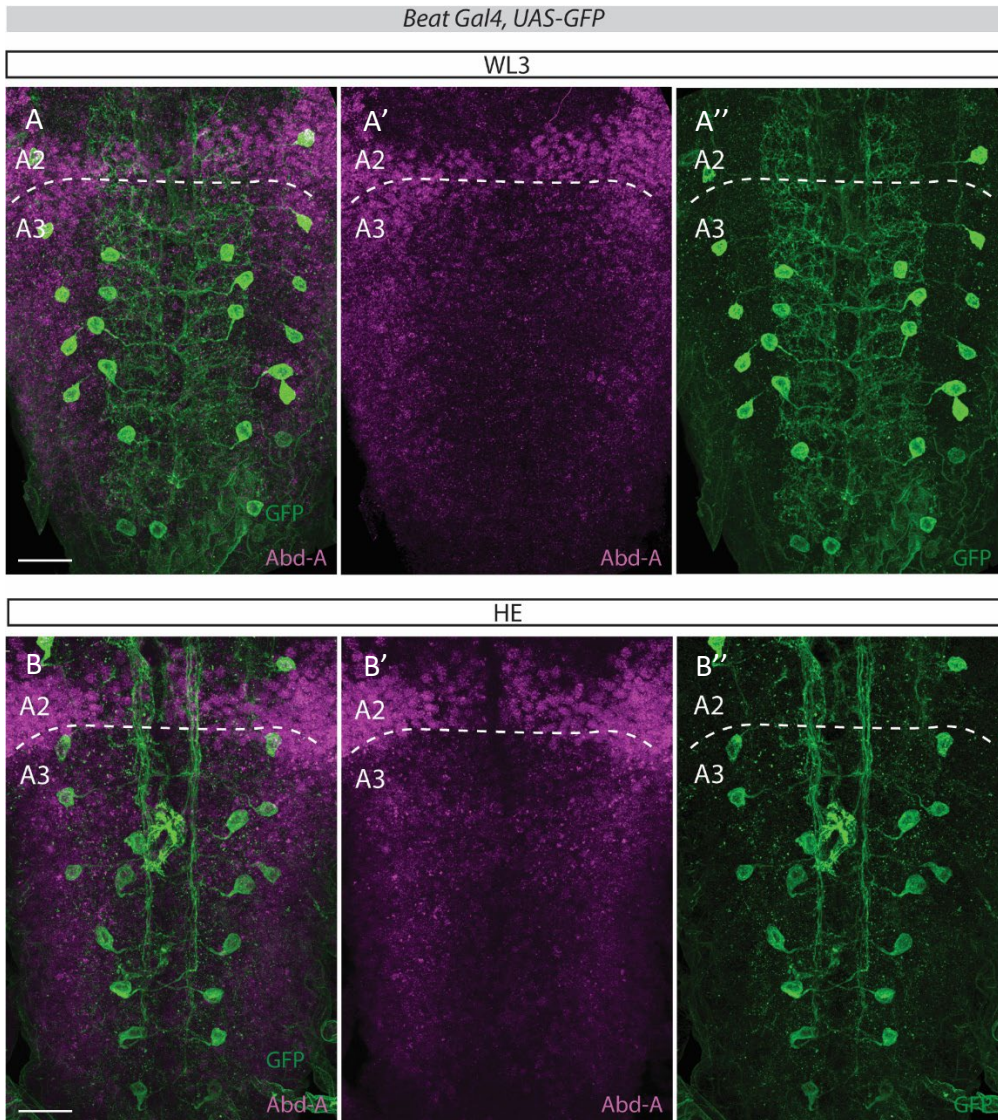


Figure 36: **A-A''**) *Beat-Va* neurons at WL3 and **B-B''**) HE labeled with *mCD8::GFP* (**green**) stained with *Abdominal-A* (**magenta**); a white dashed line denoting the boundary of *Abd-A* at the A2/A3 boundary. Scale bars are 20 microns.

The A2/A3 boundary was not the boundary of cell death that we had observed with the lateral cells, so we determined that Abd-A did likely not determine Beat-Va_L neuron survival.

Appendix G: FlyLight lines evaluated at WL3 for GAL4 strength and expression pattern

Line	Gene	Pattern (vs= very simple, s=simple, c=complex, sc=intermediate)	BDSC	Notes
GMR52G09	<i>CG42543</i> <i>mp</i>	sc	38845	
GMR55E01	<i>CG31235</i>	sc	39117	
GMR58G04	<i>CG1522</i> <i>cac</i>	sc	39194	
GMR64D10	<i>CG5907</i> <i>Frq2</i>	s	39305	
GMR68B07	<i>CG7485</i> <i>TyrR</i>	sc	39459	Weak expression
GMR74E08	<i>CG7847</i> <i>sr</i>	s	39859	
GMR75H03	<i>CG34340</i>	s	39908	
GMR77E07	<i>CG34378</i> <i>Pvf3</i>	c	39969	Very bright
GMR78B07	<i>CG42281</i> <i>bun</i>	sc	39989	
GMR83B05	<i>CG7994</i> 5- <i>HT2B</i>	vs	40352	No GFP expression
GMR84D10	<i>CG18389</i> <i>Eip93F</i>	sc	40392	
GMR85C10	<i>CG1343</i> <i>Sp1</i>	sc	40424	Bright
GMR85F10	<i>CG7734</i> <i>shn</i>	s	40434	
GMR91C05	<i>CG42242</i> <i>beat-VII</i>	sc	40578	Weak expression
GMR93G03	<i>CG31247</i> <i>tinc</i>	s	40660	
GMR93G08	<i>CG42625</i> <i>mun</i>	c	40664	Bright
GMR94E01	<i>CG8254</i> <i>exex</i>	s	40683	
GMR94G06	<i>CG33512</i> <i>dpr4</i>	sc	40701	Bright
GMR41F12	<i>CG7902</i> <i>bap</i>	s	41242	

GMR21F04	<i>CG14307</i> <i>fru</i>	s	45462	No GFP expression
GMR32F03	<i>CG7100</i> <i>CadN</i>	s	45588	
GMR13E09	<i>CG1470</i> <i>Gycbeta100B</i>	vs	45797	Weak expression
GMR39H05	<i>CG1832</i> <i>Clamp</i>	s	45873	
GMR46H01	<i>CG5954</i> <i>l(3)mbt</i>	s	45978	
GMR18A10	<i>CG11325</i> <i>GRHR</i>	s	46156	
GMR50G02	<i>CG3114</i> <i>ewg</i>	s	46282	
GMR56G03	<i>CG3143</i> <i>foxo</i>	s	46336	Weak expression
GMR72D03/TM3, Sb	<i>CG33517</i> <i>D2R</i>	c	46676	No GFP expression
GMR82A06/TM3, Sb	<i>CG11152</i> <i>fd102C</i>	c	47111	
GMR95A04	<i>CG12769</i>	c	47271	Bright
GMR44B11	<i>CG5133Doc1</i>	s	47358	
GMR52C09	<i>CG6669</i> <i>klg</i>	c	47371	
GMR54F07	<i>CG1522</i> <i>cac</i>	s	47377	Weak expression
GMR59C02	<i>CG5744</i> <i>Frg1</i>	c	47383	Bright
GMR65H09	<i>CG7887</i> <i>Takr99D</i>	sc	47389	
GMR74A06	<i>CG17390</i> <i>Oaz</i>	s	47398	Bright
GMR1E307	<i>CG6494</i> <i>h</i>	vvs	47861	Weak expression
GMR21H03	<i>CG1916</i> <i>Wnt2</i>	s	47900	
GMR36H01	<i>CG17888</i> <i>Pdpl</i>	s	47920	
GMR46C12	<i>CG17077</i> <i>pnt</i>	s	47938	Bright
GMR58H02	<i>CG3967</i>	c	47952	Bright

GMR94A09	<i>CG5518</i> <i>sda</i>	c	48007	No GFP expression
GMR24G12	<i>CG7807</i> <i>AP-2</i>	s	48053	Nice pattern
GMR29E07	<i>CG9019</i> <i>dsf</i>	s	48090	
GMR29H05	<i>CG1634</i> <i>Nr</i>	sc	48094	Bright
GMR31C03	<i>CG7100</i> <i>CadN</i>	c	48103	Bright
GMR40G11	<i>CG33956</i> <i>kay</i>	s	48143	Weak expression
GMR54E11/TM3, Sb	<i>CG5744</i> <i>Frq1</i>	c	48203	
GMR85G10	<i>CG7734</i> <i>shn</i>	s	48384	Weak expression
GMR88D01/TM3, Sb	<i>CG32447</i>	s	48395	No GFP expression
GMR94A04/TM3, Sb	<i>CG5518</i> <i>sda</i>	vs	48423	
GMR10D05	<i>CG12287</i> <i>pdm2</i>	c	48438	
GMR12G06	<i>CG32474</i> <i>dys</i>	c	48524	
GMR14A08	<i>CG8095</i> <i>scb</i>	s	48594	Messy labeling
GMR76C04/TM3, Sb	<i>CG12506</i>	c	48621	Bright
GMR91E03	<i>CG34385</i> <i>dpr12</i>	s	48631	
GMR92H04/TM3, Sb	<i>CG10134</i> <i>beat-Va</i>	sc	48632	
GMR92H12/TM3, Sb	<i>CG4846</i> <i>beat-Ia</i>	s	48633	Weak expression
GMR14G09	<i>CG10844</i> <i>Rya-r44</i>	c	48662	Inconsistent
GMR17C08	<i>CG10037</i> <i>vvl</i>	c	48761	Bright
GMR18A04	<i>CG12370</i>	c	48793	Bright
GMR19F05	<i>CG7665</i> <i>Fsh</i>	c	48855	Weak expression

GMR20B01	<i>CG6383</i> <i>crb</i>	s	48877	Inconsistent
GMR21D12	<i>CG9554</i> <i>CG2302</i> <i>nAcRalpha-7E</i>	s	48946	Bright
GMR23E05	<i>CG17299</i> <i>SNF4Agamma</i>	s	49029	
GMR23F06	<i>CG30106</i>	c	49036	Inconsistent
GMR25H08	<i>CG13777</i> <i>milt</i>	s	49146	
GMR26H11	<i>CG9656</i> <i>grn</i>	sc	49206	Weak expression
GMR21A11/TM3, Sb	<i>CG9554</i> <i>eya</i>	c	49292	Bright
GMR33G09	<i>CG10699</i> <i>Lim3</i>	s	49365	Messy labeling
GMR50H06	<i>CG4684</i> <i>nwk</i>	c	49393	
GMR60A01	<i>CG32296</i> <i>Mrtf</i>	sc	49403	
GMR70A01	<i>CG12073</i> <i>5-HT7</i>	c	49414	Bright
GMR31C11	<i>CG8355</i> <i>sli</i>	s	49671	Bright
GMR32G08	<i>CG18405</i> <i>Sema-1a</i>	s	49729	Weak expression
GMR33D08	<i>CG1856</i> <i>ttk</i>	c	49747	Bright
GMR34E05	<i>CG10704</i> <i>toe</i>	s	49789	Bright
GMR19E02	<i>CG9885</i> <i>dpp</i>	c	49833	Bright
GMR35F03	<i>CG1864</i> <i>Hr38</i>	sc	49914	Bright
GMR38E10	<i>CG9704</i> <i>Nrt</i>	c	50009	Bright
GMR40F08	<i>CG31666</i> <i>chinmo</i>	c	50095	Bright
GMR40H02	<i>CG12690</i> <i>CHES-1-like</i>	sc	50102	Bright
GMR41E11	<i>CG11020</i> <i>nompC</i>	c	50131	Bright

GMR42E12	<i>CG11153</i> <i>Sox102F</i>	s	50159	Bright
GMR44D10	<i>CG5685</i> <i>Calx</i>	c	50209	Bright
GMR45A05	<i>CG5695</i> <i>jar</i>	s	50218	Bright

Appendix H: FlyLight lines evaluated at WL3, 6APF and 18APF for remodeling

Line	Gene	Pattern (s=simple, c=complex, sc=intermediate)	BDSC	Notes
GMR52G09	<i>CG42543</i> <i>mp</i>	sc	38845	Good larval and 6APF expression. Gone by 18APF
GMR58G04	<i>CG1522</i> <i>cac</i>	sc	39194	Faint larval expression, most cells disappear by 6APF
GMR64D10	<i>CG5907</i> <i>Frq2</i>	s	39305	Bright cell bodies at larva, no expression at 6, maybe new cells express GFP by 18
GMR74E08	<i>CG7847</i> <i>sr</i>	s	39859	Not good expression
GMR75H03	<i>CG34340</i>	s	39908	Strong larval expression. Gone by 6APF
GMR77E07	<i>CG34378</i> <i>Pyf3</i>	c	39969	Good expression throughout
GMR78B07	<i>CG42281</i> <i>bun</i>	sc	39989	Simple pattern, expresses throughout
GMR85C10	<i>CG1343</i> <i>Sp1</i>	sc	40424	Only pictures for WL3 and 6APF. Looks like good expression
GMR85F10	<i>CG7734</i> <i>shn</i>	s	40434	Probably motor neuron. Not a lot of refinement
GMR93G03	<i>CG31247</i> <i>tinc</i>	s	40660	Only pictures for WL3 and 6APF. Labels 4 cells. Expression fades
GMR94E01	<i>CG8254</i> <i>exex</i>	s	40683	Strong expression. Not a lot of refinement
GMR18A10	<i>CG11325</i> <i>GRHR</i>	s	46156	Weak larval expression, strong at 18APF

GMR50G02	<i>CG3114</i> <i>ewg</i>	s	46282	Weak expression
GMR72D03/TM3, Sb	<i>CG33517</i> <i>D2R</i>	c	46676	Good expression throughout. Maybe cell death candidate
GMR82A06/TM3, Sb	<i>CG11152</i> <i>fd102C</i>	c	47111	Labels 6 cells. Not a lot of refinement through 6APF
GMR95A04	<i>CG12769</i>	c	47271	Good expression throughout. Maybe cell death candidate
GMR44B11	<i>CG5133</i> <i>Doc1</i>	s	47358	Good expression throughout. Sparse labeling Increase in cell number at 18.
GMR52C09	<i>CG6669</i> <i>klg</i>	c	47371	Good expression throughout. Cell death + refinement maybe?
GMR74A06	<i>CG17390</i> <i>Oaz</i>	s	47398	Good expression. Not a lot of refinement
GMR29H05	<i>CG1634</i> <i>Nr</i>	sc	48094	Probably motor neuron. Not a lot of refinement
GMR31C03	<i>CG7100</i> <i>CadN</i>	c	48103	Probably motor neuron. Some refinement
GMR92H04/TM3, Sb	<i>CG10134</i> <i>beat-Va</i>	sc	48632	Good expression at 6APF, Bad WL3 image?
GMR21D12	<i>CG9554</i> <i>CG2302</i> <i>nAcRalpha-7E</i>	s	48946	Not a lot refinement, maybe increase in cell number
GMR25H08	<i>CG13777</i> <i>milt</i>	s	49146	Not a lot of refinement. 4 cells/side
GMR21A11/TM3, Sb	<i>CG9554</i> <i>eya</i>	c	49292	Good expression + refinement
GMR35F03	<i>CG1864</i> <i>Hr38</i>	sc	49914	Messy

GMR42E12	<i>CG11153</i> <i>Sox102F</i>	s	50159	Inconsistent labeling
----------	----------------------------------	---	-------	-----------------------

Appendix I: Astrocyte screen results

Gene Name	CG#	Phenotype (m= mild, s= strong/ i=intact, d=debris, m=mixed, w=none)	Hit VDRC #	No Hit VDRC#
<i>beat-IIIb or CG31806</i>	CG33179	m/d	36237, 107474, 107521	107474
<i>CG13117</i>	CG13117	m/d	106941	39751
<i>CG13784</i>	CG13784	m/i	8042	
<i>Dpr-16</i>	CG12591	m/i	31986, 102628	
<i>Sema2a</i>	CG4700	m/i	15811	15810
<i>Dpr-2</i>	CG33507	m/m	29742	
<i>Dpr-8</i>	CG32600	m/m	106791	34132
<i>Dpr-9</i>	CG33485	m/m	51990	
<i>Dscam2</i>	CG32387	m/m	1100	107939
<i>Kek4</i>	CG9431	m/m	105647	

<i>CG15744</i>	CT35992	s/d	4801	
<i>Dpr-19</i>	CG13140	s/d	106092	
<i>htl</i>	CG7223	s/d	27180, 40627	
<i>ImpL2</i>	CG15009	s/d	106543	30930 30931
<i>Kek5</i>	CT10486	s/d	47771	1401
<i>MnM</i>	CG14964	s/d	43603	
<i>CG3164</i>	CG3164	s/i	42734, 108413	
<i>CG40485</i>	CG40485	s/i	106439	15492
<i>Dpr-17</i>	CG31361	s/i	8481	100978
<i>DIP-ζ</i>	CG31708	s/i	38261, 107866	
<i>Lsd-1</i>	CG10374	s/i	30884, 106891	
<i>sallimus</i>	CG1915	s/i	47301	

<i>Fasciclin III</i>	CG5803	s/m	100642	940 3091 26850
<i>fipi</i>	CG15630	s/m	37842	107797
<i>Kek6</i>	CG1804	s/m	109681	27165
<i>Lsd-2</i>	CG9057	s/m	40734, 102269	
<i>Tektin-C</i>	CG10541	s/m	31253	31253 100094
<i>vein</i>	CG10491	s/m	50358, 109437	
<i>Wrapper</i>	CG10382	s/m	105314	
<i>Atet</i>	CG2969	w		42751 100404
<i>Ama</i>	CG2198	w		22944
<i>babos</i>	CG3624*	w		956 36304
<i>bdl</i>	CG16857	w		4806 109857
<i>beaten path Vc</i>	CG14390	w		22736 102793

				24656 104444
<i>beaten path VII</i>	CG14249	w		22725 102329
<i>beat-Ia</i>	CG4846	w		4544
<i>beat-Ib</i>	CG7644	w		V101662 V330153
<i>beat-Ic</i>	beat-Ic	w		v9441 v105066
<i>beatIII-a</i>	CG12621	w		29655 45866
<i>beat-IIIc</i>	CG15138	w		27137 109015 203176
<i>beat-IV</i>	CG10152	w		52413
<i>beat-va</i>	CG10134	w		102698
<i>beat-vb</i>	CG31298	w		106502
<i>beat-vi</i>	CG14064	w		105798 6694

<i>boi</i>	CG32796	w		108265
<i>brat</i>	CG10719	w		31333 105054
<i>bwa</i>	CG13969	w		8070 101366
<i>Cat</i>	CG6871	w		6283
<i>ced6</i>	CG11804	w		16313 108101
<i>Cer</i>	CG10460	w		22751 22752
<i>CG11309</i>	CG11309	w		7513 7514
<i>CG11737</i>	CG11737	w		5807 108872
<i>CG12274</i>	CG12274	w		39319
<i>CG13506</i>	CG13506	w		14127 104632
<i>CG13707</i>	CG13707	w		29257
<i>CG14401</i>	CG14401	w		8610

<i>CG15354</i>	CG15354	w		17860
<i>CG16974</i>	CG16974	w		7993
<i>CG17839</i>	CG17839	w		3109
<i>CG18549</i>	CG18549	w		6098 107272
<i>CG31369</i>	CG31369	w		109847 110101
<i>CG31431</i>	CG31431	w		1128 104697
<i>CG4822</i>	CG4822	w		42730
<i>CG5597</i>	CG5597	w		12875
<i>CG7166</i>	CG7166	w		27117 107945
<i>CG7607</i>	CG7607	w		330258
<i>CG7611</i>	CG7611	w		108731
<i>CG9416</i>	CG9416	w		10064
<i>Contactin</i>	CG1084	w		40613

<i>crq</i>	CG4280	w		45883 45884
<i>DIP-1</i>	CG11320	w		18054
<i>dmglut</i>	CG5304	w		6938
<i>DOR</i>	CG3093	w		41186 105330
<i>Dpr-1</i>	CG13439	w		33817
<i>Dpr-10</i>	CG32057	w		18920 103511
<i>Dpr-11</i>	CG33202	w		23243 107548
<i>dpr12</i>	CG14469	w		44741 106788
<i>Dpr-13</i>	CG33996	w		17668 107676
<i>Dpr-14</i>	CG10946	w		8005 102040
<i>Dpr-15</i>	CG10095	w		29144 46245
<i>Dpr-18</i>	CG14948	w		45821

<i>Dpr-20</i>	CG12191	w		15254 101673
<i>dpr3</i>	CG15380	w		25109
<i>Dpr-4</i>	CG33512	w		28518
<i>Dpr-5</i>	CG5308	w		953
<i>Dpr-6</i>	CG14162	w		41161
<i>Dpr-7</i>	CG33481	w		46216 106546
<i>Dpr-interacting protein α</i>	CG13020	w		104044
<i>Dscam</i>	CG17800	w		25623 36233 108835
<i>Dscam4</i>	CG18630	w		42883
<i>ed</i>	CG12676	w		938 104279
<i>fandango</i>	CG6197	w		42236
<i>Fasciclin 2</i>	CG3665	w		103807

<i>Flo2</i>	CG32593	w		31525 330316
<i>frazzled</i>	CG8581	w		29910
<i>GstE3</i>	CG17524	w		6965
<i>hbs</i>	CG7449	w		40898 105913
<i>hdly</i>	CG5630	w		52066
<i>ihog</i>	CG9211	w		29897
<i>kek1</i>	CG12283	w		36252
<i>kek2</i>	CG4977	w		4745
<i>Kek3</i>	CG4192	w		6354 6356
<i>Kirre</i>	CG3653	w		109585 27227
<i>klg</i>	CG6669	w		108818
<i>Lachesin</i>	CG12369	w		35524 107450
<i>lambik</i>	CG8434	w		106679

<i>Lamtor3</i>	CG5110	w		34935 104189
<i>Lar</i>	CG10443	w		36270 107996
<i>MFS15</i>	CG15094	w		5002
<i>mth</i>	CG6936	w		102303
<i>NaPi-T</i>	CG10207	w		48951 106729
<i>Nepl6</i>	CG9508	w		103497 110244 38008
<i>Neuroglian</i>	CT4318	w		107991
<i>Neuromusculin</i>	CG43079	w		980
<i>noktochor</i>	CG14141	w		43017
<i>Nrx-1</i>	CG7050	w		36326
<i>off-track2</i>	CG8964	w		29908 106266
<i>pain</i>	CG15860	w		39477 39478

<i>Papilin</i>	CG18436	w		16523
<i>pinta</i>	CG13848	w		28263
<i>plum</i>	CG6490	w		9444 101135
<i>ppk12</i>	CG10972	w		105131
<i>prim</i>	CG15704	w		105905
<i>Pxn</i>	CG12002	w		15277 107180
<i>robo2</i>	CG5481	w		11823
<i>robo3</i>	CG5423	w		44702 330124
<i>Roughest</i>	CG4125	w		951 27223 27225
<i>roundabout 1</i>	CG13521	w		4329
<i>Sesn</i>	CG11299	w		38481 104365
<i>side</i>	CG31062	w		1283 1284 47488 47489

<i>Side</i>	CG31062	w		27049
<i>side-II</i>	CG15275	w		103687
<i>side-III</i>	CG14677	w		103669
<i>Side-IV</i>	CG14372	w		16636 102563
<i>sidestep VI</i>	CG14698	w		38809 103456
<i>side-V</i>	CG30188	w		44997
<i>Side-VII</i>	CG12950	w		106353
<i>Side-VIII</i>	CG12484	w		25576 104814
<i>SkpB</i>	CG8881	w		28975 106521
<i>sns</i>	CG13752	w		877
<i>spartin</i>	CG12001	w		16383
<i>Swip-1</i>	CG10641	w		31308 107033
<i>trol</i>	CG33950	w		24549

<i>Tsp42Ee</i>	CG10106	w		330399 7934
<i>unc-5</i>	CG8166	w		8138
<i>vinc</i>	CG3299	w		105956
<i>yellow-h</i>	CG1629	w		100481

Bibliography

- Alyagor, I., V. Berkun, H. Keren-Shaul, N. Marmor-Kollet, E. David, O. Maysel, N. Issman-Zecharya, I. Amit and O. Schuldiner (2018). "Combining Developmental and Perturbation-Seq Uncovers Transcriptional Modules Orchestrating Neuronal Remodeling." Developmental Cell **47**(1): 38-52.e36.
- Anderson, S. R., J. M. Roberts, N. Ghena, E. A. Irvin, J. Schwabkopf, I. B. Cooperstein, A. Bosco and M. L. Vetter (2022). "Neuronal apoptosis drives remodeling states of microglia and shifts in survival pathway dependence." eLife **11**: e76564.
- Arnoux, I. and E. Audinat (2015). "Fractalkine Signaling and Microglia Functions in the Developing Brain." Neural Plast **2015**: 689404.
- Arya, R., T. Sarkissian, Y. Tan and K. White (2015). "Neural stem cell progeny regulate stem cell death in a Notch and Hox dependent manner." Cell Death Differ **22**(8): 1378-1387.
- Awasaki, T., Y. Huang, M. B. O'Connor and T. Lee (2011). "Glia instruct developmental neuronal remodeling through TGF- β signaling." Nature neuroscience **14**(7): 821-823.

Bakshi, A., R. Sipani, N. Ghosh and R. Joshi (2020). "Sequential activation of Notch and Grainyhead gives apoptotic competence to Abdominal-B expressing larval neuroblasts in *Drosophila* Central nervous system." PLoS Genet **16**(8): e1008976.

Banerjee, S., M. Toral, M. Siefert, D. Conway, M. Dorr and J. Fernandes (2016). "dHb9 expressing larval motor neurons persist through metamorphosis to innervate adult-specific muscle targets and function in *Drosophila* eclosion." Dev Neurobiol **76**(12): 1387-1416.

Bello, B. C., F. Hirth and A. P. Gould (2003). "A Pulse of the *Drosophila* Hox Protein Abdominal-A Schedules the End of Neural Proliferation via Neuroblast Apoptosis." Neuron **37**(2): 209-219.

Bornstein, B., H. Meltzer, R. Adler, I. Alyagor, V. Berkun, G. Cummings, F. Reh, H. Keren-Shaul, E. David, T. Riemensperger and O. Schuldiner (2021). "Transneuronal Dpr12/DIP- δ interactions facilitate compartmentalized dopaminergic innervation of *Drosophila* mushroom body axons." Embo j **40**(12): e105763.

Bornstein, B., E. E. Zahavi, S. Gelley, M. Zoosman, S. P. Yaniv, O. Fuchs, Z. Porat, E. Perlson and O. Schuldiner (2015). "Developmental Axon Pruning Requires Destabilization of Cell Adhesion by JNK Signaling." Neuron **88**(5): 926-940.

Boulanger, A., C. Clouet-Redt, M. Farge, A. Flandre, T. Guignard, C. Fernando, F. Juge and J.-M. Dura (2011). "ftz-f1 and Hr39 opposing roles on EcR expression during *Drosophila* mushroom body neuron remodeling." Nature Neuroscience **14**(1): 37-44.

Boulanger, A., C. Thinat, S. Züchner, L. G. Fradkin, H. Lortat-Jacob and J.-M. Dura (2021). "Axonal chemokine-like Orion induces astrocyte infiltration and engulfment during mushroom body neuronal remodeling." Nature Communications **12**(1): 1849.

Boulanger, A., C. Thinat, S. Züchner, L. G. Fradkin, H. Lortat-Jacob and J. M. Dura (2021). "Axonal chemokine-like Orion induces astrocyte infiltration and engulfment during mushroom body neuronal remodeling." Nat Commun **12**(1): 1849.

Brown, H. L. D., L. Cherbas, P. Cherbas and J. W. Truman (2006). "Use of time-lapse imaging and dominant negative receptors to dissect the steroid receptor control of neuronal remodeling in *Drosophila*." Development **133**(2): 275-285.

Bu, S., S. S. Y. Lau, W. L. Yong, H. Zhang, S. Thiagarajan, A. Bashirullah and F. Yu (2023). "Polycomb group genes are required for neuronal pruning in *Drosophila*." BMC Biol **21**(1): 33.

Buchanan, J., L. Elabbady, F. Collman, N. L. Jorstad, T. E. Bakken, C. Ott, J. Glatzer, A. A. Bleckert, A. L. Bodor, D. Brittain, D. J. Bumbarger, G. Mahalingam, S. Seshamani, C. Schneider-Mizell, M. M. Takeno, R. Torres, W. Yin, R. D. Hodge, M. Castro, S. Dorkenwald, D. Ih, C. S. Jordan, N. Kemnitz, K. Lee, R. Lu, T. Macrina, S. Mu, S. Popovych, W. M. Silversmith, I. Tartavull, N. L. Turner, A. M. Wilson, W. Wong, J. Wu, A. Zlateski, J. Zung, J. Lippincott-Schwartz, E. S. Lein, H. S. Seung, D. E. Bergles, R. C. Reid and N. M. da Costa (2022). "Oligodendrocyte precursor cells ingest axons in the mouse neocortex." Proc Natl Acad Sci U S A **119**(48): e2202580119.

Cakouros, D., T. J. Daish and S. Kumar (2004). "Ecdysone receptor directly binds the promoter of the *Drosophila* caspase dronc, regulating its expression in specific tissues." J Cell Biol **165**(5): 631-640.

Carrillo, R. A., E. Özkan, K. P. Menon, S. Nagarkar-Jaiswal, P. T. Lee, M. Jeon, M. E. Birnbaum, H. J. Bellen, K. C. Garcia and K. Zinn (2015). "Control of Synaptic Connectivity by a Network of *Drosophila* IgSF Cell Surface Proteins." Cell **163**(7): 1770-1782.

Cecconi, F., G. Alvarez-Bolado, B. I. Meyer, K. A. Roth and P. Gruss (1998). "Apaf1 (CED-4 homolog) regulates programmed cell death in mammalian development." Cell **94**(6): 727-737.

Chen, Y.-T., C.-H. Kan, H. Liu, Y.-H. Liu, C.-C. Wu, Y.-P. Kuo, I. Y.-F. Chang, K.-P. Chang, J.-S. Yu and B. C.-M. Tan (2022). "Modular scaffolding by lncRNA HOXA10-AS promotes oral cancer progression." Cell Death & Disease **13**(7): 629.

Cherbas, L., X. Hu, I. Zhimulev, E. Belyaeva and P. Cherbas (2003). "EcR isoforms in *Drosophila*: testing tissue-specific requirements by targeted blockade and rescue." Development **130**(2): 271-284.

Choi, Y.-J., G. Lee and J. H. Park (2006). "Programmed cell death mechanisms of identifiable peptidergic neurons in *Drosophila melanogaster*." Development **133**(11): 2223-2232.

Choi, Y. J. (2006). "Programmed cell death mechanisms of identifiable peptidergic neurons in *Drosophila melanogaster*." **133**(11): 2223-2232.

Choi, Y. J., G. Lee, J. C. Hall and J. H. Park (2005). "Comparative analysis of Corazonin-encoding genes (Crz's) in *Drosophila* species and functional insights into Crz-expressing neurons." Journal of Comparative Neurology **482**(4): 372-385.

Choi, Y. J., G. Lee and J. H. Park (2006). "Programmed cell death mechanisms of identifiable peptidergic neurons in *Drosophila melanogaster*." Development **133**(11): 2223-2232.

Choo, M., T. Miyazaki, M. Yamazaki, M. Kawamura, T. Nakazawa, J. Zhang, A. Tanimura, N. Uesaka, M. Watanabe, K. Sakimura and M. Kano (2017). "Retrograde BDNF to TrkB signaling promotes synapse elimination in the developing cerebellum." Nat Commun **8**(1): 195.

Chung, W. S., L. E. Clarke, G. X. Wang, B. K. Stafford, A. Sher, C. Chakraborty, J. Joung, L. C. Foo, A. Thompson, C. Chen, S. J. Smith and B. A. Barres (2013). "Astrocytes mediate synapse elimination through MEGF10 and MERTK pathways." Nature **504**(7480): 394-400.

Clarembaux-Badell, L., P. Baladrón-de-Juan, H. Gabilondo, I. Rubio-Ferrera, I. Millán, C. Estella, F. S. Valverde-Ortega, I. M. Cobeta, S. Thor and J. Benito-Sipos (2022). "Dachshund acts with Abdominal-B to trigger programmed cell death in the *Drosophila*

central nervous system at the frontiers of Abd-B expression." Dev Neurobiol **82**(6): 495-504.

Clem, R. J., M. Fechheimer and L. K. Miller (1991). "Prevention of Apoptosis by a Baculovirus Gene During Infection of Insect Cells." Science **254**(5036): 1388-1390.

Corriveau, R. A., G. S. Huh and C. J. Shatz (1998). "Regulation of Class I MHC Gene Expression in the Developing and Mature CNS by Neural Activity." Neuron **21**(3): 505-520.

Cosmanescu, F., P. S. Katsamba, A. P. Sergeeva, G. Ahlsen, S. D. Patel, J. J. Brewer, L. Tan, S. Xu, Q. Xiao, S. Nagarkar-Jaiswal, A. Nern, H. J. Bellen, S. L. Zipursky, B. Honig and L. Shapiro (2018). "Neuron-Subtype-Specific Expression, Interaction Affinities, and Specificity Determinants of DIP/Dpr Cell Recognition Proteins." Neuron **100**(6): 1385-1400.e1386.

Delorenzi, M. and M. Bienz (1990). "Expression of Abdominal-B homeoproteins in *Drosophila* embryos." Development **108**(2): 323-329.

Denton, D., B. V. Shrivage, R. Simin, E. H. Baehrecke and S. Kumar (2010). "Larval midgut destruction in *Drosophila*: Not dependent on caspases but suppressed by the loss of autophagy." Autophagy **6**(1): 163-165.

Doherty, J., M. A. Logan, O. E. Tasdemir and M. R. Freeman (2009). "Ensheathing Glia Function as Phagocytes in the Adult *Drosophila* Brain." Journal of Neuroscience **29**(15): 4768-4781.

Dorothy, Emily, Amanda, R. Koyama, Alan, R. Yamasaki, Richard, Michael, Ben and B. Stevens (2012). "Microglia Sculpt Postnatal Neural Circuits in an Activity and Complement-Dependent Manner." Neuron **74**(4): 691-705.

Feinberg, I. (1982). "Schizophrenia: caused by a fault in programmed synaptic elimination during adolescence?" J Psychiatr Res **17**(4): 319-334.

Frade, J. M. and Y.-A. Barde (1998). "Microglia-Derived Nerve Growth Factor Causes Cell Death in the Developing Retina." Neuron **20**(1): 35-41.

Freeman, M. R., J. Delrow, J. Kim, E. Johnson and C. Q. Doe (2003). "Unwrapping glial biology: Gcm target genes regulating glial development, diversification, and function." Neuron **38**(4): 567-580.

Friesema, E. C., J. Jansen, H. Heuer, M. Trajkovic, K. Bauer and T. J. Visser (2006). "Mechanisms of disease: psychomotor retardation and high T3 levels caused by mutations in monocarboxylate transporter 8." Nat Clin Pract Endocrinol Metab **2**(9): 512-523.

Furber, S., R. Oppenheim and D. Prevetie (1987). "Naturally-occurring neuron death in the ciliary ganglion of the chick embryo following removal of preganglionic input: evidence for the role of afferents in ganglion cell survival." The Journal of Neuroscience **7**(6): 1816-1832.

Ganguly, K. and M.-m. Poo (2013). "Activity-Dependent Neural Plasticity from Bench to Bedside." Neuron **80**(3): 729-741.

- Gafo, G. O., P. Flodby and M. R. Capecchi (2000). "Hoxb1 controls effectors of sonic hedgehog and Mash1 signaling pathways." Development **127**(24): 5343-5354.
- Ghoumari, A. M., R. Wehrlé, O. Bernard, C. Sotelo and I. Dusart (2000). "Implication of Bcl-2 and Caspase-3 in age-related Purkinje cell death in murine organotypic culture: an in vitro model to study apoptosis." Eur J Neurosci **12**(8): 2935-2949.
- Gonçalves, C. S., E. Le Boiteux, P. Arnaud and B. M. Costa (2020). "HOX gene cluster (de)regulation in brain: from neurodevelopment to malignant glial tumours." Cellular and Molecular Life Sciences **77**(19): 3797-3821.
- Gunner, G., L. Cheadle, K. M. Johnson, P. Ayata, A. Badimon, E. Mondo, M. A. Nagy, L. Liu, S. M. Bemiller, K. W. Kim, S. A. Lira, B. T. Lamb, A. R. Tapper, R. M. Ransohoff, M. E. Greenberg, A. Schaefer and D. P. Schafer (2019). "Sensory lesioning induces microglial synapse elimination via ADAM10 and fractalkine signaling." Nat Neurosci **22**(7): 1075-1088.
- Guttenplan, K. A., M. K. Weigel, P. Prakash, P. R. Wijewardhane, P. Hasel, U. Rufen-Blanchette, A. E. Münch, J. A. Blum, J. Fine, M. C. Neal, K. D. Bruce, A. D. Gitler, G. Chopra, S. A. Liddelow and B. A. Barres (2021). "Neurotoxic reactive astrocytes induce cell death via saturated lipids." Nature **599**(7883): 102-107.
- Hakim, Y., S. P. Yaniv and O. Schuldiner (2014). "Astrocytes Play a Key Role in *Drosophila* Mushroom Body Axon Pruning." PLOS ONE **9**(1): e86178.

Hara, Y., K. Hirai, Y. Togane, H. Akagawa, K. Iwabuchi and H. Tsujimura (2013).

"Ecdysone-dependent and ecdysone-independent programmed cell death in the developing optic lobe of *Drosophila*." Developmental biology **374**(1): 127-141.

Hay, B. A., T. Wolff and G. M. Rubin (1994). "Expression of baculovirus P35 prevents cell death in *Drosophila*." Development **120**(8): 2121-2129.

Heisenberg, M. (1998). "What do the mushroom bodies do for the insect brain? an introduction." Learn Mem **5**(1-2): 1-10.

Hong, S., V. F. Beja-Glasser, B. M. Nfonoyim, A. Frouin, S. Li, S. Ramakrishnan, K. M. Merry, Q. Shi, A. Rosenthal, B. A. Barres, C. A. Lemere, D. J. Selkoe and B. Stevens (2016). "Complement and microglia mediate early synapse loss in Alzheimer mouse models." Science **352**(6286): 712-716.

Hoopfer, E. D., T. McLaughlin, R. J. Watts, O. Schuldiner, D. D. M. O'Leary and L. Luo (2006). "Wlds Protection Distinguishes Axon Degeneration following Injury from Naturally Occurring Developmental Pruning." Neuron **50**(6): 883-895.

Huang, Y., J. A. Ainsley, L. G. Reijmers and F. R. Jackson (2013). "Translational profiling of clock cells reveals circadianly synchronized protein synthesis." PLoS Biol **11**(11): e1001703.

Hughes, A. (1961). "Cell degeneration in the larval ventral horn of *Xenopus laevis* (Daudin)." J Embryol Exp Morphol **9**: 269-284.

Huh, G. S., L. M. Boulanger, H. Du, P. A. Riquelme, T. M. Brotz and C. J. Shatz (2000). "Functional requirement for class I MHC in CNS development and plasticity." Science **290**(5499): 2155-2159.

Hwang, J. S., C. Kobayashi, K. Agata, K. Ikeo and T. Gojobori (2004). "Detection of apoptosis during planarian regeneration by the expression of apoptosis-related genes and TUNEL assay." Gene **333**: 15-25.

Iram, T., Z. Ramirez-Ortiz, M. H. Byrne, U. A. Coleman, N. D. Kingery, T. K. Means, D. Frenkel and J. El Khoury (2016). "Megf10 Is a Receptor for C1Q That Mediates Clearance of Apoptotic Cells by Astrocytes." J Neurosci **36**(19): 5185-5192.

Issman-Zecharya, N. and O. Schuldiner (2014). "The PI3K Class III Complex Promotes Axon Pruning by Downregulating a Ptc-Derived Signal via Endosome-Lysosomal Degradation." Developmental Cell **31**(4): 461-473.

Iwai, Y., T. Usui, S. Hirano, R. Steward, M. Takeichi and T. Uemura (1997). "Axon Patterning Requires D N-cadherin, a Novel Neuronal Adhesion Receptor, in the *Drosophila* Embryonic CNS." Neuron **19**(1): 77-89.

Jenett, A., Gerald, T.-T. B. Ngo, D. Shepherd, C. Murphy, H. Dionne, Barret, A. Cavallaro, D. Hall, J. Jeter, N. Iyer, D. Fetter, Joanna, H. Peng, Eric, Robert, Eugene, Zbigniew, Y. Aso, Gina, A. Enos, P. Hulamm, Shing, H.-H. Li, Todd, F. Long, L. Qu, Sean, K. Rokicki, T. Safford, K. Shaw, Julie, A. Sowell, S. Tae, Y. Yu and Christopher

(2012). "A GAL4-Driver Line Resource for *Drosophila* Neurobiology." Cell Reports **2**(4): 991-1001.

Ji, H., B. Wang, Y. Shen, D. Labib, J. Lei, X. Chen, M. Sapor, A. Boulanger, J. M. Dura and C. Han (2023). "The *Drosophila* chemokine-like Orion bridges phosphatidylserine and Draper in phagocytosis of neurons." Proc Natl Acad Sci U S A **120**(24): e2303392120.

Kalcheim, C., Y. A. Barde, H. Thoenen and N. M. Le Douarin (1987). "In vivo effect of brain-derived neurotrophic factor on the survival of developing dorsal root ganglion cells." Embo j **6**(10): 2871-2873.

Kam, M. K. M., M. C. H. Cheung, J. J. Zhu, W. W. C. Cheng, E. W. Y. Sat, P. K. H. Tam and V. C. H. Lui (2014). "Perturbation of Hoxb5 signaling in vagal and trunk neural crest cells causes apoptosis and neurocristopathies in mice." Cell Death & Differentiation **21**(2): 278-289.

Kanamori, T., M. I. Kanai, Y. Dairyo, K. Yasunaga, R. K. Morikawa and K. Emoto (2013). "Compartmentalized calcium transients trigger dendrite pruning in *Drosophila* sensory neurons." Science **340**(6139): 1475-1478.

Kanamori, T., K. Togashi, H. Koizumi and K. Emoto (2015). Chapter One - Dendritic Remodeling: Lessons from Invertebrate Model Systems. International Review of Cell and Molecular Biology. K. W. Jeon, Academic Press. **318**: 1-25.

Kang, B. S., B. Y. Choi, A. R. Kho, S. H. Lee, D. K. Hong, M. K. Park, S. H. Lee, C. J. Lee, H. W. Yang, S. Y. Woo, S. W. Park, D. Y. Kim, J. B. Park, W. S. Chung and S. W. Suh (2023). "Effects of Pyruvate Kinase M2 (PKM2) Gene Deletion on Astrocyte-Specific Glycolysis and Global Cerebral Ischemia-Induced Neuronal Death." Antioxidants (Basel) **12**(2).

Kang, S. Y., S. N. Kim, S. H. Kim and S. H. Jeon (2006). "Temporal and spatial expression of homeotic genes is important for segment-specific neuroblast 6-4 lineage formation in *Drosophila*." Mol Cells **21**(3): 436-442.

Karch, F., W. Bender and B. Weiffenbach (1990). "abdA expression in *Drosophila* embryos." Genes Dev **4**(9): 1573-1587.

Karpova, N., Y. Bobinnec, S. Fouix, P. Huitorel and A. Debec (2006). "Jupiter, a new *Drosophila* protein associated with microtubules." Cell Motil Cytoskeleton **63**(5): 301-312.

Kenyon, C. (1986). "A gene involved in the development of the posterior body region of *C. elegans*." Cell **46**(3): 477-487.

Kirilly, D., Y. Gu, Y. Huang, Z. Wu, A. Bashirullah, B. C. Low, A. L. Kolodkin, H. Wang and F. Yu (2009). "A genetic pathway composed of Sox14 and Mical governs severing of dendrites during pruning." Nature neuroscience **12**(12): 1497-1505.

Kiris, E., T. Wang, S. Yanpallewar, S. G. Dorsey, J. Becker, S. Bavari, M. E. Palko, V. Coppola and L. Tessarollo (2014). "TrkA in vivo function is negatively regulated by ubiquitination." J Neurosci **34**(11): 4090-4098.

Kondo, S., N. Senoo-Matsuda, Y. Hiromi and M. Miura (2006). "DRONC coordinates cell death and compensatory proliferation." Mol Cell Biol **26**(19): 7258-7268.

Konopova, B. and M. Akam (2014). "The Hox genes Ultrabithorax and abdominal-A specify three different types of abdominal appendage in the springtail *Orchesella cincta* (Collembola)." Evodevo **5**(1): 2.

Kopec, A. M., C. J. Smith, N. R. Ayre, S. C. Sweat and S. D. Bilbo (2018). "Microglial dopamine receptor elimination defines sex-specific nucleus accumbens development and social behavior in adolescent rats." Nat Commun **9**(1): 3769.

Krämer, R., N. Wolterhoff, M. Galic and S. Rumpf (2023). "Developmental pruning of sensory neurites by mechanical tearing in *Drosophila*." Journal of Cell Biology **222**(3).

Kuo, C. T., L. Y. Jan and Y. N. Jan (2005). "Dendrite-specific remodeling of *Drosophila* sensory neurons requires matrix metalloproteases, ubiquitin-proteasome, and ecdysone signaling." Proc Natl Acad Sci U S A **102**(42): 15230-15235.

Kuo, C. T., L. Y. Jan and Y. N. Jan (2005). "Dendrite-specific remodeling of *Drosophila* sensory neurons requires matrix metalloproteases, ubiquitin-proteasome, and ecdysone signaling." Proceedings of the National Academy of Sciences of the United States of America **102**(42): 15230-15235.

Lai, Y.-W., S.-Y. Chu, J.-Y. Wei, C.-Y. Cheng, J.-C. Li, P.-L. Chen, C.-H. Chen and H.-H. Yu (2016). "*Drosophila* microRNA-34 Impairs Axon Pruning of Mushroom Body γ Neurons by Downregulating the Expression of Ecdysone Receptor." Scientific Reports **6**(1): 39141.

Lang, R. A. and J. M. Bishop (1993). "Macrophages are required for cell death and tissue remodeling in the developing mouse eye." Cell **74**(3): 453-462.

Latcheva, N. K., J. M. Viveiros and D. R. Marendza (2019). "The *Drosophila* Chromodomain Protein Kismet Activates Steroid Hormone Receptor Transcription to Govern Axon Pruning and Memory In Vivo." iScience **16**: 79-93.

Lee, G., R. Sehgal, Z. Wang, S. Nair, K. Kikuno, C.-H. Chen, B. Hay and J. H. Park (2013). "Essential role of grim-led programmed cell death for the establishment of corazonin-producing peptidergic nervous system during embryogenesis and metamorphosis in *Drosophila melanogaster*." Biology Open **2**(3): 283-294.

Lee, G., R. Sehgal, Z. Wang and J. H. Park (2019). "Ultraspiracle-independent anti-apoptotic function of ecdysone receptors is required for the survival of larval peptidergic neurons via suppression of grim expression in *Drosophila melanogaster*." Apoptosis **24**: 256-268.

Lee, G., R. Sehgal, Z. Wang and J. H. Park (2019). "Ultraspiracle-independent anti-apoptotic function of ecdysone receptors is required for the survival of larval peptidergic

neurons via suppression of grim expression in *Drosophila melanogaster*." Apoptosis : an international journal on programmed cell death **24**(3-4): 256-268.

Lee, G., Z. Wang, R. Sehgal, C.-H. Chen, K. Kikuno, B. Hay and J. H. Park (2011). "*Drosophila* caspases involved in developmentally regulated programmed cell death of peptidergic neurons during early metamorphosis." Journal of Comparative Neurology **519**(1): 34-48.

Lee, H., B. K. Brott, L. A. Kirkby, J. D. Adelson, S. Cheng, M. B. Feller, A. Datwani and C. J. Shatz (2014). "Synapse elimination and learning rules co-regulated by MHC class I H2-Db." Nature **509**(7499): 195-200.

Lee, H. H., L. Y. Jan and Y. N. Jan (2009). "*Drosophila* IKK-related kinase Ik2 and Katanin p60-like 1 regulate dendrite pruning of sensory neuron during metamorphosis." Proc Natl Acad Sci U S A **106**(15): 6363-6368.

Lee, J. H., J. Y. Kim, S. Noh, H. Lee, S. Y. Lee, J. Y. Mun, H. Park and W. S. Chung (2021). "Astrocytes phagocytose adult hippocampal synapses for circuit homeostasis." Nature **590**(7847): 612-617.

Lee, T., A. Lee and L. Luo (1999). "Development of the *Drosophila* mushroom bodies: sequential generation of three distinct types of neurons from a neuroblast." Development **126**(18): 4065-4076.

Lee, T. and L. Luo (1999). "Mosaic analysis with a repressible cell marker for studies of gene function in neuronal morphogenesis." Neuron **22**(3): 451-461.

Lee, T., S. Marticke, C. Sung, S. Robinow and L. Luo (2000). "Cell-autonomous requirement of the USP/EcR-B ecdysone receptor for mushroom body neuronal remodeling in *Drosophila*." Neuron **28**(3): 807-818.

Lee, T., S. Marticke, C. Sung, S. Robinow and L. Luo (2000). "Cell-Autonomous Requirement of the USP/EcR-B Ecdysone Receptor for Mushroom Body Neuronal Remodeling in *Drosophila*." Neuron **28**(3): 807-818.

Leuner, B. and T. J. Shors (2004). "New spines, new memories." Mol Neurobiol **29**(2): 117-130.

Levi-Montalcini, R. (1987). "The nerve growth factor 35 years later." Science **237**(4819): 1154-1162.

Levi, L. (1942). "MaRG Les consequences de la destruction d'un territoire d'innervation peripheique sur le developments des centres nerveux correspondents dans l'embryon de poulet." Arch. Biol **53**: 537-545.

Li, H., A. Watson, A. Olechwier, M. Anaya, S. K. Sorooshyari, D. P. Harnett, H.-K. Lee, J. Vielmetter, M. A. Fares, K. C. Garcia, E. Özkan, J.-P. Labrador and K. Zinn (2017). "Deconstruction of the beaten Path-Sidestep interaction network provides insights into neuromuscular system development." eLife **6**: e28111.

Lin, Y.-T., L.-S. Ro, H.-L. Wang and J.-C. Chen (2011). "Up-regulation of dorsal root ganglia BDNF and trkB receptor in inflammatory pain: an in vivo and in vitro study." Journal of Neuroinflammation **8**(1): 126.

Liu, X. Z., Q. Zhang, Q. Jiang, B. L. Bai, X. J. Du, F. Wang, L. H. Wu, X. L. Lu, Y. H. Bao, H. L. Li and T. Zhang (2018). "Genetic screening and functional analysis of CASP9 mutations in a Chinese cohort with neural tube defects." CNS Neurosci Ther **24**(5): 394-403.

Luan, H., W. C. Lemon, N. C. Peabody, J. B. Pohl, P. K. Zelensky, D. Wang, M. N. Nitabach, T. C. Holmes and B. H. White (2006). "Functional dissection of a neuronal network required for cuticle tanning and wing expansion in *Drosophila*." J Neurosci **26**(2): 573-584.

Luo, L. and D. D. O'Leary (2005). "Axon retraction and degeneration in development and disease." Annu Rev Neurosci **28**: 127-156.

Mallya, A. P., H. D. Wang, H. N. R. Lee and A. Y. Deutch (2019). "Microglial Pruning of Synapses in the Prefrontal Cortex During Adolescence." Cereb Cortex **29**(4): 1634-1643.

Manoukian, A. S. and H. M. Krause (1992). "Concentration-dependent activities of the even-skipped protein in *Drosophila* embryos." Genes Dev **6**(9): 1740-1751.

Marchetti, G. and G. Tavosanis (2017). "Steroid Hormone Ecdysone Signaling Specifies Mushroom Body Neuron Sequential Fate via Chinmo." Current Biology **27**(19): 3017-3024.e3014.

Marín-Teva, J. L., I. Dusart, C. Colin, A. Gervais, N. van Rooijen and M. Mallat (2004). "Microglia promote the death of developing Purkinje cells." Neuron **41**(4): 535-547.

Marin, I. A., A. Y. Gutman-Wei, K. S. Chew, A. J. Raissi, M. Djurusic and C. J. Shatz (2022). "The nonclassical MHC class I Qa-1 expressed in layer 6 neurons regulates activity-dependent plasticity via microglial CD94/NKG2 in the cortex." Proc Natl Acad Sci U S A **119**(23): e2203965119.

Marois, R. and T. J. Carew (1997). "Ontogeny of serotonergic neurons in *Aplysia californica*." J Comp Neurol **386**(3): 477-490.

Maysseless, O., G. Shapira, E. Y. Rachad, A. Fiala and O. Schuldiner (2023). "Neuronal excitability as a regulator of circuit remodeling." Curr Biol **33**(5): 981-989.e983.

Maysseless, O., G. Shapira, E. Y. Rachad, A. Fiala and O. Schuldiner (2023). "Neuronal excitability as a regulator of circuit remodeling." Current Biology **33**(5): 981-989.e983.

McGinnis, W. and R. Krumlauf (1992). "Homeobox genes and axial patterning." Cell **68**(2): 283-302.

Meltzer, H., E. Marom, I. Alyagor, O. Maysseless, V. Berkun, N. Segal-Gilboa, T. Unger, D. Luginbuhl and O. Schuldiner (2019). "Tissue-specific (ts)CRISPR as an efficient strategy for in vivo screening in *Drosophila*." Nature Communications **10**(1): 2113.

Mendrysa, S. M., S. Ghassemifar and R. Malek (2011). "p53 in the CNS: Perspectives on Development, Stem Cells, and Cancer." Genes Cancer **2**(4): 431-442.

- Miguel-Aliaga, I. and S. Thor (2004). "Segment-specific prevention of pioneer neuron apoptosis by cell-autonomous, postmitotic Hox gene activity." Development **131**(24): 6093-6105.
- Molliver, D. C. and W. D. Snider (1997). "Nerve growth factor receptor TrkA is down-regulated during postnatal development by a subset of dorsal root ganglion neurons." J Comp Neurol **381**(4): 428-438.
- Monedero Cobeta, I., B. Y. Salmani and S. Thor (2017). "Anterior-Posterior Gradient in Neural Stem and Daughter Cell Proliferation Governed by Spatial and Temporal Hox Control." Curr Biol **27**(8): 1161-1172.
- Muthukumar, A. K., T. Stork and M. R. Freeman (2014). "Activity-dependent regulation of astrocyte GAT levels during synaptogenesis." Nat Neurosci **17**(10): 1340-1350.
- Nakazawa, S., H. Mizuno and T. Iwasato (2018). "Differential dynamics of cortical neuron dendritic trees revealed by long-term in vivo imaging in neonates." Nat Commun **9**(1): 3106.
- Neniskyte, U. and C. T. Gross (2017). "Errant gardeners: glial-cell-dependent synaptic pruning and neurodevelopmental disorders." Nature Reviews Neuroscience **18**(11): 658-670.
- Nern, A., B. D. Pfeiffer and G. M. Rubin (2015). "Optimized tools for multicolor stochastic labeling reveal diverse stereotyped cell arrangements in the fly visual system." Proceedings of the National Academy of Sciences **112**(22): E2967-E2976.

Nussinov, R., C.-J. Tsai and H. Jang (2022). "How can same-gene mutations promote both cancer and developmental disorders?" Science Advances **8**(2): eabm2059.

Oppenheim, R. W. (1985). "Naturally occurring cell death during neural development." Trends in Neurosciences **8**: 487-493.

Osterloh, J. M. and M. R. Freeman (2009). "Neuronal death or dismemberment mediated by Sox14." Nat Neurosci **12**(12): 1479-1480.

Paolicelli, R. C., K. Bisht and M. Tremblay (2014). "Fractalkine regulation of microglial physiology and consequences on the brain and behavior." Front Cell Neurosci **8**: 129.

Paolicelli, R. C., G. Bolasco, F. Pagani, L. Maggi, M. Scianni, P. Panzanelli, M.

Giustetto, T. A. Ferreira, E. Guiducci, L. Dumas, D. Ragozzino and C. T. Gross (2011).

"Synaptic Pruning by Microglia Is Necessary for Normal Brain Development." Science **333**(6048): 1456-1458.

Pathak, D. and K. Sriram (2023). "Neuron-astrocyte omnidirectional signaling in neurological health and disease." Frontiers in Molecular Neuroscience **16**.

Penn, A. A., P. A. Riquelme, M. B. Feller and C. J. Shatz (1998). "Competition in retinogeniculate patterning driven by spontaneous activity." Science **279**(5359): 2108-2112.

Perez-Catalan, N. A., C. Q. Doe and S. D. Ackerman (2021). "The role of astrocyte-mediated plasticity in neural circuit development and function." Neural Development **16**(1): 1.

Perron, C., P. Carme, A. L. Rosell, E. Minnaert, S. Ruiz-Demoulin, H. Szczkowski, L. J. Neukomm, J.-M. Dura and A. Boulanger (2023). "Chemokine-like Orion is involved in the transformation of glial cells into phagocytes in different developmental neuronal remodeling paradigms." Development **150**(19).

Petersen, C. C. H. (2019). "Sensorimotor processing in the rodent barrel cortex." Nature Reviews Neuroscience **20**(9): 533-546.

Peterson, J. S., M. Barkett and K. McCall (2003). "Stage-specific regulation of caspase activity in *Drosophila* oogenesis." Developmental Biology **260**(1): 113-123.

Pfeiffer, B. D., A. Jenett, A. S. Hammonds, T.-T. B. Ngo, S. Misra, C. Murphy, A.

Scully, J. W. Carlson, K. H. Wan, T. R. Laverty, C. Mungall, R. Svirskas, J. T.

Kadonaga, C. Q. Doe, M. B. Eisen, S. E. Celniker and G. M. Rubin (2008). "Tools for neuroanatomy and neurogenetics in *Drosophila*." Proceedings of the National Academy of Sciences **105**(28): 9715.

Pfeiffer, B. D., A. Jenett, A. S. Hammonds, T.-T. B. Ngo, S. Misra, C. Murphy, A.

Scully, J. W. Carlson, K. H. Wan, T. R. Laverty, C. Mungall, R. Svirskas, J. T.

Kadonaga, C. Q. Doe, M. B. Eisen, S. E. Celniker and G. M. Rubin (2008). "Tools for

neuroanatomy and neurogenetics in *Drosophila*." Proceedings of the National Academy of Sciences **105**(28): 9715-9720.

Philippidou, P. and J. S. Dasen (2013). "Hox genes: choreographers in neural development, architects of circuit organization." Neuron **80**(1): 12-34.

Pinto-Teixeira, F., N. Konstantinides and C. Desplan "Programmed cell death acts at different stages of *Drosophila* neurodevelopment to shape the central nervous system." (1873-3468 (Electronic)).

Portera-Cailliau, C., R. M. Weimer, V. De Paola, P. Caroni and K. Svoboda (2005). "Diverse Modes of Axon Elaboration in the Developing Neocortex." PLOS Biology **3**(8): e272.

Quinonez, S. C. and J. W. Innis (2014). "Human HOX gene disorders." Molecular Genetics and Metabolism **111**(1): 4-15.

Read, R. D. (2018). "Pvr receptor tyrosine kinase signaling promotes post-embryonic morphogenesis, and survival of glia and neural progenitor cells in *Drosophila*." Development **145**(23).

Reay, W. R. and M. J. Cairns (2020). "The role of the retinoids in schizophrenia: genomic and clinical perspectives." Mol Psychiatry **25**(4): 706-718.

Rumpf, S., S. B. Lee, L. Y. Jan and Y. N. Jan (2011). "Neuronal remodeling and apoptosis require VCP-dependent degradation of the apoptosis inhibitor DIAP1." Development **138**(6): 1153-1160.

Schafer, D. P., E. K. Lehrman, A. G. Kautzman, R. Koyama, A. R. Mardinly, R. Yamasaki, R. M. Ransohoff, M. E. Greenberg, B. A. Barres and B. Stevens (2012). "Microglia sculpt postnatal neural circuits in an activity and complement-dependent manner." Neuron **74**(4): 691-705.

Schubiger, M., A. A. Wade, G. E. Carney, J. W. Truman and M. Bender (1998). "*Drosophila* EcR-B ecdysone receptor isoforms are required for larval molting and for neuron remodeling during metamorphosis." Development **125**(11): 2053-2062.

Schubiger, M., A. A. Wade, G. E. Carney, J. W. Truman and M. Bender (1998). "*Drosophila* EcR-B ecdysone receptor isoforms are required for larval molting and for neuron remodeling during metamorphosis." Development **125**(11): 2053-2062.

Schug, T. T., D. C. Berry, N. S. Shaw, S. N. Travis and N. Noy (2007). "Opposing effects of retinoic acid on cell growth result from alternate activation of two different nuclear receptors." Cell **129**(4): 723-733.

Scott, R. C., G. Juhász and T. P. Neufeld (2007). "Direct Induction of Autophagy by Atg1 Inhibits Cell Growth and Induces Apoptotic Cell Death." Current Biology **17**(1): 1-11.

Sekar, A., A. R. Bialas, H. de Rivera, A. Davis, T. R. Hammond, N. Kamitaki, K. Tooley, J. Presumey, M. Baum, V. Van Doren, G. Genovese, S. A. Rose, R. E. Handsaker, M. J. Daly, M. C. Carroll, B. Stevens and S. A. McCarroll (2016). "Schizophrenia risk from complex variation of complement component 4." Nature **530**(7589): 177-183.

Serrano-Pozo, A., M. P. Frosch, E. Masliah and B. T. Hyman (2011). "Neuropathological alterations in Alzheimer disease." Cold Spring Harb Perspect Med **1**(1): a006189.

Shatz, C. J. (1990). "Impulse activity and the patterning of connections during cns development." Neuron **5**(6): 745-756.

Shi, Q., K. J. Colodner, S. B. Matousek, K. Merry, S. Hong, J. E. Kenison, J. L. Frost, K. X. Le, S. Li, J. C. Dodart, B. J. Caldarone, B. Stevens and C. A. Lemere (2015). "Complement C3-Deficient Mice Fail to Display Age-Related Hippocampal Decline." J Neurosci **35**(38): 13029-13042.

Simon, D. J., J. Pitts, N. T. Hertz, J. Yang, Y. Yamagishi, O. Olsen, M. Tešić Mark, H. Molina and M. Tessier-Lavigne (2016). "Axon Degeneration Gated by Retrograde Activation of Somatic Pro-apoptotic Signaling." Cell **164**(5): 1031-1045.

Simpson, J. A. (1977). "Normal and Abnormal Development of the Human Nervous System." J Neurol Neurosurg Psychiatry **40**(11): 1125.

Sink, H. and P. M. Whitington (1991). "Location and connectivity of abdominal motoneurons in the embryo and larva of *Drosophila melanogaster*." Journal of Neurobiology **22**(3): 298-311.

Sipe, G. O., R. L. Lowery, M. Tremblay, E. A. Kelly, C. E. Lamantia and A. K. Majewska (2016). "Microglial P2Y₁₂ is necessary for synaptic plasticity in mouse visual cortex." Nat Commun **7**: 10905.

Smolič, T., P. Tavčar, A. Horvat, U. Černe, A. Halužan Vasle, L. Tratnjek, M. E. Kreft, N. Scholz, M. Matis, T. Petan, R. Zorec and N. Vardjan (2021). "Astrocytes in stress accumulate lipid droplets." Glia **69**(6): 1540-1562.

Stephenson, S. E. M., G. Costain, L. E. R. Blok, M. A. Silk, T. B. Nguyen, X. Dong, D. E. Alhuzaimi, J. J. Dowling, S. Walker, K. Amburgey, R. Z. Hayeems, L. H. Rodan, M. A. Schwartz, J. Picker, S. A. Lynch, A. Gupta, K. J. Rasmussen, L. A. Schimmenti, E. W. Klee, Z. Niu, K. E. Agre, I. Chilton, W. K. Chung, A. Revah-Politi, P. Y. B. Au, C. Griffith, M. Racobaldo, A. Raas-Rothschild, B. Ben Zeev, O. Barel, S. Moutton, F. Morice-Picard, V. Carmignac, J. Cornaton, N. Marle, O. Devinsky, C. Stimach, S. B. Wechsler, B. E. Hainline, K. Sapp, M. Willems, A.-I. Bruel, K.-R. Dias, C.-A. Evans, T. Roscioli, R. Sachdev, S. E. L. Temple, Y. Zhu, J. J. Baker, I. E. Scheffer, F. J. Gardiner, A. L. Schneider, A. M. Muir, H. C. Mefford, A. Crunk, E. M. Heise, F. Millan, K. G. Monaghan, R. Person, L. Rhodes, S. Richards, I. M. Wentzensen, B. Cogné, B. Isidor, M. Nizon, M. Vincent, T. Besnard, A. Piton, C. Marcelis, K. Kato, N. Koyama, T. Ogi, E. S.-Y. Goh, C. Richmond, D. J. Amor, J. O. Boyce, A. T. Morgan, M. S. Hildebrand, A.

Kaspi, M. Bahlo, R. Friðriksdóttir, H. Katrínardóttir, P. Sulem, K. Stefánsson, H. T. Björnsson, S. Mandelstam, M. Morleo, M. Mariani, M. Scala, A. Accogli, A. Torella, V. Capra, M. Wallis, S. Jansen, Q. Waisfisz, H. de Haan, S. Sadedin, S. C. Lim, S. M. White, D. B. Ascher, A. Schenck, P. J. Lockhart, J. Christodoulou and T. Y. Tan (2022). "Germline variants in tumor suppressor FBXW7 lead to impaired ubiquitination and a neurodevelopmental syndrome." The American Journal of Human Genetics **109**(4): 601-617.

Stevens, B., N. J. Allen, L. E. Vazquez, G. R. Howell, K. S. Christopherson, N. Nouri, K. D. Micheva, A. K. Mehalow, A. D. Huberman, B. Stafford, A. Sher, Alan, J. D. Lambris, S. J. Smith, S. W. M. John and B. A. Barres (2007). "The Classical Complement Cascade Mediates CNS Synapse Elimination." Cell **131**(6): 1164-1178.

Stevens, B., N. J. Allen, L. E. Vazquez, G. R. Howell, K. S. Christopherson, N. Nouri, K. D. Micheva, A. K. Mehalow, A. D. Huberman, B. Stafford, A. Sher, Alan M. Litke, J. D. Lambris, S. J. Smith, S. W. M. John and B. A. Barres (2007). "The Classical Complement Cascade Mediates CNS Synapse Elimination." Cell **131**(6): 1164-1178.

Stork, T., A. Sheehan, O. E. Tasdemir-Yilmaz and M. R. Freeman (2014). "Neuron-glia interactions through the Heartless FGF receptor signaling pathway mediate morphogenesis of *Drosophila* astrocytes." Neuron **83**(2): 388-403.

Stuart, D. K., S. S. Blair and D. A. Weisblat (1987). "Cell lineage, cell death, and the developmental origin of identified serotonin- and dopamine-containing neurons in the leech." J Neurosci **7**(4): 1107-1122.

Sugihara, I. (2006). "Organization and remodeling of the olivocerebellar climbing fiber projection." Cerebellum **5**(1): 15-22.

Suska, A., S. Miguel-Aliaga I Fau - Thor and S. Thor "Segment-specific generation of *Drosophila* Capability neuropeptide neurons by multi-faceted Hox cues." (1095-564X (Electronic)).

Tang, G., K. Gudsnuk, S.-H. Kuo, Marisa L. Cotrina, G. Rosoklija, A. Sosunov, Mark S. Sonders, E. Kanter, C. Castagna, A. Yamamoto, Z. Yue, O. Arancio, Bradley S. Peterson, F. Champagne, Andrew J. Dwork, J. Goldman and D. Sulzer (2014). "Loss of mTOR-Dependent Macroautophagy Causes Autistic-like Synaptic Pruning Deficits." Neuron **83**(5): 1131-1143.

Tasdemir-Yilmaz, O. E. and M. R. Freeman (2014). "Astrocytes engage unique molecular programs to engulf pruned neuronal debris from distinct subsets of neurons." Genes Dev **28**(1): 20-33.

Terry, R. D., E. Masliah, D. P. Salmon, N. Butters, R. DeTeresa, R. Hill, L. A. Hansen and R. Katzman (1991). "Physical basis of cognitive alterations in Alzheimer's disease: synapse loss is the major correlate of cognitive impairment." Ann Neurol **30**(4): 572-580.

Thomaidou, D., M. C. Mione, J. F. Cavanagh and J. G. Parnavelas (1997). "Apoptosis and its relation to the cell cycle in the developing cerebral cortex." J Neurosci **17**(3): 1075-1085.

Thompson, C. K. (2011). "Cell death and the song control system: a model for how sex steroid hormones regulate naturally-occurring neurodegeneration." Dev Growth Differ **53**(2): 213-224.

Thummel, C. S. (1996). "Flies on steroids — *Drosophila* metamorphosis and the mechanisms of steroid hormone action." Trends in Genetics **12**(8): 306-310.

Toyoshima, Y., S. Sekiguchi, T. Negishi, S. Nakamura, T. Ihara, Y. Ishii, S. Kyuwa, Y. Yoshikawa and K. Takahashi (2012). "Differentiation of neural cells in the fetal cerebral cortex of cynomolgus monkeys (*Macaca fascicularis*)." Comp Med **62**(1): 53-60.

Tremblay, M., R. L. Lowery and A. K. Majewska (2010). "Microglial interactions with synapses are modulated by visual experience." PLoS Biol **8**(11): e1000527.

Truman, J. W. and L. M. Riddiford (2019). "The evolution of insect metamorphosis: a developmental and endocrine view." Philosophical Transactions of the Royal Society B: Biological Sciences **374**(1783): 20190070.

Truman, J. W. and L. M. Riddiford (2023). "*Drosophila* postembryonic nervous system development: a model for the endocrine control of development." Genetics **223**(3).

- Truman, J. W., R. S. Thorn and S. Robinow (1992). "Programmed neuronal death in insect development." J Neurobiol **23**(9): 1295-1311.
- Trush, O., C. Liu, X. Han, Y. Nakai, R. Takayama, H. Murakawa, J. A. Carrillo, H. Takechi, S. Hakeda-Suzuki, T. Suzuki and M. Sato (2019). "N-Cadherin Orchestrates Self-Organization of Neurons within a Columnar Unit in the *Drosophila* Medulla." The Journal of Neuroscience **39**(30): 5861-5880.
- Tung, T. T., K. Nagaosa, Y. Fujita, A. Kita, H. Mori, R. Okada, S. Nonaka and Y. Nakanishi (2013). "Phosphatidylserine recognition and induction of apoptotic cell clearance by *Drosophila* engulfment receptor Draper." J Biochem **153**(5): 483-491.
- Turrigiano, G. (2012). "Homeostatic synaptic plasticity: local and global mechanisms for stabilizing neuronal function." Cold Spring Harb Perspect Biol **4**(1): a005736.
- Ueno, M., Y. Fujita, T. Tanaka, Y. Nakamura, J. Kikuta, M. Ishii and T. Yamashita (2013). "Layer V cortical neurons require microglial support for survival during postnatal development." Nature Neuroscience **16**(5): 543-551.
- Viswanathan, S., M. E. Williams, E. B. Bloss, T. J. Stasevich, C. M. Speer, A. Nern, B. D. Pfeiffer, B. M. Hooks, W.-P. Li, B. P. English, T. Tian, G. L. Henry, J. J. Macklin, R. Patel, C. R. Gerfen, X. Zhuang, Y. Wang, G. M. Rubin and L. L. Looger (2015). "High-performance probes for light and electron microscopy." Nature methods **12**(6): 568-576.

Wang, T., M. Liu and M. Jia (2023). "Integrated Bioinformatic Analysis of the Correlation of HOXA10 Expression with Survival and Immune Cell Infiltration in Lower Grade Glioma." Biochemical Genetics **61**(1): 238-257.

Wang, Y., M. Rui, Q. Tang, S. Bu and F. Yu (2019). "Patronin governs minus-end-out orientation of dendritic microtubules to promote dendrite pruning in *Drosophila*." eLife **8**: e39964.

Wang, Z., G. Lee, R. Vuong and J. H. Park (2019). "Two-factor specification of apoptosis: TGF- β signaling acts cooperatively with ecdysone signaling to induce cell- and stage-specific apoptosis of larval neurons during metamorphosis in *Drosophila melanogaster*." Apoptosis **24**(11-12): 972-989.

Watts, R. J., E. D. Hoopfer and L. Luo (2003). "Axon Pruning during *Drosophila* Metamorphosis: Evidence for Local Degeneration and Requirement of the Ubiquitin-Proteasome System." Neuron **38**(6): 871-885.

Weil, M., M. D. Jacobson and M. C. Raff (1997). "Is programmed cell death required for neural tube closure?" Curr Biol **7**(4): 281-284.

Werneburg, S., P. A. Feinberg, K. M. Johnson and D. P. Schafer (2017). "A microglia-cytokine axis to modulate synaptic connectivity and function." Curr Opin Neurobiol **47**: 138-145.

Whiddon, Z. D., J. B. Marshall, D. C. Alston, A. W. McGee and R. F. Krimm (2023). "Rapid structural remodeling of peripheral taste neurons is independent of taste cell turnover." PLoS Biol **21**(8): e3002271.

Williams, D. W. and J. W. Truman (2005). "Cellular mechanisms of dendrite pruning in *Drosophila*: insights from in vivo time-lapse of remodeling dendritic arborizing sensory neurons." Development **132**(16): 3631-3642.

Wilson, A. M., R. Schalek, A. Suissa-Peleg, T. R. Jones, S. Knowles-Barley, H. Pfister and J. W. Lichtman (2019). "Developmental Rewiring between Cerebellar Climbing Fibers and Purkinje Cells Begins with Positive Feedback Synapse Addition." Cell Reports **29**(9): 2849-2861.e2846.

Winbush, A. and J. C. Weeks "Steroid-triggered, cell-autonomous death of a *Drosophila* motoneuron during metamorphosis." (1749-8104 (Electronic)).

Winbush, A. and J. C. Weeks (2011). "Steroid-triggered, cell-autonomous death of a *Drosophila* motoneuron during metamorphosis." Neural Dev **6**: 15.

Xiao, Y., L. Petrucco, L. J. Hoodless, R. Portugues and T. Czopka (2022).

"Oligodendrocyte precursor cells sculpt the visual system by regulating axonal remodeling." Nature Neuroscience **25**(3): 280-284.

Xie, Y., A. T. Kuan, W. Wang, Z. T. Herbert, O. Mosto, O. Olukoya, M. Adam, S. Vu, M. Kim, D. Tran, N. Gómez, C. Charpentier, I. Sorour, T. E. Lacey, M. Y. Tolstorukov,

B. L. Sabatini, W. A. Lee and C. C. Harwell (2022). "Astrocyte-neuron crosstalk through Hedgehog signaling mediates cortical synapse development." Cell Rep **38**(8): 110416.

Xiong, W. C., H. Okano, N. H. Patel, J. A. Blendy and C. Montell (1994). "repo encodes a glial-specific homeo domain protein required in the *Drosophila* nervous system." **8**(8): 981-994.

Xu, P., M. Das, J. Reilly and R. J. Davis (2011). "JNK regulates FoxO-dependent autophagy in neurons." Genes Dev **25**(4): 310-322.

Yamaguchi, Y. and M. Miura (2015). "Programmed Cell Death in Neurodevelopment." Developmental Cell **32**(4): 478-490.

Yang, C. H., S. Rumpf, Y. Xiang, M. D. Gordon, W. Song, L. Y. Jan and Y. N. Jan (2009). "Control of the postmating behavioral switch in *Drosophila* females by internal sensory neurons." Neuron **61**(4): 519-526.

Yaniv, S. P., N. Issman-Zecharya, M. Oren-Suissa, B. Podbilewicz and O. Schuldiner (2012). "Axon regrowth during development and regeneration following injury share molecular mechanisms." Curr Biol **22**(19): 1774-1782.

Yao, T. P., B. M. Forman, Z. Jiang, L. Cherbas, J. D. Chen, M. McKeown, P. Cherbas and R. M. Evans (1993). "Functional ecdysone receptor is the product of EcR and Ultraspiracle genes." Nature **366**(6454): 476-479.

Yu, X. M., I. Gutman, T. J. Mosca, T. Iram, E. Ozkan, K. C. Garcia, L. Luo and O. Schuldiner (2013). "Plum, an immunoglobulin superfamily protein, regulates axon pruning by facilitating TGF- β signaling." Neuron **78**(3): 456-468.

Yu, Xiaomeng M., I. Gutman, Timothy J. Mosca, T. Iram, E. Özkan, K. C. Garcia, L. Luo and O. Schuldiner (2013). "Plum, an Immunoglobulin Superfamily Protein, Regulates Axon Pruning by Facilitating TGF- β Signaling." Neuron **78**(3): 456-468.

Zhang, H., Y. Wang, Jack Jing L. Wong, K.-L. Lim, Y.-C. Liou, H. Wang and F. Yu (2014). "Endocytic Pathways Downregulate the L1-type Cell Adhesion Molecule Neuroglian to Promote Dendrite Pruning in *Drosophila*." Developmental Cell **30**(4): 463-478.

Zhang, Y., S. A. Sloan, L. E. Clarke, C. Caneda, C. A. Plaza, P. D. Blumenthal, H. Vogel, G. K. Steinberg, M. S. Edwards, G. Li, J. A. Duncan, 3rd, S. H. Cheshier, L. M. Shuer, E. F. Chang, G. A. Grant, M. G. Gephart and B. A. Barres (2016). "Purification and Characterization of Progenitor and Mature Human Astrocytes Reveals Transcriptional and Functional Differences with Mouse." Neuron **89**(1): 37-53.

Zhao, T., T. Gu, H. C. Rice, K. L. McAdams, K. M. Roark, K. Lawson, S. A. Gauthier, K. L. Reagan and R. S. Hewes (2008). "A *Drosophila* gain-of-function screen for candidate genes involved in steroid-dependent neuroendocrine cell remodeling." Genetics **178**(2): 883-901.

Zheng, X., J. Wang, T. E. Haerry, A. Y. H. Wu, J. Martin, M. B. O'Connor, C.-H. J. Lee and T. Lee (2003). "TGF- β Signaling Activates Steroid Hormone Receptor Expression during Neuronal Remodeling in the *Drosophila* Brain." Cell **112**(3): 303-315.

Zhu, S., R. Chen, P. Soba and Y.-N. Jan (2019). "JNK signaling coordinates with ecdysone signaling to promote pruning of *Drosophila* sensory neuron dendrites." Development **146**(8): dev163592.

Zirin, J., D. Cheng, N. Dhanyasi, J. Cho, J.-M. Dura, K. VijayRaghavan and N. Perrimon (2013). "Ecdysone signaling at metamorphosis triggers apoptosis of *Drosophila* abdominal muscles." Developmental Biology **383**(2): 275-284.